MODIFICATION OF CERAMIC MEMBRANE SURFACE BY NANOPARTICLE COATING FOR IMPROVED WETTABILITY DURING OIL-WATER SEPARATION

A dissertation submitted in fulfilment of the requirements for the degree Master of Engineering in Mechanical Engineering

In the Faculty of Engineering & Technology

Vaal University of Technology

VAAL UNIVERSITY
OF TECHNOLOGY

ENGINEERING &
TECHNOLOGY

Student Name: Tshepo G. Maome

Student Number: 20107935

B Tech: Mechanical Engineering

Supervisor: Prof Thomas B. Tengen

Co-Supervisor: Prof Alfayo A. Alugongo

Co-Supervisor: Assistant Prof Peter B. Sob

Date: 07 March 2022

ABSTRACT

The developed oil-water separation membranes used in membrane technology are currently inefficient due to their poor morphological and topographical properties during nanoparticle coating. Researchers have developed different wettable membrane surfaces using jet spray coating. Most of these developed membranes are inadequate due to poor morphological and topographical properties normally observed as clusters, creating a rougher membrane surface that hinders wettability. This has resulted in the existing membrane fouling and degradation during the oil/water separation process and again due to different responses to corrosion and rusting. In the current study, membrane clusters were minimised on the ceramic membranes to create a smoother surface, improving membrane wettability. These clusters were minmised at optimal coating force, optimal coating distance and optimal coating angle.

Part one of the study was to model and simulate different parameters that decreased clusters using the jet-spray coating. A theoretical model was derived from the first principles and all the external and internal forces that impact membrane clusters were considered during the model derivation. These forces are the force due to applied pressure from the spray gun, the force of nano-particles, the force of viscosity, the upward force on solid wall due to nanoparticles, the downward force on solid wall due to nanoparticles and the reaction force on the solid wall due to nanoparticles. The tools of stochastic theory and the concept of fluid dynamics were used in the modelling process. The total coating force from the jet spray gun nozzle was increased from $0{,}2x10^7$ kN to $2{,}4x10^7$ kN, which gave optimal coating force. The coating distance from the jet spray gun nozzle to the membrane surface was increased from 10 mm to 24 mm, which gave optimal coating distance. The jet spray angle in the spray region was also increased from 1º to 9º with reference from the vertical axis to the membrane surface, which gave optimal coating angle. This lead to optimal spread of nanoparticles on the membrane surface thus resulting to optimal cluster minimisation during the coating process. This decreased cluster sizes during nanoparticle coating, resulting in a smooth membrane surface, thus leading to lowered surface energy on the membrane.

Part two of the study was to fabricate the ceramic membrane with fewer clusters on the surface for improved wettability using the jet-spray coating. It was important to produce the ceramic membrane surfaces with minimised membrane clusters by considering the optimal parameters revealed to minimise these membrane clusters during coating. Nanoparticle coating was performed under a controlled laboratory environment, and the optimal parameters that were studied to minimise membrane clusters were revealed. These parameters are coating force, coating distance and coating angle. More coating rounds were applied on ceramic samples and clusters were minimised during these coating rounds. The coated samples were analyzed by a scanning electron microscope and the nanoparticles on the membrane surfaces were characterised for optimal performance during oil-water separation. The scattering, orientation, morphology, spatial distribution, surface roughness, surface smoothness, contact angles,

surface density of the particles, pore size network, mean size of the coated nanoparticle on the membrane surface after different coating rounds were characterised and analysed to minimise membrane cluster during nanoparticle coating. It was shown that more clusters were observed in 1st LP, 2nd LP, 3rd LP and 4th LP coating rounds when compared to 1st HP, 2nd HP, 3rd HP and 4th HP coating rounds. It was also shown that material surface roughness increased the formation of clusters in membrane surface as more clusters were observed in rough membrane surface when compared to the smooth membrane surface. The microstructure revealed a smoother membrane surface where membrane clusters were minimised.

Part three of the study was to compare the newly designed ceramic membrane with the previously designed ceramic membrane from previous the literature. The correlation was done on the experimental results obtained in this study with the experimental results obtained from the previous literature. Different coating rounds were performed from the current study and the previous literature to design nanostructured ceramic membranes with fewer clusters on the surface. The results in the last coating round in this study, revealed a smooth membrane with a homogeneous substrate with fewer clusters and small sizes compared to other coating rounds.

Keywords: Clusters, Wettability, Ceramics, Nanoparticle coating, Surface energy, and Surface tension.

Declaration of Dissertation

I declare that this dissertation was written entirely by me without the assistance of anyone. It is being submitted for the degree of Master of Engineering in Mechanical Engineering at the Vaal University of Technology, Vanderbijlpark, South Africa. It has never been submitted for any other University's degree or examination.

Statements

1. This dissertation is being submitted in fulfilment of the requirements for the degree of Master of Engineering in Mechanical Engineering.
2. This dissertation is the result of my own independent work/investigation, except where otherwise stated. Other sources are acknowledged by giving explicit references and a list of references is appended.
3. If accepted, I consent for my dissertation to be available for online publication, photocopying and interlibrary loan, and the title and summary to be made available to outside organisations.

Signature of Candidate……

Date: 07 March 2022

Publications and Conference Proceedings

1. **T.G. Maome, P.B. Sob, A.A Alugongo and T.B. Tengen, (2020). Minimising Clusters on Ceramic Membrane during Nanoparticle Coating by Jet-Spray for Efficient Wettability during Oil-Water Separation.** In Proceedings of the 8'th International Conference on Advancements and Futuristic Trends in Mechanical and Materials Engineering (AFTMME 2020). ISSN: 2249-7250, Vol 10, No.1.

Acknowledgement

Firstly, I would like to thank the "**All Mighty Creator**" for his unconditional blessings throughout my entire research, "**Praise to GOD**". This academic journey has never been easy at all and as a result, a few people made my ordeal bearable. Throughout their moral support, I'm proudly saying this dissertation is here.

Secondly, I would like to thank my wife, **Moipone Maome**, my son, **Kutloano Maome** and my daughter **Dintle Maome**. Through their love and support throughout the years, this work is possible. They have always been there for me, and I am grateful for their love and generosity. I would like to thank my mother, **Mathapelo Maome,** for her spiritual support and encouragement throughout my research.

Thirdly, I would like to thank my supervisor, **Prof Thomas Tengen**. His technical and academic expertise fine-tuned my academic journey in the right direction. I would like to thank my co-supervisor, **Prof Alfayo Alugongo,** for his contribution to my research. Special thanks to my other co-supervisor, **Dr Peter Sob,** for his long-lasting mentoring throughout my research, channelling my research route towards the right direction. I would not have gained proper mentoring throughout my research without them.

To the **Vaal University of Technology, Vanderbijlpark, South Africa, Faculty of Engineering and Technology, particularly the Department of Mechanical Engineering, Industrial Engineering & Operations Management**, I would like to thank this institution for the knowledge it has provided to me.

I would like to thank the **Sefako Makgatho Health Science University management** and **Dr James-Wesley Smith** for all the microscopic analysis in this dissertation.

To all my fellow **Postgraduate Students**, thank you for offering the great company throughout the years. Wishing you all the best of luck and **GOD bless you**.

Dedication

This is dedicated to my late father (**Motlalepula Maome**), whose death touched my life profoundly. May his soul continue to Rest in Peace.

Table of Contents

List of Figures

List of Tables

List of Symbols and Acronyms

Al	Aluminum
Al_2O_3	Alumina
Ag	Silver
CFV	Cross-flow Velocity
CNN	Cable News Network
$CuSO_4$	Copper Sulphate
EDS	Energy Dispersion Spectroscopy
EES	Engineering Equation Solver
Fe	Iron
F	Fluorine
HP	High Pressure
H_2O_2	Hydrogen Peroxide
ITO	Indium Tin Oxide
K	Potassium
Kev	Kilo Electrons Volt
L-b-L	Layer-by-layer
LLDP	Liqui-liquid Porosimetry
LP	Low Pressure
MF	Microfiltration
Mg	Magnesium
Na	Sodium
NF	Nanofiltration
O	Oxygen
P	Pressure
PAN	Polyacrylonitrile
PDA	Polydopamine
PE	Polyethylene

PES	Polyethersulfone
PF	Permeation Flux
PP	Polypropylene
PTFE	Polytetrafluoroethylene
PVDF	Polyvinylide fluoride
Q	Flow Rate
S	Sulphur
SEM	Scanning Electron Microscope
Si	Silicon
T	Temperature
TEM	Transmission Electron Microscope
TFC	Thin-film Composite
TFN	Thin-film Nanocomposite
TMP	Trans-membrane Pressure
UF	Ultrafiltration
UV	Ultra Violet
$ZrCl_4$	Zirconium Tetrachloride
ZrO_2	Zirconium Oxide

CHAPTER ONE

INTRODUCTION

1.1 Background of the study

Water, as a vital need to both industrial and domestic applications, is contaminated due to mining processing, oil exploration, pharmaceutical processing and agricultural processing (Wang*et al.*, 2018) (Yu *et al.*, 2017) (Rezaei *et al.*, 2011) (Achilli *et al.*, 2009). With the progress of society globally, water contamination is increasingly becoming a serious concern (Cai *et al.*, 2018). This contaminated water is not suitable for both domestic and industrial consumption (Wang*et al.*, 2018) (Wang *et al.*, 2009). The aquatic environment and health of humans are seriously threatened by offshore oil spills and oily industrial wastewater (Wang*et al.*, 2018). Communities that depend on fishing for the sustainability of their livelihood are seriously affected.

In February 2019, an oil spill occurred during offshore bunkering operations in the Algoa Bay, Port of Ngqura, Port Elizabeth city in South Africa (NEWS 24, 2019). It was reported that approximately 200 to 400 litres of oil were spilt into the sea as a result of overflow during the fuel oil transfer. In November 2013, an oil pipeline blasted in Sinopec, Qingdao city in China and resulted in a large amount of oil spills into the ocean (Liu *et al.*, 2015). This created damage to the coastlines and the near-shore water, thus causing disasters for marine animals and organisms. In April 2010, an explosion occurred in a BP Deepwater Horizon oil rig, releasing approximately 4 million barrels of oil into the Gulf Coast of Mexico (CNN, 2018) (Chu *et al.*, 2015). After seeing these great damages due to oil spillages, it was important for the researchers to design and fabricate functional membrane materials and adsorbents to deal with oil-water separation. Thus, there is a need for the contaminated water to be treated to separate the oil from water. Effective and economic oil-water separation is a hotspot research area with massive industrial and domestic benefits (Ramachandran and Nosonovsky, 2016) (Magdysyuk *et al.*, 2016). In this regard, oil-water separations have been attracting significant attention due to the ever-increasing environmental regulations (Magdysyuk *et al.*, 2016).

Many studies have focused on developing effective oil-water separation methods for pollution control and oil spill recovery (Wang*et al.*, 2018). The established oil-water separation techniques mainly include gravity sedimentation, centrifugation, electrolytic separation, adsorption separation and biodegradation (Wang*et al.*, 2018) (Wang *et al.*, 2016) (Munirasu *et al.*, 2016). However, these methods are inefficient and expensive to run (Wang*et al.*, 2018) (Wang *et al.*, 2016) (Munirasu *et al.*, 2016). These challenges greatly depend on the types of membrane materials selected to offer the best wettable properties. Researchers never considered selecting the membrane with better surface properties and further modifying it to provide optimum wettability during oil-water separation (Wang*et al.*, 2018) (Shannon *et al.*, 2008).

Membrane materials that are used in membrane wettability design for oil-water separation are ceramics, polymers, textiles, clay, glass and sediments (Wang*et al.*, 2018) (Yu *et al.*, 2017) (Chu, *et al.*, 2015). These materials have different wetting properties when coated with nanoparticles due to their surface roughness, which impacts membrane wettability (Weston *et al.*, 2015). The main factors influencing the membrane surface wettability are the surface energy and the surface roughness (Wang*et al.*, 2018) (Kubiak *et al.*, 2011) (Miwa *et al.*, 2000). One of the common problems observed from these developed membrane materials is severe membrane fouling by oil droplets (Padaki *et al.*, 2015) (Zhu *et al.*, 2014). However, membrane fouling remains a technical challenge to date in the oil-water separation industries (Wei *et al.*, 2018) (Padaki *et al.*, 2015).

Polymeric membrane materials have weak mechanical strength, they are used for low separation requirements, and they have a tendency to foul more quickly (Ma *et al.*, 2016) (Le and Nunes, 2016) (Padaki *et al.*, 2015). As a result, they require frequent cleaning in between filtration processes (Ma *et al.*, 2016). These membrane materials have small pore channels, requiring high pressure to maintain the permeate flux. This can be energy-intensive (Ma *et al.*, 2016), which is a problem in oil-water separation (Yu *et al.*, 2017). Textile membrane materials are flexible, cheaper to buy without size limitations, and have better mechanical stability (Chu, *et al.*, 2015) (Zhang and Seeger, 2011). These membrane materials can only be used for a lesser amount of oil-water mixture arising from oil spills and other industrial organic pollutants since it's impractical to discharge all of the oil-water mixtures onto the materials (Liu *et al.*, 2015). Clay membrane materials possess low thermal stability, and they are cheaper to buy than other membrane materials (Yu *et al.*, 2017). However, it takes a longer period to observe separation when using clay materials, which is a problem in oil-water separation (Yu *et al.*, 2017). Glass membrane materials possess low thermal stability and have relatively small pores, which is a problem in oil-water separation due to that high temperature will result in damaging the membrane atomic structure (Fang, 2015) (Kong and Li., 1999). Sediment membrane materials have higher thermal stability but low surface roughness (Fang, 2015) (Kong and Li., 1999). However, they can only be used for a smaller amount of oil-water separation, which is a problem in oil-water separation (Wang*et al.*, 2018).

Ceramic membrane materials have high chemical stability, good mechanical strength and high thermal stability (Xing, 2017) (Rezaei *et al.*, 2011) (Achilli *et al.*, 2009). They have higher fluxes due to their higher porosity and are more hydrophilic when compared to other membranes (Xing, 2017) (Rezaei *et al.*, 2011) (Achilli *et al.*, 2009). Furthermore, they are easy to clean and have a long and reliable lifetime (Le and Nunes, 2016). Ceramic materials have advantages over other materials that are used for wettability. These advantages are high chemical stability, good mechanical strength, high thermal stability, higher fluxes due to their higher porosity (Xing, 2017) (Rezaei *et al.*, 2011) (Achilli *et al.*, 2009). They are easy to clean, they have a long and reliable lifetime are more hydrophilic when compared to other membranes (Rezaei *et al.*, 2011), which is a focus of this study to design a

hydrophilic/oleophobic membrane which will allow more water to flow through the membrane while leaving the oil behind,.

Therefore, these developed technologies are limited in industrial and domestic applications since the membrane may be easily contaminated should a large quantity of oil flow through the membrane. Therefore, there is a great need to develop a hydrophilic/oleophobic ceramic membrane, which allows more water to flow through the membrane while leaving the oil behind, hence being a modified ceramic membrane. The current project focused on designing a ceramic membrane with improved surface properties for the most enhanced efficiency in the oil-water separation.

1.2 Rationale and motivation

Most developed technologies using ceramics for oil-water separation focused on parameters such as surface tension, and they have been based on limited model derivations. Major factor such as "surface energy" has not been considered in detail in model derivations. These developed technologies for oil-water separation are mostly hydrophobic/oleophilic, which means they are "water repellent" and "oil attracting" (Liu *et al.*, 2016) (Ramachandran and Nosonovsky, 2016) (Zhu *et al.*, 2014) (Xu *et al.*, 2012) (Zhang *et al.*, 2012). These technologies result in high fouling capabilities during the separation process and also results in extreme cluster formation during nanoparticle coating on the membrane, and this greatly impacts membrane wettability (Ma *et al.*, 2017) (Le and Nunes, 2016) (Ditsch *et al.*, 2005). Hence, these currently developed technologies have limited industrial and domestic applications, and therefore, it is imperative to do modification of ceramic membrane material surface for wettability. This will be highly beneficial to improve ceramic membrane inefficiencies.

1.3 Problem Statement

Materials used in membrane technology are ceramics, glass, polymers, clay, textiles and sediments (Yu *et al.*, 2017) (Chu, *et al.*, 2015). Glass, polymers, clay, textiles and sediments are inefficient in oil-water separation (Yu *et al.*, 2017) (Chu, *et al.*, 2015). These materials have different wetting properties when coated with nanoparticles due to their different surface roughness (Weston *et al.*, 2015). Polymer membranes possess weak mechanical strength, poor cycling performance and small pore channels (Le and Nunes, 2016) (Ma *et al.*, 2016). Textile membranes possess poor thermal stability. They can only be used to separate a lesser amount of oil-water mixture arising from oil spills and other industrial organic pollutants (Liu *et al.*, 2015). Clay membranes possess low thermal stability and take a longer period to achieve separation (Yu *et al.*, 2017). Glass membranes possess low surface roughness and low thermal stability (Fang, 2015). Sediment membranes have low surface roughness (Fang, 2015). Ceramic materials possess better surface properties over other materials that are used in wettability in that they

have high chemical stability, good mechanical strength and high thermal stability (Xing, 2017) (Rezaei *et al.*, 2011) (Achilli *et al.*, 2009).

The formation of clusters is commonly observed on ceramic membrane material surfaces during nanoparticle coating, and this creates more surface roughness (Cai *et al.*, 2016) (Zhou *et al.*, 2015) (Ferrando*et al.*, 2008), which affects membrane wettability negatively. Most of the researchers overlooked the idea of removing these clusters after nanoparticle coating. However, this has a significant effect on membrane performance. Furthermore, ceramic materials result in membrane fouling and degradation during wettability when used as hydrophobic/oleophilic membranes (Ma *et al.*, 2017) (Le and Nunes, 2016) (Rezaei *et al.*, 2011) (Ditsch *et al.*, 2005). This necessitates a backwashing process to be performed after every filtration run, which is a very difficult process to be performed. It is time-consuming it is hazardous, and, due to that, it might lead to damage of the membrane atomic structure (Padaki *et al.*, 2015). According to Zhu *et al.* (2014), an efficient filtration membrane for oil-water separation should ideally possess hydrophilic/oleophobic surface properties. Although ceramic materials possess better surface properties, there has not been much research carried out on the joint effects of surface properties, cluster formation during nanoparticle coating and coating strategy on the material surface to give the most enhanced wettability properties. In this regard, the project focused on designing a nanostructured ceramic membrane with improved surface properties that led to optimal wettability for oil-water separation.

1.4 Research aims

The main aim of the research was to design a nanostructured ceramic membrane material with more improved surface properties for enhanced wettability to achieve efficient oil-water separation.

1.5 Research objective and specific objectives

The main objective of the current dissertation was to design a modified ceramic membrane material surface using a jet-spray coating to achieve improved wettability for efficient oil-water separation. The specific objectives dealt with were:

1. To investigate the coating strategies used on ceramic membranes and propose the best one to give improved membrane surface properties
2. To model and simulate ceramic membrane surface properties for improved wettability
3. To fabricate the ceramic membrane system
4. To experimentally validate the membrane

1.6 Dissertation Outline

This dissertation is divided into several chapters. Chapter One briefly provides the background of the existing challenges faced by membrane technologies used in the oil-water separation processes. It also explains the one-of-a-kind strategy and methodology utilised to address the current membrane difficulties in membrane technology. Chapter Two discusses the literature review that covers the membrane wettability used in oil-water separation processes, such as the orientation of nanoparticles, nanoparticle scattering effect, nanoparticle clusters, nanoparticle coating techniques, surface roughness and smoothness, membrane surface characterisation and velocity distribution on the membrane surface during coating**.** Chapter Three describes the theoretical model derivation, simulation and manufacturing process of a nanostructured ceramic membrane with a more efficient oil-water separation process. Chapter Four discusses the results obtained during practical modelling and simulation, experimental results and the comparison between the newly developed nanostructured ceramic membrane with the developed nanostructured ceramic membrane from the previous literature. Chapter Five gives the overall conclusion based on the facts obtained in the study. Chapter Six gives the recommendations for future studies.

CHAPTER TWO

LITERATURE REVIEW

2.1 Introduction

The current chapter of this dissertation provides the overall literature review of the membrane technology used in oil-water separation. It broadens the understanding of the current problems faced by membrane separation technology. It leads to a deeper understanding of the current issues with membrane separation technology. Oil-water separation technologies, membrane clusters, nanoparticle coating, coating techniques, membrane fouling, and degradation challenges are all discussed in this chapter. This chapter discusses previous work and the limitations that membrane technologists, scientists, and engineers face. Their accomplishments and contributions are also illustrated. Compared to other researchers' shortcomings and successes, the dissertation's logic and innovation are often illustrated. The new ceramic membrane surface, which has been engineered to provide optimum wettability, is also highlighted and compared to the previous study from other researchers. Material with better wettability and surface properties are a benchmark for experimentation and validation. Different coating techniques used to coat materials have been broadly investigated, and the best one that offers better wettability was selected during modelling. In this research, the membrane surface was characterised for optimal wettability using a new approach of surface energy-driven wettability.

2.2 Oil-water separation technology

Oil-water separation has attracted attention due to the ever-increasing amounts of oily water produced from daily activities in mining and industrial services (Wei *et al.*, 2018) (Ramachandran and Nosonovsky, 2016). Nanotechnology has developed rapidly and led to the material science revolution, offering new possibilities for oil-water separation (Wei *et al.*, 2018). There are unique wettable materials used to separate oil-water mixtures globally (Bai *et al.*, 2019) (Padaki *et al.*, 2015). Membrane materials are made up of nanoparticles on their surfaces (Sob *et al.*, 2020). These materials can either be hydrophilic/oleophobic (allowing water to pass through while rejecting oil) or hydrophobic/oleophilic (allowing oil to pass through while rejecting water) on porous substrates. The effective membrane for oil-water separation is dependent on the size of the membrane pore sizes. Recent studies on membrane wettability revealed that ceramic porous membranes are more promising in membrane wettability if membrane pore sizes can be properly characterised (Sob *et al.*, 2020) (Das *et al*., 2016). This is a critical observation, which is a very important factor during the oil-water separation process (Sob *et al.*, 2020) (Atallah *et al.*, 2017) (Das *et al*., 2016) (Abbasi *et al.*, 2010). It was therefore necessary for this research to use membrane technology to alleviate oil/water separation processes.

2.3 Membrane preparation technology

There is a lot of progress in the industrial production of oil, petroleum refineries, pharmaceutical, medical and mining industries. This has led to the fast increase in the generation of oily wastewater during industrial processes in the form of oil-in-water emulsions, which is commonly reported with concentrations ranging between 50 and 1000 mg/L (Sob *et al.*, 2020) (Kim *et al.*, 2017) (Padaki *et al.*, 2015). The direct disposition of these emulsions to the environment is unsafe for human inhabitants or aquatic life (Garmsiri *et al.*, 2017). The particle sizes of oil droplets in oil-water mixtures, which are stable, can be smaller than 20 μm. It is very difficult to separate the oil-water mixture using the gravitational method and other methods (Zhu *et al.*, 2013) (Zhou *et al.*, 2010). There is a range of membrane technology used in oil-water separation. These include gravity sedimentation, centrifugation, electrolytic separation, adsorption separation, biodegradation, coagulation method, flocculation method, air flotation method, chemical de-emulsification method, ultrasonic separation method, and membrane filtration method (Sob *et al.*, 2020) (Sob *et al.*, 2019) (Wang *et al.*, 2018) (Munirasu *et al.*, 2016) (Padaki *et al.*, 2015) (Zhu *et al.*, 2013) (Zhou *et al.*, 2010).

2.4 Materials used to design membrane surface in membrane technology

There are many materials used in membrane wettability design for oil-water separation (Wang *et al.*, 2018). Some of these materials are glass, ceramics, polymers, clay, textiles and sediments (Yu *et al.*, 2017) (Chu *et al.*, 2015). These membrane materials have different wetting properties when coated with hydrophobic/oleophilic and oleophobic/hydrophilic nanoparticles due to their different surface properties, impacting membrane wettability (Weston *et al.*, 2015).

Polymer membranes possess weak mechanical strength, poor cycling performance and small pore channels (Le and Nunes, 2016) (Ma *et al.*, 2016). These membranes are only used for low energy requirements, and they are unable to separate volatile compounds and have a tendency to foul more quickly (Padaki *et al.*, 2015). Textile membranes possess poor thermal stability, and they can only be used for a lesser amount of oil-water mixture arising from oil spills and other industrial organic pollutants (Liu *et al.*, 2015). Clay membranes possess low thermal stability and take a longer period to achieve separation (Yu *et al.*, 2017). Glass membranes possess low surface roughness and low thermal stability (Fang, 2015). Sediment membranes have low surface roughness and high thermal stability (Sob *et al.*, 2020) (Fang, 2015). Some of these materials also suffer from corrosion and thermal instability, increasing membrane fouling and degradation during wettability (Le and Nunes, 2016).

2.5 Ceramic Materials used in membrane technology

Ceramic membranes are used for microfiltration (MF) and ultrafiltration (UF) processes. Ceramic membrane materials possess high thermal stability, high chemical stability, high mechanical and pressure resistance (Sob *et al.*, 2020) (Ben Ali *et al.*, 2018) (Xing, 2017) (Abbasi *et al.*, 2010) (Achilli *et al.*, 2009) (Wang *et al.*, 2009) (Riley, 2000). They also possess higher flux capability due to their higher porosity (Rezaei *et al.*, 2011). They offer resistance to mechanical, thermal and chemical stresses, and as a result, this allows a better membrane performance (Rezaei *et al.*, 2011). They are easy to clean and have a long and reliable lifetime (Le and Nunes, 2016). These membranes offer poor stability under severe conditions (Chen *et al*., 2016). They are brittle and require careful handling. They possess more surface roughness, which affects membrane wettability (Rezaei *et al.*, 2011). When used as hydrophobic membranes, ceramic membrane materials offer less sealing due to their different thermal expansion (Chen *et al*., 2016). This is a serious problem as oil-water separation's efficiency, stability, and controllability are poor (Sob *et al.*, 2020) (Long *et al.*, 2016). However, different parameters greatly affect the permeation and separability during oil-water separation, such as trans-membrane pressure (TMP), cross-flow velocity (CFV), oil concentration in the feed and different methods of membrane cleaning through a measure of average permeate flux, oil removal efficiency and also the total concentration of organic compounds (Ebrahimi *et al.*, 2010).

The wettability of the ceramic membrane can be optimised by adjusting the membrane pore size distribution during wettability (Sob *et al.*, 2020) (Das *et al.*, 2016). This is a critical observation, which is a very important factor during the oil-water separation process (Sob *et al.*, 2020) (Atallah *et al.*, 2017) (Das *et al.*, 2016) (Abbasi *et al.*, 2010). Therefore, as earlier indicated, the optimal coating force gives optimal coating pressure, optimal coating distance, and optimal coating angle, which offer optimal membrane wettability during oil-water separation. This problem has been solved in this current dissertation since the membrane surface properties have been adequately characterised to achieve optimal membrane wettability during nanoparticle coating. Over the past years, there have been several studies on ceramic membranes to effectively increase membrane permeate flux by studying the layer of the wettable membrane (Sob *et al.*, 2020) (Gu *et al.*, 2016) (Ren *et al.*, 2015) (Tuyen *et al.*, 2009). Research reports ceramic membranes as having produced highly hydrophilic membrane surfaces owing to the intrinsic hydrophilicity of Si3N4. Recent studies on membrane wettability revealed that ceramics porous membranes are more promising in membrane wettability if membrane pore sizes can be properly characterised. Ceramics offer better wettability as compared to other materials (Le and Nunes, 2016) (Chen *et al*., 2016) (Padaki *et al.*, 2015) (Rezaei *et al.*, 2011) (Achilli *et al.*, 2009). Hence it was recommended for use in this current research.

2.5.1 Types of Ceramic Materials used in membrane technology

Types of ceramic materials that are used in wettability are alumina (Al_2O_3), zirconia (ZrO_2), and titanium dioxide (TiO_2) (Sob *et al.*, 2020) (Atallah *et al.*, 2017) (Xing, 2017) (Suresh *et al.*, 2017) (Das *et al.*, 2016) (Masuda *et al.*, 2015) (Padaki *et al.*, 2015) (Abbasi *et al.*, 2010). The other type of ceramic membrane material that is used in wettability is the mullite–alumina ceramic membrane (Abbasi *et al.*, 2010). This ceramic membrane has very high chemical and thermal stability and is very cheap. It can be prepared by extruding and calcining kaolin clay. Kaolin is cheap; it provides low plasticity and high refractory properties (quartz), which contributes to mechanical and thermal stability (Chen *et al*., 2016). It possesses good chemical properties (carbonates), which provide porous texture, sodium carbonate and boric acid, which improves dispersion properties, thereby creating homogeneity and sodium metasilicate, which brings higher mechanical strength to the membrane (Emani *et al.*, 2014) (Mittal *et al.*, 2011) (Abbasi *et al.*, 2010). This membrane is mainly used in microfiltration (MF) processes (Abbasi *et al.*, 2010). The preparation of ceramic membranes with excellent surface characteristics is still a challenge for treating a large volume of oil-water mixtures (Kumar. *et al.* 2015). There are significant literature surveys on another type of ceramic materials used in membrane wettability such as silicon nitride (Si3N4) porous ceramic membranes and solid solutions (-SiAlON) (Sob *et al.*, 2020) . These ceramics materials possess high strength, fracture toughness, thermal stability, and chemical stability (Sob *et al.*, 2020) (Riley, 2000). There is also an added advantage of interwoven rod in Si3N4 crystals, which offer a high membrane ratio of length/diameter in the membrane pores with a smaller pore size distribution, which improved membrane pore sizes and wettability. Therefore, ceramic materials are more suitable and possess better membrane wettability (Sob *et al.*, 2020).

Another advantage of Ceramics Si3N4 is that it is nontoxic and helpful in maintaining the natural environment (Sob *et al.*, 2020) (Neumann *et al.*, 2004) (Dion *et al.*, 1994), which is very important. Research report revealed Si3N4 hollow-fibre ceramic membranes produced by combined phase-inversion method and sintering gave an excellent permeate flux and ultrahigh salt rejection during wettability (Sob *et al.*, 2020) (Zhang *et al.*, 2013) (Zhang *et al.*, 2012). A synthesised study by Wang Jun-wei et al. (2018) on SiAlON planar ceramic membranes, which had a similar structure to Si3N4, revealed good performance in membrane distillation during experimentation (Sob *et al.*, 2020) (Wang *et al.*, 2018) (Wang *et al.*, 2016). However, the experimentation processon_-Si3N4 was expensive based on raw material (Si3N4 powder) acquisition and the high sintering temperature (1700 ^{O}C) required. The reaction bonded and sintered Si3N4 (SRBSN) ceramics are very popular today due to their lower production cost and their reaction takes place at a lower temperature (~1300 ^{o}C).

2.5.1.1 Alfa-AL2O3 (α-AL2O3) ceramic membrane used in oil-water separation

This ceramic membrane material is chemically inert and is the most commonly used type of ceramic for wettability (Rezaei *et al.*, 2011). This membrane is used as a hydrophobic membrane in microfiltration (MF) for the treatment of oil-water separation. It results in efficient separation of oil, but it also results in extreme fouling formation observed during each MF run. This requires the process to stop and perform backwashing in intervals. Backwashing is typically done after every 90 minutes of every MF run to improve membrane performance for the next MF run. The backwashing process is used to remove oil droplets and particles that block the membrane surface pores (Padaki *et al.*, 2015) (Rezaei *et al.*, 2011). Backwashing in ceramic membranes is highly hazardous and difficult to process, and it might damage the membrane surface atomic structure (Padaki *et al.*, 2015) (Rezaei *et al.*, 2011). Membrane fouling remains a technical challenge in the oil-water separation industries (Wei *et al.*, 2018) (Padaki *et al.*, 2015). It should be noted that hydrophobic-oleophilic membranes are easily fouled by oils as opposed to hydrophilic-oleophobic membranes (Ma *et al.*, 2017) (Song *et al.*, 2015)..

2.5.1.2 Polymeric-ceramic composite membrane used in oil-water separation

Polymer-modified ceramic membranes have recently drawn much interest due to their excellent thermal, chemical stability, and fouling resistance (Chu *et al.*, 2005). These composite membranes are used mainly in UF as a hydrophilic membrane for the treatment of oily-water emulsion (Yu *et al.*, 2017) (Chu *et al.*, 2005); hence the change of membrane surface hydrophilicity had to be studied. Many researchers have used dip coating methods to prepare ceramic-polymeric membranes (Mittal *et al.*, 2011). Ceramic-polymeric composite membrane retains oil "droplets", resulting in cake formation / thick oil layer over the membrane surface. This cake formation is fouling. Mueller *et al.* (1997) reported similar results for oil-water emulsion separation with ceramic-polymeric composite membrane. The thick oil layer/fouling formation over the membrane surface affects membrane permeation as the flux declination increases (Zhu *et al.*, 2014). Fouling increases surface roughness, affecting membrane performance (Zhu *et al.*, 2014) (Zhong*et al.*, 2013). This type of ceramic membrane results in efficient oil-water separation, but it can only be used for lower concentrations of oil from oil-water mixtures (Mittal *et al.*, 2011); hence it was not recommended for use in this research.

2.5.1.3 Mullite and mullite–alumina ceramic membranes used in oil-water separation

These ceramic membranes are very cheap because they are prepared by extruding and calcining kaolin clay (Abbasi *et al.*, 2010). This membrane is used as a hydrophobic membrane in microfiltration (MF) for the treatment of oil-water separation. Oil rejection of the mullite ceramic membranes was found to be more than 94% for the synthetic oily wastewater and 84% for the real wastewater (Emani *et al.*, 2014) (Abbasi *et al.*, 2010). It was observed that permeation flux (PF) increases with increasing volumetric

flow rate (Q), temperature (T), pressure (P) and alumina content of the mullite–alumina membranes. It results in mild fouling formation during each MF run due to increasing volumetric flow rate and temperature on the membrane, reducing permeation flux (PF) significantly. Due to fouling, the process requires more pumping power to achieve the required high flow rates, and this is not economically feasible (Padaki *et al.*, 2015) (Rezaei *et al.*, 2011) (Abbasi *et al.*, 2010). After each MF run, membrane cleaning is required to remove fouling to improve surface permeability. The fouling problem is generally observed on all ceramic membranes and can be resolved by cleaning the membrane using a backwashing method after every MF run. As reported by Padaki *et al.* (2015) and Rezaei *et al.* (2011), backwashing is extremely hazardous and very difficult to process and, in most cases, it leads to damaging the membrane surface morphological and topological structures. Although this membrane results in fouling during oil-water separation, it has advantages over other ceramic membranes. It is very cheap, it is easy to prepare and it offers high mechanical strength, high thermal stability and high chemical stability (Chen *et al*., 2016) (Le and Nunes, 2016) (Abbasi *et al.*, 2010) (Achilli *et al.*, 2009).

2.5.2 Ceramic Membranes pore sizes

The pore sizes of ceramic membranes are used in most popular oil/water separation technologies to selectively enable materials of some size (nano-scale) to move through the membranes while maintaining other materials of large scale (Sob *et al.*, 2020) (L. H. Chen *et al.*, 2018). These membrane materials have small pore channels; therefore, they require high pressure to maintain the permeate flux, and this can be energy-intensive (L. H. Chen *et al.*, 2018) (Ma *et al.*, 2016). Therefore, it is imperative to include careful characterisation of nanoparticle coating and membrane pore sizes in the design of this membrane. For an effective and reliable oil/water separation process, membranes with customised selectivity and pore sizes are needed (Sob *et al.*, 2020) (Sob *et al.*, 2019) (Le and Nunes, 2016) (Ma *et al.*, 2016). Separation membranes with these capabilities have been reported to have low porosity and poor membrane permeation channels, resulting in severe membrane fouling and degradation (Sob *et al.*, 2020) (Peng *et al.*, 2016). In the process of oil/water separation, the membrane surface poorly separates oil and water mixtures, which leads to a fast decline in performance during the separation process (Sob *et al.*, 2020) (Si *et al.*, 2015). These technologies are costly, as they usually require the use of additional energy during operation (Sob *et al.*, 2020). Furthermore, their preparations and applications are very complex and complicated (Sob *et al.*, 2020) (Peng *et al.*, 2016). There is therefore a great need to come up with a separation technology that is low cost, low consumption of energy and easy to handle.

2.6 Liquid-liquid displacement porosimetry

In membranes with limited pore sizes, the liquid-liquid porosimetry (LLDP) approach is commonly used to provide information on pore size distribution (Sob *et al.*, 2020) (Wang *et al.*, 2018) (Peng *et al.*, 2016). By using similarity between the pressures added in the device and the membrane pore size radius open to the membrane flux, the LLPD is based on the concepts of air-liquid displacement or the process of extended bubble point technique., which is given by (Wang *et al.*, 2018) (Peng *et al.*, 2016). This technique is promising since it evaluates the active pores in the nano-scale and sub-nanometer during membrane wettability (Wang *et al.*, 2018) (Peng *et al.*, 2016). Additionally, it is used to study membrane pore size distribution in ultrafiltration (UF) and nanofiltration (NF) membrane systems due to their relatively low applied pressures in the system, which does not cause membrane compaction during wettability. Some studies on polymeric membranes having pore sizes from 0.4 μm to 8 nm have been reported to be useful in the LLDP method during the membrane optimisation process.

This system uses pairs of immiscible liquids with low interfacial tension since the membrane pore sizes can be measured at relatively low pressures. The method consists of filling the membrane surface with the relevant wetting liquid, and the liquid is then allowed to be displaced. Membrane pressure drop has been monitored through the membrane rate of flow of oil and water, and the corresponding membrane pore radius, which opens at a given applied pressure, can be calculated using the Cantor equation. During the experiment, the trans-membrane pressure is increased, and the corresponding membrane pore radius and flow rate are obtained. The membrane pore size distributions of the membrane permeability are determined. This thesis uses the Hagen-Poiseuille equation by considering the cylindrical pores, volume flow, and membrane number of pore sizes during wettability.

2.7 Oil-Water Separation Challenges experienced in Membrane Technology

The current developed technologies with special surface wettable properties are ineffective in the oil-water separation process (Sob *et al.*, 2020) (Ramachandran and Nosonovsky, 2016) (Peng *et al.*, 2016) (Cheng *et al.*, 2013) (Zhang *et al.*, 2012) (Yang *et al.*, 2006). The developed technologies on wettability have revealed conflicting wettable surfaces. Studies on wettable nanostructured surfaces have been conducted with deposited mixtures, while emulsion research has been limited (Solomon *et al.*, 2014). Several studies have revealed the major issue of the formation of clusters which is commonly observed on ceramic membrane material surfaces during nanoparticle coating, and this creates more surface roughness (Sob *et al.*, 2020) (Sob *et al.*, 2019) (Cai *et al.*, 2016) (Zhou *et al.*, 2015) (Ferrando *et al.*, 2008) (Ditsch *et al.*, 2005) which affect membrane wettability negatively. Most of the researchers overlooked the idea of removing these clusters after nanoparticle coating. However, this has a significant

effect on the membrane performance. A little attention has been paid identifying the best coating strategy on material surface to combat the formation of these clusters, which is the focus of this dissertation.

Furthermore, ceramic materials result in membrane fouling and degradation during wettability when used as hydrophobic/oleophilic membranes (Le and Nunes, 2016) (Chu *et al.*, 2005). This then necessitates a backwashing process to be performed after every filtration run, which is a very difficult process to be performed. It is expensive, time-consuming, hazardous, and hazardous, which might lead to damage of the atomic membrane structure (Padaki *et al.*, 2015).

This dissertation focused on surface energy-driven separability, suitable membrane characterisation of the pore size network, the best nanoparticle-coating on the membranes, and the suitable material selected for nanoparticle-coating so as to design a wettable membrane that is efficient and sustainable in the oil-water separation process.

2.8 Membrane fouling and degradation experienced on the membrane surface during oil-water separation

Membrane fouling and degradation has been one of the biggest challenges in mostly hydrophobic membranes. Membrane fouling happens when particles seal off the membrane pores and prevent the flow of liquid during wettability. The filters or membranes used face drawbacks of poor membrane permeability, membrane capacity, or both (Sob *et al.*, 2020). The membrane capacity of these technologies defines the amount of fluid per membrane area before membrane fouling, or degradation is reported (Sob *et al.*, 2020) (Radjenović *et al.*, 2008). The membrane capacity also defines the trans-membrane pressure drop or pressure as the amount of fluid per membrane area during wettability (Sob *et al.*, 2020) (Radjenović *et al.*, 2008). There is also intermediate blocking, which is similar to complete blocking during membrane wettability. A portion of particles usually block the membrane pore, and there is usually an accumulation of particles being deposited (Sob *et al.*, 2020) (Radjenović *et al.*, 2008). Another membrane fouling called cake filtration is reported during wettability when particles usually accumulate on the surface of the wettable membrane. There is a porous cake of increasing thickness that, during membrane wettability, prevents the flow of fluids. Such fouling cannot occur in this study's newly proposed membrane technology. When it comes to modelling processes, it is assumed that all fouls which enter a membrane pore are deposited and accumulated uniformly with axial position during membrane wettability (Sob *et al.*, 2020). Therefore, membrane modelling is usually predicted by membrane capacity independent of membrane flow rate during wettability (Sob *et al.*, 2020). This explains that models are individually used singly or in combination to discuss experimental results obtained during membrane wettability. Similarly, other researchers discovered that data for the fouling of micro-porous track-etched membranes could be fitted initially into either a standard or complete

model and subsequently, by the cake model (Sob *et al.*, 2020) (Radjenović *et al.*, 2008). Most empirical models assume that membrane fouling and degradation are proportional to the volume filtered but not to the filtration rate (Sob *et al.*, 2020).

An efficient filtration membrane for oil-water separation should ideally possess hydrophilic/oleophobic surface properties. These membranes allow more water to flow through the membrane while leaving the oil behind, which results in improved fouling (Zhu *et al.*, 2014) (Mittal *et al.*, 2011). Rougher surfaces in ceramic materials are reported to be easily fouled by oils compared to smoother surfaces (Zhong *et al*., 2013). Fig.2.1 shows the principle of membrane fouling under different surface properties. Oil droplets typically accumulate in the deep valleys of the rough membranes, thus forming a cake/fouling layer on the membrane surface. However, this causes severe flux decline in the rough surface rather than in the smooth surface during oil-water separation (Zhong *et al*., 2013) (Kubiak *et al.*, 2011) (Miwa *et al.*, 2000). Ceramic membranes that possess smoother surfaces are reported to have more enhanced wettability than those that possess rougher surfaces (Kubiak *et al.*, 2011) (Miwa *et al*., 2000). This is based on the lotus scientific effect (Ge *et al.*, 2019) (Kubiak *et al.*, 2011) (Miwa *et al.*, 2000). As a result, these study limitations must be addressed by creating membranes with suitable wettable surfaces that are effective in the oil-water separation process.

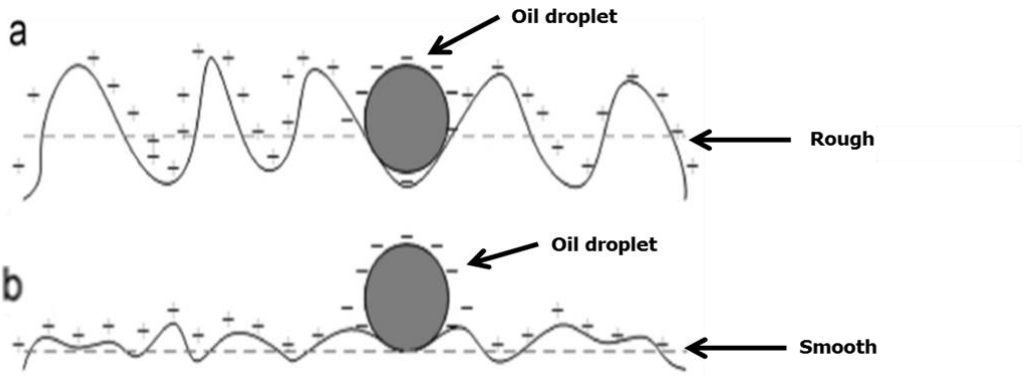

Figure. 2.1 Schematic diagram showing membrane fouling under different surface properties: (a) rough membrane; (b) smooth membrane (Zhong et al., 2013).

Some researchers reported a decline in flux during membrane wettability leading to fouling of micro-porous track-etched membranes (Sob *et al.*, 2020) (Zhong *et al*., 2013) (Radjenović *et al.*, 2008). It was, however, observed that it did not follow the trend of any of the individual fouling models used during membrane wettability, and membrane fouling was reported to occur through a combination of complete blocking. Most studies on membrane fouling and degradation showed the effects of complete membrane blockage and caking fouling mechanisms within the medical industries (Sob *et al.*, 2020) (Radjenović

et al., 2008). Pre-filtration processes were used, and persistent membrane fouling was reported (Sob *et al.*, 2020) (Radjenović *et al.*, 2008). It was also reported that while previously derived models on membrane wettability are used, there are still several membrane inefficiencies during wettability.

The common strategy used to combat fouling is to design the membranes to be hydrophilic by either (a) hydrophilically modifying the ceramic membrane by using polymers-based composite membranes; (b) by blending ceramic membrane with hydrophilic agents during manufacturing; and (c) grafting or (d) coating hydrophilic polymers on the ceramic membrane surface (Sob *et al.*, 2020) (Zhou *et al.*, 2013). It is also reported that membrane fouling can be minimised or reduced by narrowing the pore size or even blocking the pores of the microfiltration (MF) and ultrafiltration (UF) microporous membrane surfaces (Sob *et al.*, 2020). Most often, the pore size enlarges, thus reducing salt rejection. As equally reported, many coating layers have inadequate mechanical and chemical properties that do not sustain long-term operations (Sob *et al.*, 2020). The model derived in this study assumes the forces of nanoparticles, the force of water, a force of walls, the force of viscosity, and all other external forces during membrane wettability. The membrane pore sizes were characterised, and the coating of the nanoparticles on the membrane pore sizes was also characterised to get the optimal membrane wettability with increasing membrane resistance.

2.9 Microfiltration (MF) and Ultrafiltration (UF) used in oil-water separation

MF and UF are very popular in the process of oil-water separation (Sob *et al.*, 2020) (Le and Nunes, 2016) (Ma *et al.*, 2016). These technologies have been reported to suffer from fouling and cost factors (Sob *et al.*, 2020). This is because membranes used in MF and UF are mostly hydrophobic and are based on the size of contaminants. These technologies filter particles within the size range of (100–1000 nm). Materials used for the fabrication of MF and UF are ceramics and polymers (Sob *et al.*, 2020) (Wu *et al.*, 2015) (Si *et al.*, 2015). These materials give different wetting properties when coated with nanoparticles due to their different surface properties (Weston *et al.*, 2015). Ceramics have advantages over polymers because they possess high thermal resistance, high chemical stability, and good mechanical strength.

Ceramics are also good since they offer better cleaning conditions and a long and reliable lifetime. The main disadvantage of ceramics is that they are quite expensive and very difficult to fabricate in sufficient quantities due to their brittleness. Ceramics also possess a great weakness of sealing pores when integrating in modules and cause major problems with inefficient filtration processes. The most common commercial polymers used for MF and UF membranes are polyethersulfone (PES), polyvinylide fluoride (PVDF), polyethylene (PE), polypropylene (PP), and polytetrafluoroethylene (PTFE). These materials have weak mechanical strength and poor cycling performance (Le and Nunes, 2016) (Ma *et al.*, 2016). As a result, frequent cleaning and replacement of polymeric membranes may be required in

between filtration processes (Ma *et al.*, 2016). These membranes are only used for low energy requirements. They are unable to separate volatile compounds and have the tendency to foul more quickly (Padaki *et al.*, 2015), which results in flux decline and rejection due to deterioration, particularly when treating oily wastewater. These membrane materials have small pore channels. Therefore, they require high pressure to maintain the permeate flux, which can be energy-intensive (Ma *et al.*, 2016). All the listed polymers are hydrophobic except PES. It should also be noted that PE, PP and PTFE are insoluble in organic solvents, specifically at room temperature, thereby making the manufacturing process very difficult. Most porous membranes used are based on PP and PTFE designs usually produced by mechanical stretching of extruded films.

2.10 Nanofiltration (NF) used in oil-water separation

This filtration is said to have better performance than other filtration designs used in oil/water separation. The membrane formation technologies based on nanoparticles exhibit high flux that prevents membrane fouling (Sob *et al.*, 2020) (Peng *et al.*, 2016) (Liu *et al.*, 2015). The manufacturing method is NIPS, which produces integrated porous asymmetric membrane selective layers at the top or a non-selective porous structure used as substrates for multi-layered membrane preparation. The main polymeric materials for NF are PES, PVDF, and polyacrylonitrile (PAN). Another cross-linked polymer constitutes the deposition of the selective layer, and the coating is performed by dip-coating or interfacial polymerisation (Sob *et al.*, 2020) (Peng *et al.*, 2016) (Liu *et al.*, 2015). Surface coatings are usually modified incorporating nanoparticles and grafting polymerisation that helps to reduce selectivity or membrane blockage (Sob *et al.*, 2020) (Peng *et al.*, 2016) (Liu *et al.*, 2015). This is achieved through an interfacial polymerisation technique: poly-condensation of water-soluble and organic-soluble monomers, usually on a porous support system to produce thin-film composite (TFC) membranes. This technique is quite simple and easy to apply, capable of creating a very thin selective layer of less than 100 nm and based on the polyamides. This thin layer determines the membrane overall efficiency during the wettability process. More efforts to improve NF performance during wettability include influencing the selective layer by changing monomers and adding additives into the aqueous or organic solutions during the experiment or by modifying the surface of the formed polyamide layer being used during experimentation.

It should be noted that the incorporation of nanoparticles into the selective layer during polymerisation has been previously studied to form thin-film nanocomposite (TFN) for proper wettability (Sob *et al.*, 2020) (Liu *et al.*, 2015) (Cheng *et al.*, 2015). Therefore, TFN membranes are being considered benchmarks in the field of NF for the aqueous separations process. However, grafting polymerisation via UV/photo-grafting electron beam irradiation plasma treatment and other researchers have extensively studied layer-by-layer (L-b-L) methods to produce nanofiltration (NF) membranes with high hydrophilic properties and low fouling during the membrane wettability process.

These methods are well developed under laboratory conditions, but their application is very limited. Although membranes that offer high performance and proper selectivity to salt are available, membranes with tailored selectivity and pore sizes are needed for an efficient and stable oil/water separation process. More so, the use of NF membranes is also rapidly growing for different applications. In this research, a new class of resistant porous membrane networks and selective layers are being developed with a stable and efficient oil/water separation process using sediment materials coated with nanoparticles for hydrophilicity, which lower the surface energy of water through the membrane pore sizes.

2.11 Coating strategies used in wettability

Several techniques are used to coat materials to possess hydrophilic/oleophobic and hydrophobic/oleophilic properties. Such techniques are suspension plasma spray, dip coating, spin coating, electrochemical deposition method, phase inversion technique and jet-spray coating (Sob *et al.*, 2020) (Balzarotti *et al*., 2019) (Chen *et al.*, 2018) (Shahien and Suzuki, 2017) (Cai *et al.*, 2016) (Xu *et al.*, 2012). These coating techniques offer different responses to wettability (Sob *et al.*, 2020) (Kubiak *et al.*, 2011). Different coating techniques give different effects on flow rate depending on the variety of materials used for nanoparticle coating and the methods used to characterise these nanoparticle coating techniques (Sob *et al.*, 2020) (Zheng *et al.*, 2015). In this research, the membrane surface was characterised for optimal wettability using a new approach of surface energy-driven wettability.

2.11.1 Suspension plasma spraying technique

Suspension plasma spraying is a type of coating method widely used to coat the membrane surface with nanoparticles. This process has the high-speed capability with high deposition rates with the capability of coating complex shapes, and it is relatively low in cost (Shahien and Suzuki, 2017) (Cai *et al.*, 2016) (Fauchais and Vardelle, 2011). The process is based on supplying the feedstock powder material into a very high-temperature plasma jet that is rapidly heated and accelerated with its high-velocity flow. Fig.2.2 demonstrates the suspension plasma spraying system. The advantage of using this method is that it is possible to deposit different ceramic coatings at low power (27kw) with only argon gas as plasma gas. This technique makes it easy to vary operating parameters such as plasma flow rate and electric power inlet. However, this method is very expensive since it requires only argon as plasma gas. The particles collide on the substrate surface and quickly solidify to form a coat during coating, and this causes cracks in the pores. To overcome the above-mentioned challenges, it is recommended to spray nano-sized powders on the affected substrate (Shahien and Suzuki, 2017).

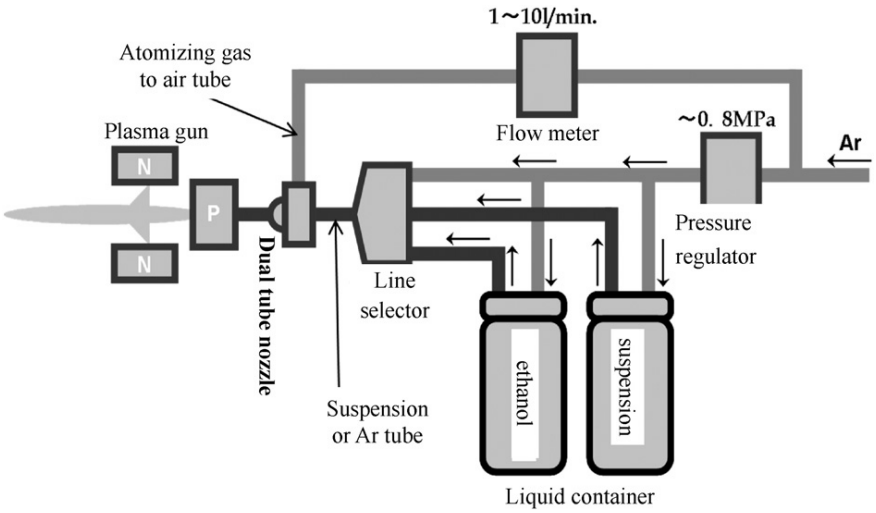

Figure. 2.2 Schematic diagrams of the suspension plasma spraying system (Shahien and Suzuki, 2017).

2.11.2 Dip coating technique

Dip coating is preferred for complex geometry membranes (Balzarotti *et al*., 2019) (Xu *et al.*, 2012). Such membranes have closely spaced struts which can prompt capillary forces. However, this results in channel/cell clogging. To avoid this, an air jet is used to maintain coating thickness. In some cases, there are drawbacks introduced using gas blowing to control wash coat thickness. Fig.2.3 demonstrates the flow chart resume of the dip-coating method. According to Balzarotti et al. (2019), this method results in liquid entrainment. For this reason, the spin coating technique has been used to remove the entrained liquid (Balzarotti *et al*., 2019). Dip coating technique results in random surface coverage and incomplete coverage (Balzarotti *et al*., 2019) (Xu *et al.*, 2012).

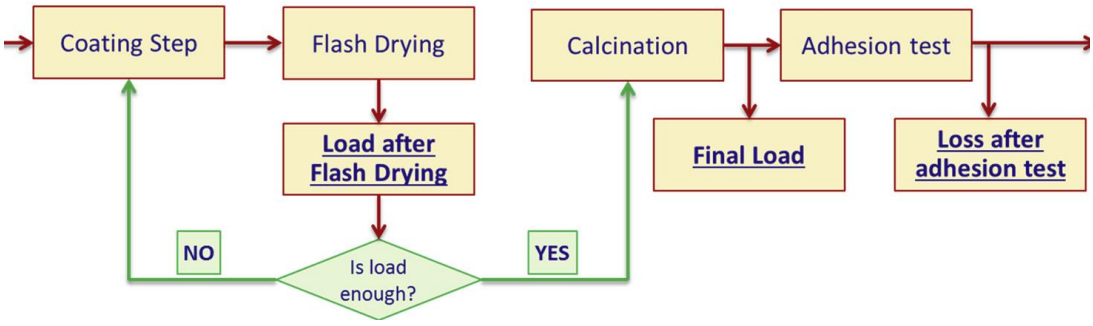

Figure. 2.3 Schematic diagram of the dip coating system (Balzarotti et al., 2019).

2.11.3 Spin coating technique

The spin coating technique is well-known in many industrial sectors for flat coating surfaces (Balzarotti *et al*., 2019). In this process, a coating solution is dropped on a vacuum pump, normally on a fixed rotational speed of 400 to 1200 rpm for a certain spinning time (from 30 s to 10 min), see Fig.2.4. Spin coating is only limited to coat flat substrates and not complex substrates (Balzarotti *et al*., 2019). Unfortunately, most of the spin coating literature has been devoted to flat substrates coating investigation. Only a few publications concerning the coating of complex substrates exist (Balzarotti *et al*., 2019). None of these papers provides a comprehensive explanation of the use of the spin-coating technique (Balzarotti *et al*., 2019).

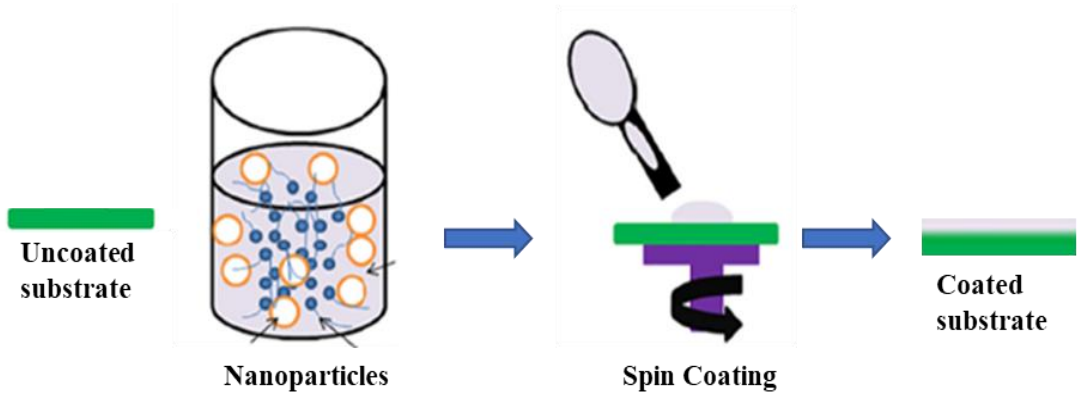

Figure. 2.4 Schematic diagram of the spin-coating technique (Meena *et al.*, 2019).

2.11.4 Jet-spray coating technique

Coating strategies used on ceramic membranes were investigated to propose the best one to give improved membrane surface properties. Jet-spray coating technique is a type of coating technology that is used to fabricate appropriate porous ceramic membranes used in microfiltration (MF), ultrafiltration (UF) and nanofiltration (NF) processes (Chen *et al.*, 2018). Fig.2.5 demonstrates the jet-spray system.

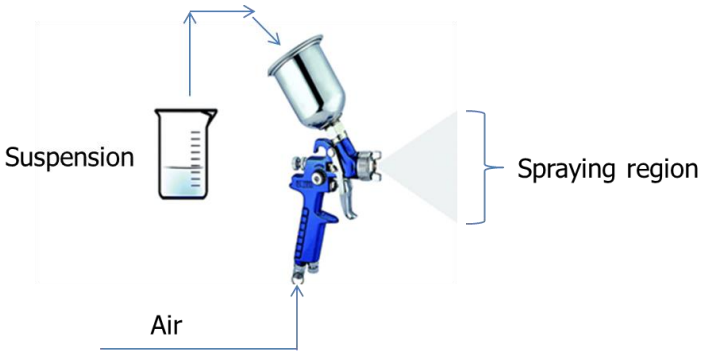

Figure. 2.5 Schematic diagram of the jet-spray system.

The process is based on spraying the ceramic membrane with nanoparticle suspension a very high pressure and temperature. From the previous literature, the jet-spray coating has been reported to be effective in reducing the penetration of membrane-forming particles in ceramic coating (Chen *et al.*, 2018). The jet-spray coating incorporates the following parameters: coating pressure, coating distance, and coating angle (Chen *et al.*, 2018). These were major parameters used in model derivation in this current study. Jet-spray coating gives different clustering on the membrane surface as compared to other coating strategies (Sob*et al.*, 2019) (Chen *et al.*, 2018) (Gestel *et al.*, 2008). This is due to the fact that it offers a better scattering effect of nanoparticles on the membrane surface during coating; hence it was proposed as the best coating strategy for use in this current study.

2.12 The model of surface energy used in membrane wettability against surface tension driven separability

The importance of surface energy and surface tension in particle separation has been confirmed (Sob *et al.*, 2020) (Peng *et al.*, 2016) (Liu *et al.*, 2015) (Cheng *et al.*, 2015) (Khan, 2015) (Ke *et al.*, 2014) (Zhou *et al.*, 2013). Surface tension-driven separability has received a lot of attention from researchers, but surface energy-driven separability has not received a lot of attention (Sob *et al.*, 2020) (Liu *et al.*, 2016) (Ramachandran and Nosonovsky, 2016) (Solomon *et al.*, 2014) (Cheng *et al.*, 2013). Several models on wettability studies have been derived or from the traditional Young's models (Peng *et al.*, 2016) (Liu *et al.*, 2015) (Cheng *et al.*, 2015) (Khan, 2015) (Ke *et al.*, 2014) (Zhou *et al.*, 2013). Most of the Young-modified models centred on surface tension-driven separability, with only a few experiments on surface energy-driven separability, which could have more wetting-molecule parameters. Surface energy is defined as the work performed per unit area where Surface tension is the force on the surface of the liquid that prevents the liquid from flowing (Sob *et al.*, 2020) (Zhou *et al.*, 2013). This does not include the area over which the fluid will flow if needed, which is considered by surface energy (Sob *et al.*, 2020). As a result, surface tension primarily quantifies a solid surface's wetting properties, which are determined by the values of forces at the contact point and the contact angles between molecules (oil or

water) and the surface (Peng *et al.*, 2016) (Liu *et al.*, 2015) (Cheng *et al.*, 2015) (Khan, 2015) (Ke *et al.*, 2014). Surface energy deals with the work (force and the displacement) required for liquids to move across the membrane pores/channels. As a result, surface energy considers the surface area of the membrane surface over which the particles are separated. Therefore, the work done by nanoparticles on the membrane surface i.e. the force of viscosity, force of nanoparticles, frictional resistance force during wettability studies should impact membrane wettability which can be observed during surface energy-driven separability study and these are overlooked in surface tension driven separability.

This dissertation aims to design a membrane with a stable and more efficient oil-water separation process. The membrane characteristics that influence the properties or surface energy arise from the random nature of the membrane constituent structures, such as random nanoparticle size, random surface pore morphology and random spatial distribution of membrane pores. Therefore, it is essential to employ the tools of stochastic theory to study those characteristics and the impacts on surface energy, which is the approach adopted in this dissertation.

2.13 The stochastic effect of nanoparticles size, morphology, spatial distribution on flow rate through a nanostructured membrane surface

Membrane technologies offer different flow rates during wettability because of random nanoparticles on the solid membrane surface. Different membrane pore size characterization and different characterization of membrane coating have a different impact on membrane wettability (Gao and Yan, 2012). These bring into mind, the nanoparticles' random nature, size, morphology, and spatial distribution that impact wettability. Different membrane pore size characterization and membrane coating techniques offer different membrane flow rate performance (Sob *et al.*, 2020) (Sob*et al.*, 2019) (Ten Brink *et al.*, 2015) (Gao and Yan, 2012) (Tuteja *et al.*, 2008).

Most results revealed poor membrane wettability due to poor membrane design (Sob *et al.*, 2020) (Ten Brink *et al.*, 2015) (Gao and Yan, 2012) (Tuteja *et al.*, 2008). Several investigations have been carried out on factors that affect the flow of water in a membrane surface during oil-water separation (Sob *et al.*, 2020) (Ten Brink *et al.*, 2015) (Gao and Yan, 2012) (Tuteja *et al.*, 2008). The flow rate through a membrane during oil-water separation is influenced by membrane pores/channels, the spatial distribution of membrane pores/channels and the morphology of coated nanoparticles in the membrane channels/pores, according to most studies (Sob *et al.*, 2020) (Ten Brink *et al.*, 2015) (Gao and Yan, 2012) (Tuteja *et al.*, 2008). The stochastic effect of nanoparticles scattering, the morphology of nanoparticles in the membrane pores, and the spatial distribution of the membrane pores due to their orientation and their impact on wettability have not been investigated in detail (Sob *et al.*, 2020) (Ten Brink *et al.*, 2015) (Gao and Yan, 2012) (Tuteja *et al.*, 2008). Most of the models used for surface tension

and surface energy in wettability don't reflect the relevant stochastic nature of nanoparticles (Sob *et al.*, 2020) (Ten Brink *et al.*, 2015) (Gao and Yan, 2012) (Tuteja *et al.*, 2008).

2.14 Optimum membrane wettability

To achieve optimal membrane wettability, the membrane surface should have exceptional surface properties where the mixture of oil and water will be separated to a point where both clean oil and clean water are collected separately (Sob *et al.*, 2020) (Sob*et al.*, 2019). The spatial distribution of the membrane due to membrane channel orientation should be taken into consideration. The morphology of membrane nanoparticle sizes in the membrane channels and their impact on the rate of flow of oil-water mixture through the membrane surface should be well investigated (Sob *et al.*, 2020). It is also possible to optimize membrane performance by studying these parameters that impact membrane wettability. This research studies the effect of nanoparticle sizes on the membrane surface, the morphology of the nanoparticle sizes, the spatial distribution across the membrane from the point of oil-water inlet, the point of exit where oil is collected, and the coating technique employed during nanoparticle coating. For water and oil to separate through a membrane surface, the nanoparticle coating will have a unique property of hydrophobicity (Sob *et al.*, 2020).

2.15 The benefits of hydrophobic membrane surface in wettability

The benefits of hydrophobicity of a membrane surface are that it is self-cleaning (Sob *et al.*, 2020) (Ten Brink *et al.*, 2015) (Gao and Yan, 2012) (Tuteja *et al.*, 2008). Dirt is removed during the backflow of oil molecules. The shape of water droplets on the super-hydrophobic surface is closely spherical due to the force of nanoparticles, and there is a backflow of oil out of the membrane channel since hydrophobicity mean water-repelling water and only pure oil is backflow through the membrane channel (Sob *et al.*, 2020) (Ten Brink *et al.*, 2015) (Gao and Yan, 2012) (Tuteja *et al.*, 2008). As the water touches a hydrophobic membrane surface, there is a point of contact and water contact angles defines the wettability surface, which is affected by membrane surface roughness and the type of technique used during coating (Sob *et al.*, 2020) (Ten Brink *et al.*, 2015) (Gao and Yan, 2012) (Tuteja *et al.*, 2008).

The contact angles between the water droplet and the channel's rigid surface are determined. The water droplet and the rigid surface of the membrane pore size typically form a tangent line (Sob *et al.*, 2020) (Ten Brink *et al.*, 2015) (Gao and Yan, 2012) (Tuteja *et al.*, 2008) (Feng *et al.*, 2008). This is the logic of Young's equation on wetting angles of liquid on a solid surface proposed in 1805 (Sob *et al.*, 2020) (Ten Brink *et al.*, 2015) (Gao and Yan, 2012) (Tuteja *et al.*, 2008) (Cao *et al.*, 2008) (Feng *et al.*, 2008).

Several experiments have been conducted to prove that smooth surfaces offer better wettability as compared to rough surfaces. This is due to their low contact angles, as shown in Young's equations (Yan *et al.*, 2011). However, the stochastic nature of these external and internal factors that impact membrane wettability, specifically, the flow rate of the oil-water mixture through the membrane surface, have not been well investigated to design a membrane with better wettability (Sob *et al.*, 2020) (Gao and Yan, 2012) (Tuteja *et al.*, 2008) (Feng *et al.*, 2008). Therefore, it is important to study the random effect of nanoparticles, surface morphology, topology, the best coating technique and how these impact the flow rate of water through the membrane surface. The research is therefore aimed at designing a membrane surface with an efficient oil-water separation.

2.16 Challenges faced by separation technologies

The problem of oil leaks can be overcome by employing effective and safe separation technology (CNN, 2018) (Peng *et al.*, 2016) (Liu *et al.*, 2015) (Cheng *et al.*, 2015) (Khan, 2015) (Wu *et al.*, 2015). Owing to the various oil-water mixture ratios, designing separation technologies that are effective in oil-water separation has been incredibly challenging (Sob *et al.*, 2020) (CNN, 2018) (Peng *et al.*, 2016) (Liu *et al.*, 2015) (Cheng *et al.*, 2015) (Khan, 2015) (Duan *et al.*, 2015) (Wu *et al.*, 2015) (Ke *et al.*, 2014).

For water to be effectively separated from the oil-water mixture, the surface energy of water molecules should be lowered during wettability (Peng *et al.*, 2016) (Wang *et al.*, 2015) (Cheng *et al.*, 2015) (Duan *et al.*, 2015) (Wu *et al.*, 2015) (Si *et al.*, 2015) (Ke *et al.*, 2014) (Zhou *et al.*, 2013). Therefore, membrane technologies used for oil-water separation depend mainly on surface energy parameters.

Membrane technologists have not developed a membrane channel taking into consideration the parameters that affect surface roughness (Sob *et al.*, 2020) (Wang *et al.*, 2015) (Cheng *et al.*, 2015) (Duan *et al.*, 2015) (Wu *et al.*, 2015) (Jiang and Hsieh, 2014) (Ke *et al.*, 2014) (Zhou *et al.*, 2013) (Zhu *et al.*, 2013). In this dissertation, the model derivation is based on the concept of stochastic approach incorporating the velocity of nanoparticles, the total coating force, the coating pressure, the coating distance and the coating angle and their impact on wettability. This leads to lowered surface energy, in which the design of a membrane surface will be with less clusters formed on the surface to give better wettability for oil-water separation.

2.17 Membrane Surface Wetting Properties

Membrane Surface wetting properties are considered hydrophobic if the water contact angle is higher than 90 degrees, or the contact angle is considered hydrophilic if this angle is less than 90^{o} (Sob *et al.*, 2020) (Sob*et al.*, 2019) (Song and Rojas, 2013) (Subhash*et al.*, 2012). A super-hydrophobic surface is a surface with a high-water contact angle ($>150^{0}$) (Cheng *et al.*, 2013). There are also special wetting

properties, which are typically referred to as wetting properties that are not frequently encountered in wettability studies (Sob *et al.*, 2020). Some of those unique wettable properties are extremely water repellent (super-hydrophobic) and oil repellent (super-oleophobic) or repelling both water and oil (homophobic) (Sob *et al.*, 2020) (Wang *et al.*, 2016). There are also surfaces that are air hydrophilic and also oleophobic (Sob *et al.*, 2020) (Wang *et al.*, 2016) (Cheng *et al.*, 2013). Since oil has a lower surface tension than water, which has a higher surface tension, these types of surfaces are difficult to create (Wang *et al.*, 2016).

Another kind of surface patterned wettable surfaces that are partly hydrophobic or partly hydrophilic also exist, bringing more complexity in studying the wettable surfaces of nanostructured membranes (Sob *et al.*, 2020) (Sob*et al.*, 2019) (Wang *et al.*, 2016). These are the major challenges researchers and scientists face in designing a membrane that can offer efficient oil-water separation. It is shown that poor membrane designs are based on poor characterization of nanoparticle coating on wettable membrane surfaces. Therefore, for the proper design of a wettable surface that will be more efficient in oil-water separation, the characterization of the best nanoparticle coating is very important. This dissertation focuses on these aspects to close the current research gap. Therefore, in the current dissertation, a membrane surface with a more efficient wettability surface has been designed for efficient and controlled oil-water separation.

2.18 Membrane wettability

Several parameters or variables are involved during membrane wettability (Sob *et al.*, 2020) (Peng *et al.*, 2016) (Wang *et al.*, 2015) (Cheng *et al.*, 2015) (Duan *et al.*, 2015) (Wu *et al.*, 2015) (Si *et al.*, 2015) (Ke *et al.*, 2014) (Jiang and Hsieh, 2014) (Zhou *et al.*, 2013) (Zhu *et al.*, 2013). Most of the parameters involved during membrane wettability were ignored in the previous modelling of membrane wettability (Sob *et al.*, 2020) (Peng *et al.*, 2016) (Wang *et al.*, 2015) (Cheng *et al.*, 2015) (Wu *et al.*, 2015) (Si *et al.*, 2015) (Zhu *et al.*, 2013) (Zhou *et al.*, 2013). Some of these variables are influenced by external factors such as external pressures (P) being applied on the membranes that other models ignored (Sob *et al.*, 2020) (Wang *et al.*, 2015) (Cheng *et al.*, 2015) (Duan *et al.*, 2015) (Wu *et al.*, 2015) (Si *et al.*, 2015) (Ke *et al.*, 2014) (Jiang and Hsieh, 2014) (Zhou *et al.*, 2013) (Zhu *et al.*, 2013) (Zhou *et al.*, 2013). Temperature is also an important factor that affects fluid viscosity, membrane forces, and surface energy during wettability. Gravitation (g) and specific weight of water and oil are other major factors that affect surface energy during wettability (Sob *et al.*, 2020).

Other membrane dynamic forces are internally applied forces such as the force of water (F_w), which acts in the opposite direction to the direction of the flow of water, the frictional force (F_r) acting in the opposite direction of the force of water, the force of wall (F_{wl}), due to the reaction of the water on the solid wall of the membrane and the force of viscosity (F_v), which defines the rate at which water flows

through the membrane. The force from nanoparticles (F_n) is also due to membrane coating. The force from nanoparticles plays an important role in membrane wettability since it lowers the surface energy. Water molecules at the surface of the coated membrane are spherical in shape due to the effects of hydrophobic.

2.19 The effect of surface roughness on a membrane during wettability

Surface roughness has a significant impact on the wettability of membrane surfaces (Kubiak *et al.*, 2011). Oil molecules flowing through a rough or smooth membrane channel impact differently on membrane performance during oil-water separation (Sob *et al.*, 2020) (Sob *et al.*, 2019). The surface of the nanostructured membrane designed in this dissertation is hydrophilic, thus allowing water to flow through the membrane and at the same time pushing oil out of the membrane channel through the back-flow pipe. During this process, there was a *drag force, shear force, lift force* and the *resultant force* on the separated oil-water molecules in the membrane channel (Sob *et al.*, 2020). Previously, research findings on ceramic membrane surface properties used for wettability have not considered membrane *surface roughness, surface smoothness, shear stress, nanoparticle velocity* during coating and the *resultant force during* the oil-water separation process. Therefore, the derived model in this dissertation is vital and relevant in membrane wettability.

It should be noted that oil-water molecules that are being separated are usually under the influence of these parameters therefore their oil-water separating efficiency depends on these parameters. This informed the design of new membrane technology with better separating efficiency.

2.20 The effect of vibrant forces on Surface energy and their impact on membrane wettability

Most nanostructured membranes used for oil-water separation are designed based on dynamic forces that impact wettability (Sob *et al.*, 2020) (Peng *et al.*, 2016) (Wang *et al.*, 2015) (Cheng *et al.*, 2015) (Ke *et al.*, 2014) (Jiang and Hsieh, 2014). These dynamic forces are the force of nano-particle (F_{nano}), the force of viscosity ($F_{viscosity}$), the force of water (F_{water}), the force of solid surface and water (F_{down}), force on the solid surface and oil (F_{upward}) and force of friction ($F_{friction}$). There are also externally applied forces such as input pressure and gravitation. These dynamic forces on the membrane also impact the change in membrane temperature (T) that affects membrane viscosity which affects the scattering of nanoparticles on the membrane surface (Sob *et al.*, 2020) (Peng *et al.*, 2016) (Wang *et al.*, 2015) (Duan *et al.*, 2015) (Wu *et al.*, 2015) (Si *et al.*, 2015) (Cheng *et al.*, 2015) (Ke *et al.*, 2014) (Jiang and Hsieh, 2014) (Zhou *et al.*, 2013). In most membrane designs, nanoparticle flow rates are impacted by these dynamic forces (Sob *et al.*, 2020) (Peng *et al.*, 2016) (Wang *et al.*, 2015) (Cheng *et al.*, 2015) (Duan *et al.*, 2015) (Wu *et al.*, 2015) (Si *et al.*, 2015) (Ke *et al.*, 2014) (Jiang and Hsieh, 2014) (Zhou *et al.*, 2013).

Therefore, to design a membrane surface that is efficient and stable in wettability, these dynamics forces were well investigated.

Membrane dynamic forces and their parameters during wettability have not been well investigated during oil-water (Peng *et al.*, 2016) (Wang *et al.*, 2015) (Cheng *et al.*, 2015) (Duan *et al.*, 2015) (Wu *et al.*, 2015) (Si *et al.*, 2015) (Ke *et al.*, 2014) (Jiang and Hsieh, 2014) (Zhou *et al.*, 2013). Most existing models used in membrane wettability are designed based on limited dynamic forces (Sob *et al.*, 2020) (Peng *et al.*, 2016) (Wang *et al.*, 2015) (Cheng *et al.*, 2015) (Duan *et al.*, 2015) (Wu *et al.*, 2015) (Si *et al.*, 2015) (Ke *et al.*, 2014) (Jiang and Hsieh, 2014) (Zhou *et al.*, 2013). To design a membrane surface with proper wettability and stability, all the physical properties such as membrane dynamic forces must be taken into account (Sob *et al.*, 2020) (Peng *et al.*, 2016) (Wang *et al.*, 2015) (Cheng *et al.*, 2015) (Duan *et al.*, 2015) (Wu *et al.*, 2015) (Si *et al.*, 2015) (Ke *et al.*, 2014) (Jiang and Hsieh, 2014) (Zhou *et al.*, 2013). The focus should then be placed on parameters or variables that affect wettability, which was ignored by other models of wettability.

2.21 Surface energy and surface tension and their impact during wettability

Surface tension and surface energy are commonly used in membrane wettability. Their impacts on membrane wettability are based on membrane shear stress, fluid viscosity, shear stress distribution, velocity distribution, change in membrane temperature, and the forces on the membrane surface (Sob *et al.*, 2020) (Sob*et al.*, 2019). Most often, researchers focus on surface tension driven separability that deals with a few parameters that affect the membrane wettability process. Different parameters or variables in membrane technologies affect surface tension and surface energy. Surface energy-driven separability primarily involves the time spent constructing a new surface (Sob *et al.*, 2020).

For work to be done, there is always a change in distance due to applied forces. As work is being done to separate oil and water, there is shearing in the membrane due to the different layers of oil-water mixture and surface roughness or smoothness of the membrane channel because of nanoparticle coating. There is also a velocity distribution in the membrane channels due to the coating of the nanoparticles on the membrane surface. There is a change in membrane temperature during the wettability process that impacts the membrane shear stress, affecting the velocity distribution and viscous flow in the channel, which impacts surface tension and surface energy-driven separability. Surface energy deals with the total inward force on the surface and the surface area in which the molecules act during wettability.

The force in surface tension is the tensile force acting on a liquid on a membrane surface. The force is affected by the temperature of the separated particles, which affects the separated particles' viscosity. The difference between the parameters and variables in surface tension and surface energy-driven

separability has not been previously investigated (Peng *et al.*, 2016) (Wang *et al.*, 2015) (Cheng *et al.*, 2015) (Duan *et al.*, 2015) (Wu *et al.*, 2015) (Si *et al.*, 2015).

Most relationships on surface tension and surface energy used in modelling and simulation assume that surface tension and surface energy are the same (Peng *et al.*, 2016) (Cheng *et al.*, 2015) (Duan *et al.*, 2015) (Wu *et al.*, 2015) (Si *et al.*, 2015) (Ke *et al.*, 2014) (Jiang and Hsieh, 2014). This has always been true in membrane technology having uniform membrane channels, and it is not the case for a membrane surface with different orientated channels used in wettability. It is important to recall that surface tension is the tensile force on the surface of the liquid that prevents the liquid from flowing. This does not include the area over which the liquid may flow and if it has to flow, which surface energy considers during oil-water separation. Therefore, surface tension and surface energy should not be the same from empirical definitions.

The modelling and simulation process of surface tension and surface energy and their parameters and variables in this dissertation show that if a membrane surface has different orientations, the surface tension and surface energy are not the same, and therefore, this will have different impacts on wettability. This dissertation modelled the relationship between surface tension and surface energy in a viscous flow in membrane channels.

2.22 External and Internal forces during membrane wettability

These internal and external forces are random in nature during membrane wettability (Peng *et al.*, 2016) (Wang *et al.*, 2015) (Cheng *et al.*, 2015) (Duan *et al.*, 2015) (Wu *et al.*, 2015) (Si *et al.*, 2015) (Ke *et al.*, 2014) (Jiang and Hsieh, 2014) (Yang and Cranston, 2014) (Kong *et al.*, 2014) (Zhou *et al.*, 2013) (Zhu *et al.*, 2013) (Prasad *et al.*, 2008). Membrane wettability is usually analysed based on surface tension and surface energy (Peng *et al.*, 2016) (Wang *et al.*, 2015) (Cheng *et al.*, 2015) (Yang and Cranston, 2014) (Zhou *et al.*, 2013) (Zhu *et al.*, 2013). Surface tension-driven separability deals with the force on the water droplet in the membrane surface (Peng *et al.*, 2016) (Wang *et al.*, 2015) (Cheng *et al.*, 2015) (Ke *et al.*, 2014). The wettability of a membrane is not only affected by the forces on the water molecules and the surface length of the membrane, but also by the surface area of the membrane and the ability of the water molecules to flow, which is energy driven. These are affected by the orientation of the channel in which the water is flowing. The effect of membrane dynamic forces is tested on surface energy-driven separability to test their impacts on wettability in order to design a nanostructured membrane with better surface properties and stable wettability during oil-water separation.

2.23 The benefits of using hydrophobic ceramic membrane surface in wettability

The advantage of hydrophobicity of a membrane surface is that it is self-cleaning (Gao and Yan, 2012) (Tuteja *et al.*, 2008). Contaminants are removed during the backflow of oil molecules. The shape of water droplets on the super-hydrophobic surface is closely spherical due to the force of nanoparticles, and there is a backflow of oil out of the membrane channel since hydrophobicity mean water-repelling and only pure oil is flown back through the membrane channel (Sob *et al.*, 2020) (Gao and Yan, 2012) (Tuteja *et al.*, 2008) (Feng *et al.*, 2008). There is a point of contact as water comes into contact with a hydrophobic membrane surface. The water contact angles determine the wettability of a surface, which is predominantly determined by the membrane roughness, nanoparticle particle sizes, membrane morphology, membrane topology and spatial distribution (Sob *et al.*, 2020) (Gao and Yan, 2012) (Tuteja *et al.*, 2008) (Feng *et al.*, 2008).

The contact angles are measured by the water droplet and the solid surface of the membrane. It is usually a tangent line between the water droplet and the solid surface of the membrane pore size (Sob *et al.*, 2020) (Gao and Yan, 2012) (Tuteja *et al.*, 2008) (Feng *et al.*, 2008). Young's equation on wetting angles of liquid on solid surfaces suggested this in 1805 (Sob *et al.*, 2020) (Gao and Yan, 2012) (Tuteja *et al.*, 2008) (Feng *et al.*, 2008). The most important factor from different theoretical and experimental findings is that the solid surface of water droplet contact must be smooth for proper correlation of surface tension and surface energy and for proper mechanical equilibrium conditions (Sob *et al.*, 2020) (Gao and Yan, 2012) (Tuteja *et al.*, 2008) (Feng *et al.*, 2008) (Feng *et al.*, 2002).

Several studies have been carried out to demonstrate that smooth surfaces offer better wettability in terms of their low contact angles, as shown in Young's equations (Sob *et al.*, 2020) (Sob*et al.*, 2019) (Yan *et al.*, 2011). Nonetheless, the stochastic nature of these external and internal factors that affect membrane wettability, more especially the flow rate of the oil-water mixture through the membrane surface, have not well been investigated to design a membrane with better wettability (Sob *et al.*, 2020) (Tuteja *et al.*, 2008) (Feng *et al.*, 2008) (Feng *et al.*, 2002). Consequently, it is important to study the random effect of nanoparticles, morphology, topology and spatial distribution and how they affect the flow rate of water through the membrane surface. Therefore, the study aims to design a membrane surface with an optimal flow of water during oil/water separation.

2.24 Wettability of Nanostructure Membrane used in Oil-water Separation Technology

The wettable surface is the most important property in the oil-water separation process (Sob *et al.*, 2020) (Tuteja *et al.*, 2008) (Feng *et al.*, 2008) (Feng *et al.*, 2002). Recent studies have opened up some massive research areas that can be exploited in the medical field, specifically in treating complicated illnesses and even in designing clean water systems for industrial and domestic applications (Sob *et al.*, 2020).

Surface wetting properties are usually quantified by measuring the contact angles of a sessile liquid drop on a solid surface in the air (Sob *et al.*, 2020) (Huang and Lai, 2015) (Cheng *et al.*, 2013). Other approaches are being used to measure the captive bubble (Cheng *et al.*, 2013).

2.25 The correlation between surface tension and surface energy in a membrane during oil-water separation

Several relationships exist between surface tension and surface energy during membrane wettability (Peng *et al.*, 2016) (Cheng *et al.*, 2015) (Cheryan and Rajagopalan, 1998). Most of these relationships are established for the design of the membrane surface (Peng *et al.*, 2016) (Cheng *et al.*, 2015) (Cheryan and Rajagopalan, 1998). These physical activities are given by the parameters or variables that affect surface tension and surface energy in a designed membrane. The physical activities are mostly the membrane surface area, nanoparticles coating on the membrane channel, surface length, pressure difference across the membrane surface, the shear stress distribution in the membrane due to the coating of the membrane channel by nanoparticles, the fluid velocity distribution in the membrane due to nanoparticles coating, the flow rate in the membrane channel, the fluid viscosity due to nanoparticles coating, changes in temperature on the membrane surface, the membrane temperature and the forces on the membrane channel.

These parameters, when related to surface tension or surface energy, have different effects on membrane wettability or flow rate. The relationships between these parameters are based on the membrane design and the type of nanoparticle coating that offers shear stress in the membrane channel during wettability. Membrane technologists and engineers have dealt with membranes that have uniform channels in most membranes (Sob *et al.*, 2020) (Peng *et al.*, 2016) (Cheng *et al.*, 2015) (Duan *et al.*, 2015) (Wu *et al.*, 2015) (Si *et al.*, 2015) (Ke *et al.*, 2014) (Jiang and Hsieh, 2014) (Cheryan and Rajagopalan, 1998), while nanoparticles coating, shear stress, shear stress distribution, velocity distribution, pressure difference and their impact on surface tension and surface energy have not been investigated in details.

2.26 Stability and Durability of Nanostructured Ceramic Membrane in Oil/Water Separation Technology

The pore sizes of the produced nanostructured membrane are major factors to examine in order to achieve proper stability and durability in ceramic membranes (Huang and Lai, 2015) (Zheng *et al.*, 2015). Suitable pore size can effectively allow water to pass through while preventing oil penetration. Furthermore, owing to the coating of the super-oleophobicity nanostructured membrane, a high-water holding capability will potentially sustain a robust super-oleophobicity of the nanostructured membrane by creating a very solid water sheet (Sob *et al.*, 2020) (Zheng *et al.*, 2015).

It has been observed that the flow rate of water out of wettable membranes is highly dependent on the pore size distribution networks, as different nanostructured membranes with different pore sizes before and after nano-coating have different flow rates. This may be due to the engineered nanostructured membrane absorbing more water, as is the case in this study (Sob *et al.*, 2020) (Zheng *et al.*, 2015). Furthermore, as revealed in the current study, the pore sizes of nanostructured membranes, when coated, have varying flow rates of water out of the membranes depending on the pore size diffusion network and their characterization. As a result, the coated nanostructured membrane must reach a statistical pore scale for the criteria of a reliable super-oleophobicity oil/water isolation. According to this study, the nano-coatings have various effects on flow rate depending on the morphology of materials used for nanoparticle coating and the methods of nanoparticle coating characterization (Sob *et al.*, 2020) (Zheng *et al.*, 2015).

It is necessary to note that certain selective nanostructured membranes can experience pore network blockage during the oil/water separation process (Sob *et al.*, 2020). As a result, due to blockage, the flow rate of water during the oil/water separation process cannot always be constant, and hence the idea of stability and durability in ceramic membranes is necessary. This study has explored that aspect by designing a backflow pipe with oleophilic properties to attract only those particles that can induce membrane fouling. A new logic of surface energy-driven wettability was developed after the membrane surface was defined for optimum wettability. The random design of nanoparticles, as well as their scale, morphology, and spatial distribution, influence wettability.

2.27 SEM & TEM Microscopy

Electron microscopy provides visual information on membrane structure and porosity through magnification by scanning electron microscope (SEM) and transmission electron microscope (TEM) during the characterization of nanoparticles (Sob *et al.*, 2020) (Sob *et al.*, 2019) (Huang and Lai, 2015) (Duan *et al.*, 2015) (Jiang and Hsieh, 2014) (Ditsch *et al.*, 2005). Microscopy, such as high electron beam energy, damages surfaces of polymeric membranes, and therefore, material observation and characterization are not efficient (Sob *et al.*, 2020) (Sob*et al.*, 2019) (Duan *et al.*, 2015) (Jiang and Hsieh, 2014). SEM ensures accuracy and validation of findings during characterization on how particles are distributed on the membrane surface during coating (Ren *et al.*, 2015). It also depicts the nanoparticle clusters produced during nanoparticle-coating, as shown in Fig. 5 and Fig. 6.

The SEM has its own limitation during observation since it does not give a deeper insight into the finer porosity, but it is vital in observing the surface spread of coated nanoparticles (Sob *et al.*, 2020) (Sob *et al.*, 2019). Therefore, SEM is more recommended and has been used in the current dissertation to characterize the surface spread of nanoparticles on the membrane surface and inter-separation distances that impact membrane wettability. TEM is more acceptable since it has a much higher resolution (0.2

nm) than SEM and other microscopies (Sob *et al.*, 2020) (Sob*et al.*, 2019). The problem with TEM is that the sample must be etched and well-polished for analysis. The membrane coated with nanoparticles on the surface accompanied by etching or polishing the sample for TEM can dislocate the coated nanoparticle, and therefore, TEM may not be used for nanoparticle characterization.

In this current study, ceramic samples were not cleaned for microscopic analysis due to that the surface roughness of the hydrophobic nano4stone was the main parameter to be measured. These samples were embedded in epoxy resin blocks, and later, the thin section to be analysed was prepared. The holders in which the ceramic samples were placed for microscopy analysis were 25mm diameter round. The ceramic samples were electrically non-conducting during analysis, and a conducting surface coating was applied to provide a proper path for the incident electrons to flow to the ground during analysis.

To achieve higher resolution during SEM imaging, advanced detectors were used during SEM analysis. These were used to selectively detect the different locations as indicated by spectrum 1 to spectrum 5 called site of interest. The site of interest is where the lens was able to capture the results. This was to ensure accuracy and elementary validation of findings on how particles were distributed on the membrane surface during coating. During the SEM analysis, the detector used was an In- Lens SE detector (Zeiss Supra 40, FE-SEM, Oberkochen, Germany). It must be noted that the In-Lens was only able to pick images in a straight path. Therefore, the In-Lens was unable to pick up images in the curve section of the glass membrane and as such, the sections were black in the SEM captured images. The nanoparticles' sizes, shape, orientation, morphology, and dispersion of lateral dimensions were measured.

It should be noted that the STEM detector being placed under the samples was used to capture images in transmission mode in the SEM during the experiment. This consists of sample holders which guide the transmitted electrons onto the electron multiplier in the form of a gold plate under the bright field. All the transmitted electrons are collected by the E-T detector. At the same time, the screening ring being operated prevented the X-rays from being emitted by the sample to reach the EDS detector, and therefore, it is important to remove the ring before an EDS analysis. Moreover, a TEM grid transmission setup was used, and the TEM detector was able to analyse four samples on the holders, and EDS analysis was carried out immediately.

The various SEM and EDS configurations images were captured for LP and HP. The coating thickness, surface spread, roughness, smoothness, contact angles, inter-separation distances, size, morphology, spatial distribution were observed and measured using SEM, image J particle analyser and energy dispersive X-ray spectroscopy. The viscosities of nanoparticle scattering were measured at room temperature using a rheometer (Physica MCR301, Anton PaarGmbh Graz, Austria). The densities of nanoparticles were also measured at room temperature with a densitometer (30 PX, Metler Toledo, Viroflay France).

The following EDS detectors were used to analyze 8 mm^2 ceramic, coated ceramic and hydrophobic nanoparticles (Thermo Scientific, USA), a 10 mm^2, SDD (Bruker, Germany), a 100 mm^2, SDD (Thermo Scientific, USA), with an annular 60 mm^2 Flat QUAD SDD (Bruker, Germany). The SDD annular is being inserted between the pole shoe and the experimental sample to give a very large solid angle of the X-rays being emitted by the sample. For the TEM analysis, the samples were not polished since the coated nanoparticles were on the surface of the membrane. A standard TEM thin foil 3mm in diameter were prepared for analysis by electrolytic twin-jet (at $-30^{\circ}C$, 30 V) in Struers Tenupol 2 filled with 6% solution of perchloric acid in methanol. It was imperative to analyze the uncoated sample for ceramic membrane and its descriptive statistical analysis to detect elements in it and to observe the surface properties.

2.28 Clusters observed during SEM and TEM analysis

In Fig.2.6, Ogi et al. (2006) prepared the surface morphology and cross-sections of nanoparticles from commercial indium tin oxide (ITO) nanoparticles using a dip-coating method. An ITO film prepared using commercial nanoparticles had a rough surface, and this is because the commercial nanoparticles resulted in clustering on the membrane surface.

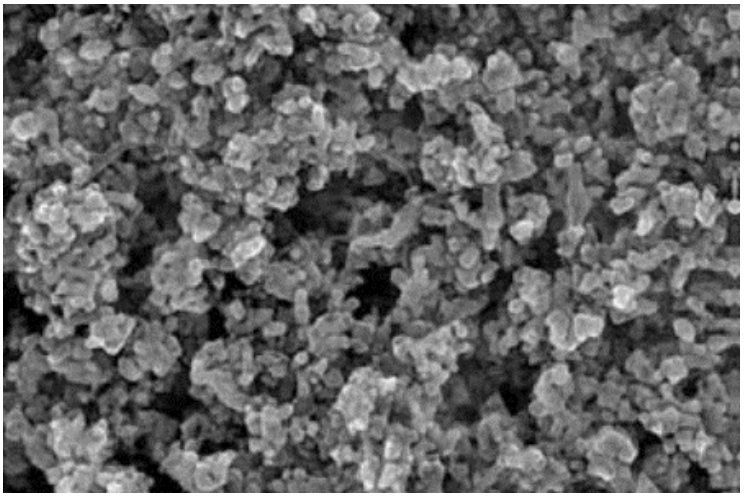

Figure 2.6 SEM image of clusters on a ceramic membrane (Ogi et al., 2006)

Gao and Xu (2019) reported on depositing the polydopamine (PDA) on ceramic aluminium oxide (Al_2O_3) membrane surface using the *self-polymerization technique*. The original Al_2O_3 ceramic membrane surface is a smooth membrane, but clusters were observed on the membrane surface after coating with PDA, as depicted in Fig.2.7 (a). To reduce the developed clusters during the coating rounds, researchers further deposited Silver (Ag) nanoparticles to achieve an optimum speed of nanoparticles

with little success being reported as clusters were still observed, as shown in Fig. 2.7 (b) (Gao and Xu, 2019).

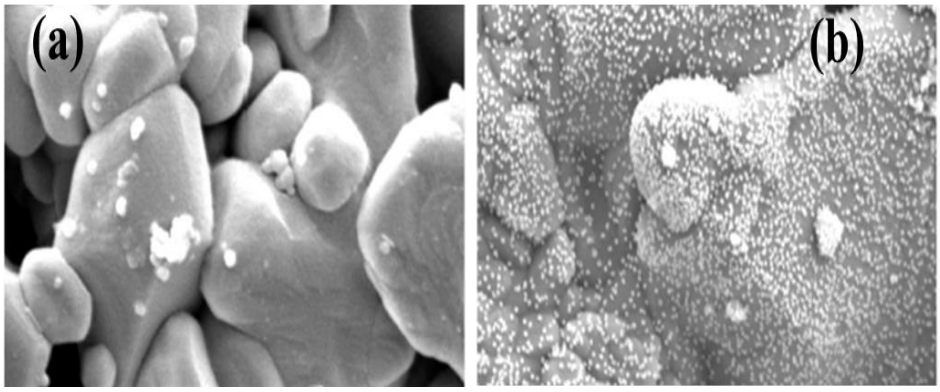

Figure 2.7 SEM images of clusters on PDA coated Al_2O_3 ceramic membrane (a) followed by clusters on PDA coated Al_2O_3 ceramic membrane after Ag nanoparticle deposition (b) (Gao and Xu, 2019)

HP and LP coating have been reported to give different clustering on the membrane surface (Sob *et al.*, 2019). With different coating rounds, clusters appear differently on the membrane, and this is due to a different scattering effect of nanoparticles on the membrane surface during coating rounds (Sob *et al.*, 2019). Sob et al (2019) reported more and larger clusters observed on LP jet-spray coating as compared to HP jet-spray coating as depicted on Fig.2.8 (a) & 2.8 (b).

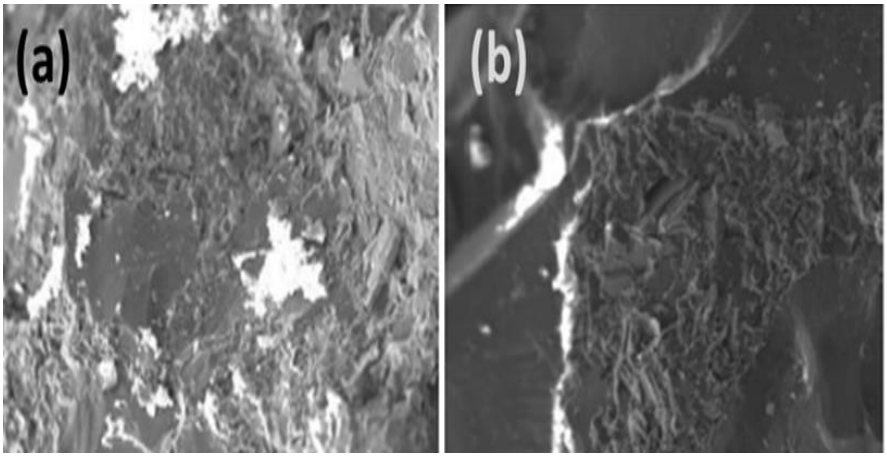

Figure 2.8 SEM images of clusters on LP jet spray-coated membrane (a), and clusters on HP jet spray-coated membrane (b) (Sob et al., 2020) (Sob et al., 2019)

Ditsch et al. (2005) produced a nanostructured membrane by nano-coating a polymer membrane with magnetic nanoparticles, as shown in Fig.2.9. Clusters were observed after nanoparticle coating. A secondary hydrophilic, low molecular-weight polymer was further used to minimise clusters, with limited success.

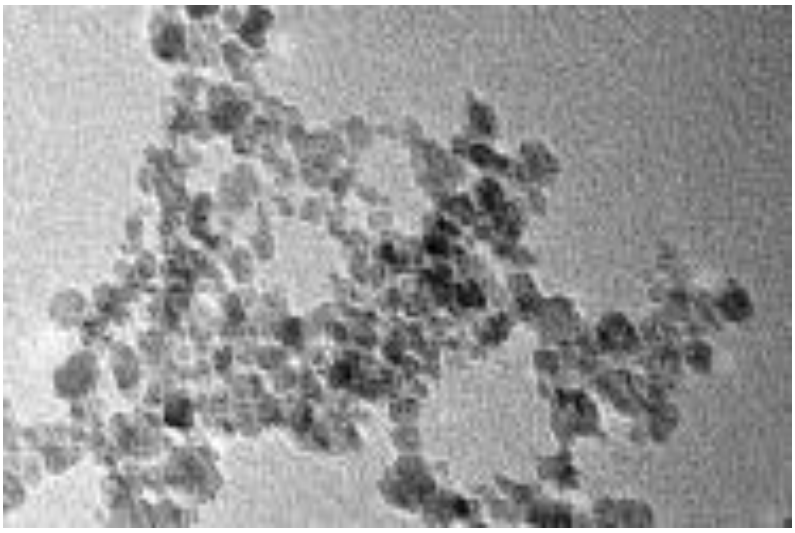

Figure 2.9 TEM image of clusters on polymeric membrane (Ditsch et al., 2005)

Stebounova et al. (2011) produced a nanostructured membrane using silver (Ag) nanoparticles. Clusters were observed on the membrane surface as shown in Fig. 2.10 (a). To reduce the developed clusters during coating, researchers deposited polyacrylate sodium on the solute to achieve optimum spread of nanoparticles, with limited success being reported as clusters were still observed, as shown in Fig. 2.10 (b) (Stebounova *et al*., 2011)

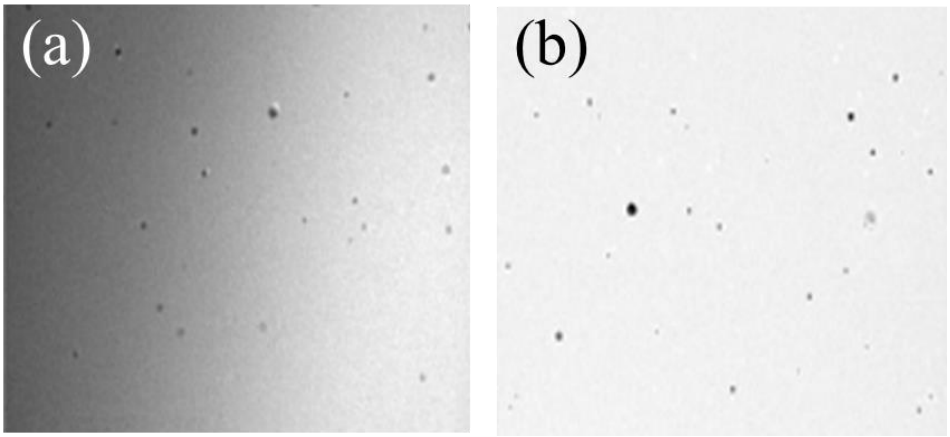

Figure 2.10 TEM images of clusters on the Ag coated membrane surface (a), and clusters on the Ag coated membrane surface with polyacrylate sodium (b) (Stebounova et al., 2011)

In this study, a nanostructured ceramic membrane was produced using jet-spray coating in HP and LP coating rounds. Clusters were observed after nanoparticle coating in LP rounds, as shown in Fig.2.11.

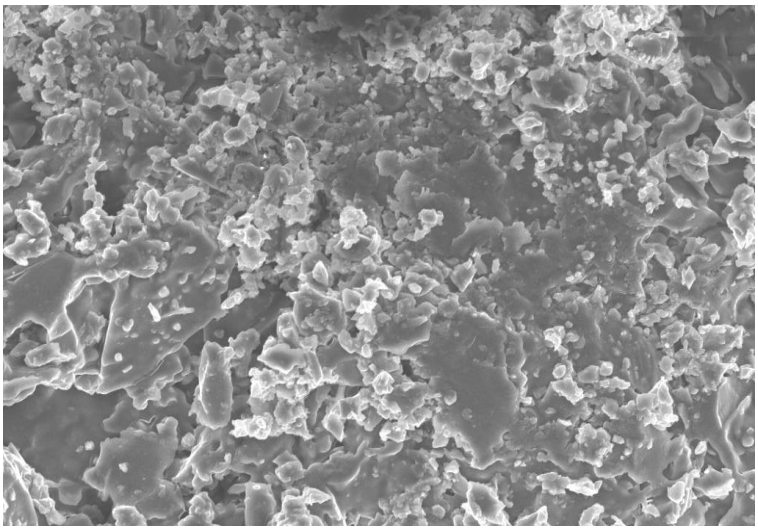

Figure 2.11 SEM images showing clusters on the ceramic membrane after nano-coating

The SEM has its own limitation during observation since it does not give a deeper insight into the finer porosity, but it is vital in observing the surface spread of coated nanoparticles (Sob *et al.*, 2020) (Sob*et al.*, 2019) (Tai *et al.*, 2015). Therefore, SEM is more recommended and used in the current dissertation to characterize the surface spread of nanoparticles on the membrane surface and inter-separation distances that impact wettability. TEM is more acceptable since it has a much higher resolution (0.2 nm) than SEM and other microscopies (Sob *et al.*, 2020) (Sob*et al.*, 2019). The problem with TEM is that the sample must be etched and well-polished for analysis. The membrane coated with nanoparticles on the surface accompanied by etching or polishing the sample for TEM can dislocate the coated nanoparticles and therefore, TEM may not be used for nanoparticle characterization.

2.29 Summary of the reviewed literature

The challenges faced by membrane technologists and scientists in developing membrane technologies that are effective and have reliable wettability during oil-water separation were discussed in detail in this chapter. The first part of the chapter looked at the literature from a global viewpoint, focusing on the emerging problems that membrane technologists are facing. The different separation technologies used in water purification processes were discussed, and their limitations were equally examined.

Materials such as glass, ceramics, polymers, clay, textiles and sediments were investigated from the previous literature. Ceramic material was recommended for the design of the current membrane technology due to its availability and advantages. Membrane surface characterization and nanoparticle coating characterizations were also analyzed with their effects on wettability during oil-water separation. This concept is understood by using the tools of the stochastic approach.

Coating strategies were investigated from the previous literature. Jet-spray coating has been reported to be effective in ceramic coatings due to that it offers a better scattering effect of nanoparticles on the membrane surface during coating. It also gives better clustering on the membrane surface as compared to other coating strategies. The following parameters: coating pressure, coating distance and coating angle were revealed as the major parameters to be incorporated in the jet-spray coating when fabricating the ceramic membrane system. These parameters were also related to the transition of rough membrane surface to the smooth membrane. This concept is clearly understood by using the tools of fluid dynamics. It was revealed from the literature that a membrane with less or fewer clusters gives a smooth surface with less surface energy, as this was the purpose of the current study. The relationship between surface tension and surface energy-driven separability were compared and analyzed. The use of surface energy-driven separability against surface tension driven separability was also highlighted. The motivation and rationale of surface energy-driven separability against surface tension were highlighted. The literature explored in this chapter related a better understanding of membrane technology used in oil-water separation around the globe.

The next chapter presents the derivation of a model which will minimise clusters on the ceramic membrane surface using the aforementioned parameters: coating pressure, coating distance and coating angles.

CHAPTER THREE

RESEARCH DESIGN AND METHODOLOGY

3.1 Introduction

Since the current study is aimed at modifying ceramic membrane surface for efficient wettability during oil-water separation, this chapter deals with identifying the best coating strategy used for improved ceramic membrane surface properties and establishes parameters that will be modelled to produce an efficient wettable ceramic membrane surface.

3.2 Research design

Fig.3.1 demonstrates the process flow of ceramic membrane surface modification. It indicates some of the internal factors that affect material wettability during oil-water separation. It also indicates some of the external factors which will have an effect on material coating processes and their wettability during nano-particle coating. In designing the ceramic nanostructured membrane, the following parameters were modelled for efficient wettability during oil-water separation: coating force, coating pressure, coating distance and coating angle. The model identified was tested using the concept of the stochastic approach. The model was tested on surface energy-driven separability.

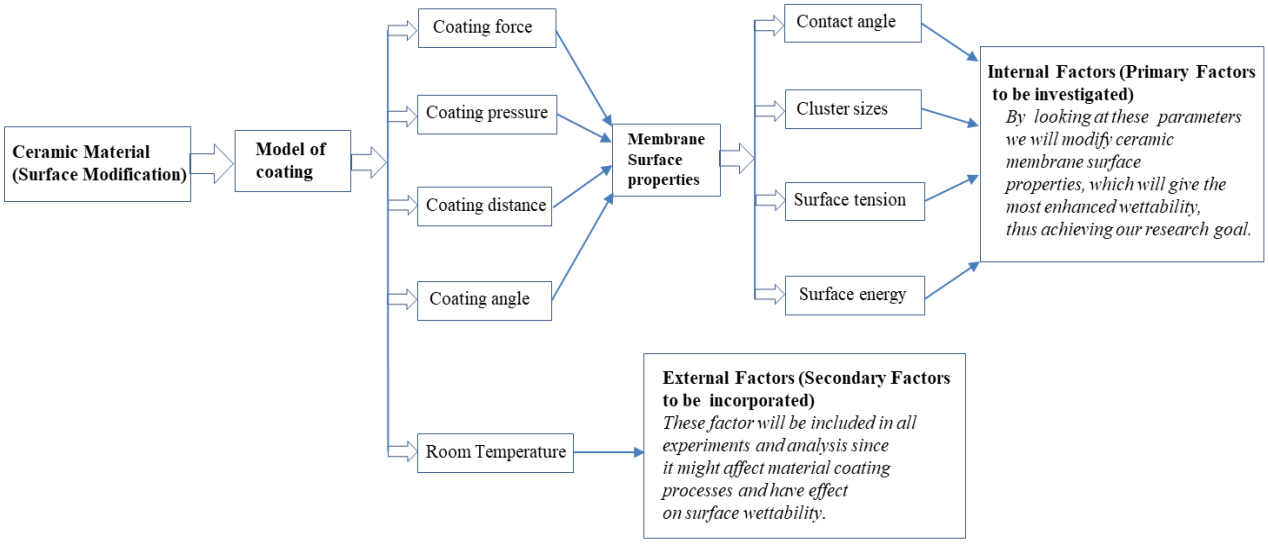

Figure 3.1: Schematic diagram showing the modelling of surface tension and surface energy driven separability

To achieve the research goal, the focus was on characterisation of the cluster sizes on the wettable nanostructured membrane. The approaches followed a sequence of coating nanoparticles on wettable membranes using a jet-spray guns then tested the model on surface energy-driven separability. Therefore, the major experimental parameters variables were nanoparticle coating, coating force, coating pressure, coating distance, coating angle and surface energy.

Membranes technology is extremely important today because it operates without the use of chemicals and requires less electricity, as well as the fact that it is simple to use and has a well-organized conduction mechanism (Sob *et al.*, 2020) (Padaki *et al.*, 2015). The first series of experiments involved manufacturing and testing suitable membranes for oil/water separation.

3.3 Research approach

This project was approached in three stages. Stage one focused on a theoretical modelling and simulation based on ceramic membrane material modification of surface properties by nanoparticle coating. Stage two was experimentation. Stage three was comparison of the newly designed ceramic membrane with the previously designed ceramic membrane from previous the literature. Our theoretically developed models of surface wettability (e.g., coating force, coating angle and coating distance) guided the manufacturing process and nanoparticle coating strategy of the wettable membrane surfaces. A ceramic membrane system was fabricated by using hydrophobic-oleophilic nano4stone nanoparticles containing *Fluorine S5* as the control element. The coating technique that was used in this project is the jet-spraying technique. This technique has a high deposition rate and is flexible to reach any substrate shape (Chen *et al.*, 2018) (Gestel *et al.*, 2008). It has unique properties such as thickness uniformity and offers high scattering effects across the surface (Chen *et al.*, 2018) (Gestel *et al.*, 2008).

Characterization was done using scanning electron microscopy (SEM), transmission electron microscopy (TEM), energy dispersion spectroscopy (EDS) and Image J particle analyser. This work focused on the effects of different coating rounds of LP and HP to identify the optimum coating pressure, which will give a better scattering effect of nanoparticles, thus reducing clusters on the wettable membrane. Since the morphology of membranes, nanoparticle sizes, and scattering of nanoparticles on the membrane are naturally random, the concept of stochastic approach was used. The stochastic approach promotes the analysis of spontaneous phenomena, as reported by Sob *et al.* (2020). The improved relationship between ceramic membrane surface properties was established. Such properties are surface smoothness, contact angle, surface tension and surface energy.

3.3.1 Theoretical modelling and simulation

3.3.1.1 Modelling and simulation of surface energy driven separability

The study employed the relevant theoretical models in modelling the surface energy-driven separability. The stochastic effects of nanoparticle size, the morphology of membrane channels and spatial distribution of membrane on surface energy were investigated this section of the thesis. The relationship between surface tension and surface energy in membrane viscous flow during oil/water separation was also investigated for the design of the current membrane surface with more efficient wettability. The relationship between the parameters of flow during nanoparticle coating and surface energy-driven separability during oil-water separation was also investigated for a stable wettability process.

Membrane dynamic forces on surface energy and their impact during oil-water separation were also incorporated in the modelling of the current membrane surface. Membrane inter-separation distances during nanoparticle scattering were also modelled theoretically to obtain the optimal inter-separation distances that gave optimal wettability. The relevant engineering simulation was done using Engineering Equation Solver (EES).

Fig.3.2 (a) and Fig.3.3 (a) shows a jet spray gun during high pressure (HP) coating and low pressure (LP) during coating, used to produce nanostructured membrane for oil/water separation. Impurities (which may be oil or water) must flow through the produced membrane surface. For water oil to be effectively separated from the coated membrane surface, the effect of nanoparticles on the coated ceramic solid membrane surface must be taken into consideration. Nanoparticles coated on the ceramic membrane surface have different surface roughness, which affects the surface energy of the ceramic membrane surface. The roughness or smoothness of the ceramic's membrane surface, which led to the frictional resistance force F_R (higher for a rough ceramic surface and lower for a smooth ceramic surface), played a significant role how water and oil flew on the membrane surface. Other forces such as the force of nano-particle (F_{nano}) to lower the surface energy on the membrane surface, the force of viscosity ($F_{viscosity}$), the force on nanoparticles due to applied pressure from the spray gun ($F_{nano/pressure}$), the force on solid wall and nanoparticle (F_{down}) and the force on wall and nanoparticle (F_{upward}) are shown in Fig. 3.2 (b) and Fig. 3.3 (b). Fig.3.2 (a) shows a jet-spray gun during coating and Fig.3.2 (b) depicts a rough ceramic membrane surface during coating rounds and the mobility of nanoparticles on the membrane surface, which must be modelled. External and internal parameters that affect surface homogeneity must be studied. From Fig.3.2 (b) the different forces that impacted surface homogeneity are greatly dependent on the pressure of the jet spray gun, the distance of the jet spray gun from the membrane during coating and the frictional resistance force (F_R) that impacted the force of nano-particles (F_{nano}), the force of viscosity ($F_{viscosity}$), the force on nanoparticle to due applied pressure

($F_{nano/pressure}$), the force on solid wall and nanoparticle ($F_{downward}$) and the force on wall and nanoparticle (F_{upward}).

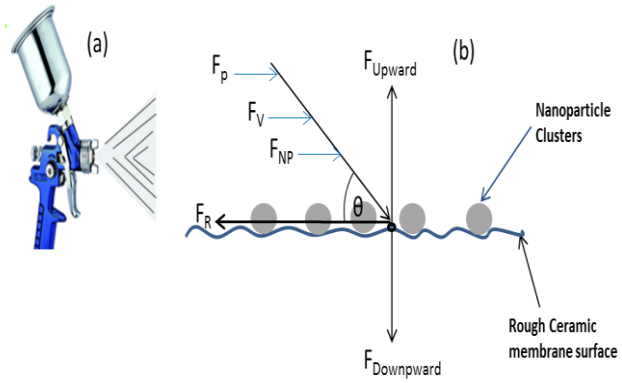

Figure 3.2 (a) Jet spray gun during coating and (b) movement of nanoparticles on a rough membrane surface during coating

It was observed during coating on rough ceramic membrane surfaces that the frictional force must be high for the nanoparticles to move through the rough membrane surface during the coating process.

Fig.3.3 (a) shows a jet-spray coating on a smooth ceramic membrane surface, and Fig.3.3 (b) depicts the mobility of nanoparticles on a smooth ceramics surface under the influence of low resistant force when compared with a rough membrane surface. Therefore, membrane frictional resistance forces are vital forces when minimizing the formation of clusters in ceramics membrane surfaces. The coating pressure and frictional resistance force must be maintained at optimal levels but in a steady state to maintain proper movement and a better scattering effect of particles on the membrane surface. Fig.3.3 (a) revealed membrane coating for a smooth ceramic surface. However, the frictional forces were low when compared to a rough membrane surface during coating rounds in order to minimize the formation of clusters, as shown in Fig.3.3 (b)

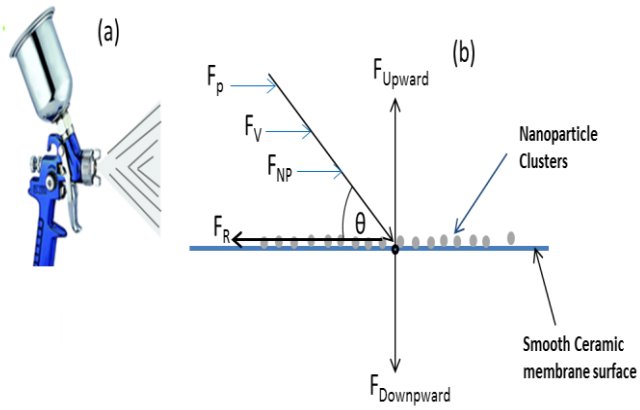

Figure 3.3 (a) Jet spray gun during coating and (b) movement of nanoparticles on a smooth membrane surface during coating

Before modelling the frictional resistance force and scattering effect that impact membrane surface clusters in a ceramic membrane, it is important to look at the total forces acting on a rough membrane and smooth membrane during ceramic membrane coating and is given as:

$$F_{Total} = F_{(NP\cos\theta)} + F_{(Viscosity)} + F_{(Spray\ gun\ pressure)} + F_{(Downwards)} - F_{(Frictional\ resistance)} \quad (1)$$

The equation (1) gives a total force that acts on a membrane surface during the coating process. The formation of membrane clusters is due to membrane surface roughness. The frictional resistance force influences this surface roughness during coating. A rough membrane surface requires higher frictional force and a smooth membrane surface requires low frictional force for membrane clusters to be minimized. Therefore, there is a need to investigate the optimal frictional force in rough and smooth membrane surfaces to minimize the surface clusters during coating. Figure 3.4 revealed the forces that are acting on a coated membrane surface during the coating process when using the jet spray gun. From Fig.3.4, the jet spray propulsion during nanoparticle coating depends on the jet diameter, coating pressure or force, fluid viscosity, velocity, the distance of the jet spray gun from the coating membrane and the coating angles of the ceramic membrane used in the coating. These parameters affect membrane surface clusters and must be modelled to minimize membrane clusters during coating.

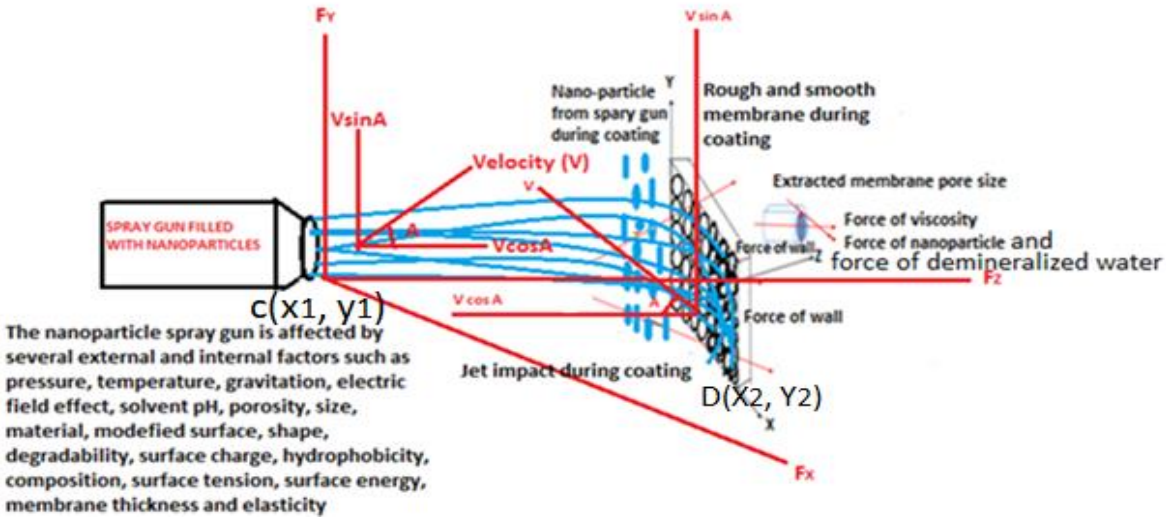

Figure 3.4 Schematic diagram of jet impact propulsion forces during membrane coating by jet spray gun (Sob et al., 2020)

Since the motion of nanoparticles during coating is parabolic as shown in Fig.3.4, the jet spray gun makes an angle θ with the horizontal and vertical component velocity at point C is given as $V\cos\theta \ \ and\ V\sin\theta$ as shown in Fig.3.4. If another point at D, there are coordinates (x, y) before the nanoparticles strike the ceramic membrane, and the particles travel at a given time (t) to hit the ceramic membrane surface as shown in Fig.3.4. The $x\ and\ y$ component in terms of velocity, the angle of projection and time of projection are given as $x = V\cos\theta\ (t)$ and $y = V\sin\theta(t) - \frac{1}{2}gt^2$. From the x component of the velocity, t can be computed as $t = \frac{x}{V\cos\theta}$ Substituting t in y yielded:

$$y = x\ \frac{\sin\theta}{\cos\theta} - \frac{gx^2}{2V^2\cos\theta\cos\theta} \tag{2}$$

From equation (2) the impact of membrane clusters during jet spray coating can be analysed based on the coating angles of the jet spray gun θ, the speed of nanoparticles from the jet spray gun V and the distance the jet spray gun is kept away from the ceramic membrane during coating. The coating process revealed the flow of nanoparticles that can be related to flow in the open surface since the coating process was done in a controlled laboratory environment. The velocity from Fig.3.4 can be derived based on the physical reality during the coating process. The nanoparticle discharge by the jet spray, as shown in Fig.3.4, would have covered an external distance S_3 while spending external time, t_3, as the nanoparticles flew from the jet spray gun to the ceramic membrane being coated. To estimate these external characteristics, flow characteristics were measured from the jet spray gun to the coated membrane as shown in Fig.3.4.

Since the nanoparticles hit the membrane surface after fleeing the S_3 at a time t_3, the impact of the jet spray gun is felt on the membrane surface. This impact can be related to the mass flow rate on the

membrane surface discharge by the jet spray gun given as $M_3 = \rho A_3 V_3$ where ρ the density of nanoparticle, A_3 is the nanoparticle coating cross-sectional area of the surface and V_3 is the velocity of nanoparticles during coating. The average time t_3 spent by nanoparticles to get to the membrane surface was measured using a stopwatch. It was obtained by calculating the time it took the nanoparticle to flow from the jet spray gun and when the nanoparticle struck the ceramic membrane during coating. This was done after repeated trials and by taking the average time t_3, and assuming that the average time flow at a constant speed V_3. The average distance travelled by the nanoparticle during jet spray coating can be received from the speed formula $S_3 = V_3 t_3$. Therefore, the distance covered by nanoparticles during jet spray coating is given as:

$$\Delta S = S_3 - S_1 = \frac{M_3 t_3}{\rho A_3} - S_1 \tag{3}$$

The change of distance covered by nanoparticles during coating can be computed by looking at the specific capacity from the jet spray gun given by assuming a limit of a function. This function depends on a single point (x,y) at the injection point of the jet spray gun given as the specific capacity $q$which is given as $q = \lim_{\Delta s \to o} \frac{\Delta Q}{\Delta S}$, where ΔQ defines the nanoparticle flowing through the surface of the jet spray gun during coating. Δs is the faction of the coated surface.

The function of specific capacity during jet spray coating depends on the angular distribution of the jet spray gun during coating and is given as:

$$q_\theta = \frac{\partial Q}{\partial \theta} \tag{4}$$

where ∂Q is the capacity of variation of nanoparticles during jet spray coating and $\partial \theta$ is the angular variation of the jet spray gun during nanoparticle coating. The change in the capacity of variation of nanoparticles and the variation of the angle of the jet spray gun impact membrane clusters, and it must be studied for an optimal operation that decreases the formation of clusters during jet spray coating. From Bernoulli's equation, we can get the change in pressure during jet spray coating, impacting the speed of nanoparticles at different coating angles that impact the formation of membrane clusters. The volume flow rate between the two points can be given by the continuity equation, $V_2 = (A_1 V_1 / A_2)$. The change in pressure during jet spray coating is given as:

$$\Delta P = \frac{1}{2}\rho \left[\frac{A_1}{A_2} V_1\right]^2 - \frac{1}{2}\rho V_1^2 \tag{5}$$

where ρ is the density of nanoparticles and V_1 is the velocity of nanoparticles at entrance A_1 in the jet spray gun and A_2 is the area of the jet spray gun at the discharge. The derived model of the function of coating pressure, coating angle of the jet spray gun and the distance moved by the nanoparticles through the spray region during coating, was tested on the model of nanoparticle coating and scattering of

nanoparticles on the ceramic membrane surface and on the model of surface energy-driven separability as derived by Sob et al. (2019) and is given by equation (6) to (8) as:

$$r = r_0 - \frac{2\lambda}{\lambda + n} r_p \quad \text{(Sob } et\ al.\text{, 2019)} \tag{6}$$

where r_0 is the size of the aperture without coated nanoparticles, λ the density of nanoparticles coated on the membrane channel and n the maximum number of particles that can be coated on the membrane channel surface to give a complete membrane smoothness that leads to the lowest surface energy.

$$n = \frac{2r\, r_p - r_p^2}{r_p^2} \quad \text{(Sob } et\ al.\text{, 2019)} \tag{7}$$

$$denergy = \frac{PA_1S_3}{A_3} = \frac{PA_1}{2\rho r} = \frac{\mathrm{P.r}}{2} \quad \text{(Sob } et\ al.\text{, 2019)} \tag{8}$$

From expression (6), the effect of the nanoparticle size r_p can be inferred. It should be recalled that the nanoparticles are coated on the internal surface of the membrane channel with some spacing between them. Equations (1-8) are solved simultaneously using engineering equation solver software (f-chart software, madison, w153744, USA and the results are presented and discussed below. Fig.3.5 depicts different sizes of nanoparticle clusters on a membrane surface and their effect on inter-separation distances. The bigger the clusters the smaller the inter-separtion distances indicating a rough membrane surface and vice-versa.

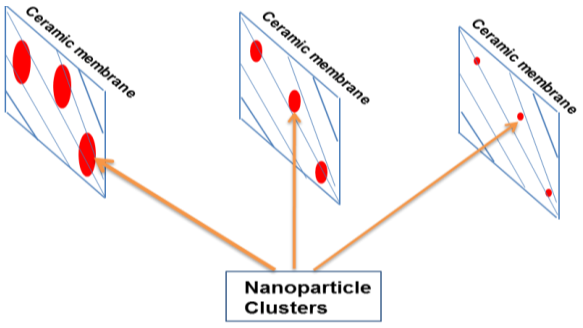

Figure 3.5 Schematic diagram of ceramic membrane surfaces with different cluster sizes

The proposed models derived in this study were tested with the following data from Sob et al (2019), ρ = 1000 kg/m^3, h = 6.626 x 10^{-34} J.s, μ = 0.000720 m^2/s, S_1 = 0.3 m, Vvol = 0.12 m^3, t_2 = 150 sec, t_3 = 120 sec, A_1 = 0.08 m, A_2 = 0.04 m, F = 100 KN. ρ = 1000, S_1 = 0.3, V = 200 m/s, t_2 = 3 sec, t_3 = 1 sec, σ = 0.002, A_1 = 0.08 m^2, A_2 = 0.04 m^2, F = 100 KN. The obtained results will be presented and discussed in Chapter four.

3.3.2 Experimental Approach

3.3.2.1 Ceramic sample preparation for Nanoparticle Coating

Ceramic hydrophobic nano4stone nanoparticles, ceramics and spray gun were purchased for the experiment. A quantity of half a kilogram ceramic samples were crushed into small grain sizes of 8 mm^{2,} using a ceramic crusher, see Fig.3.6 (a). The sample sizes were measured using a vernier caliper. Ceramic material was washed with a pre-clean detergent two times to remove foreign particles, which may result in preventing proper blending of nanoparticles on the membrane during coating, as shown in Fig. 3.6 (b). Ceramic material was then allowed to dry under room temperature for 24 hours, as shown in Fig. 3.6 (c).

Before coating, the uncoated ceramic membrane samples were put separately in a zip-lock plastic bag to be sent for microscopic analysis, as shown in Fig. 3.6 (f). Nano4Stone sample was put separately in a small plastic jar to be sent for microscopic analysis to observe all elements and identify the control element which will be monitored during result discussion, as shown in Fig. 3.6 (g).

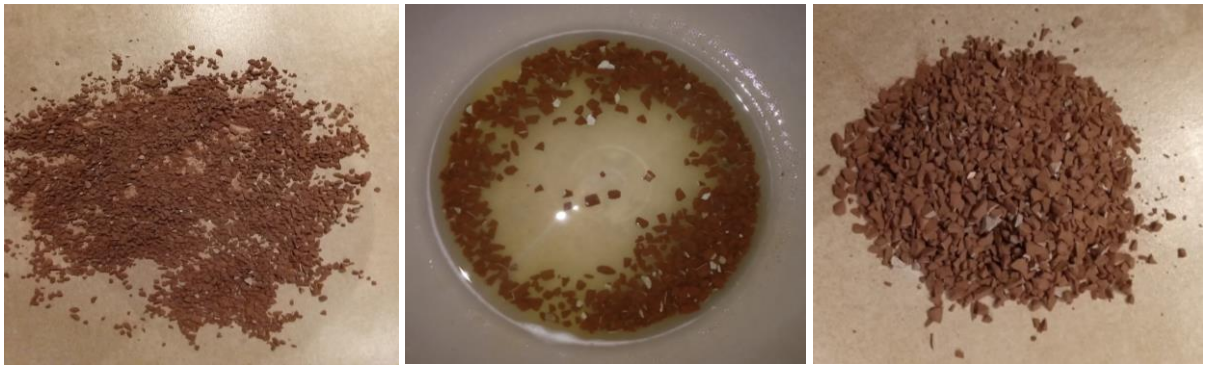

(a) (b) (c)

(d) (e) (f)

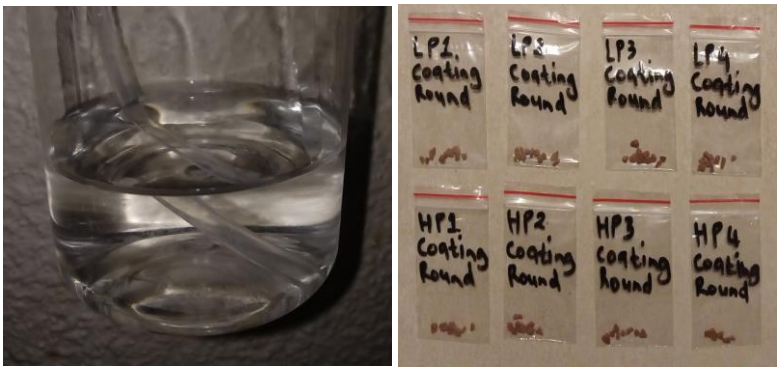

(g) (h)

Figure 3.6 (a) Crushed ceramic membrane (b) Ceramic membrane grains submerged in a pre-clean detergent (c) Ceramic membrane grains dried up after cleaning (d) Coating the ceramic membrane using jet spray coating (e) Drying up ceramic membrane samples after coating (f) Ceramic membrane control sample (g) Nano4Stone control sample (h) Parcelled ceramic membrane samples for microscopic analysis.

3.3.2.2 Manufacturing of ceramic membrane surface by jet-spray

Jet-spray coating was done under different coating rounds. During coating, the coating force was varied from $0{,}2x10^7$ kN to $2{,}4x10^7$ kN, the jet spray gun used for coating was varied between 10-24 mm away from the membrane surface at an angle between 1 to 9º with reference from the vertical axis to the membrane surface, as shown in Fig.3.6 (d). These parameters were maintained when coating all-ceramic beads. Four coating rounds were employed on different ceramic grains for both LP and HP. Membranes were coated in the following order: first coat, second coat, third coat and fourth coat for both HP and LP rounds. The coating was done in two minutes intervals between coating rounds for both LP and HP. After coating, the ceramic grains were dried up for 24 hours at room temperature, as shown in Fig. 3.6

(e). The coated ceramic membrane samples were then put separately in zip-lock plastic bags to be sent for microscopic analysis, as shown in Fig. 3.6 (h).

3.3.2.3 Sample Preparation for Microscopy (SEM, TEM and EDS)

Ceramic samples were not cleaned for microscopic analysis due to that the surface roughness of the hydrophobic nano4stone was the main parameter to be measured. These samples were embedded in epoxy resin blocks, and later, the thin section to be analysed was prepared. The holders in which the ceramic samples were placed for microscopy analysis were 25mm diameter round. The ceramic samples were electrically non-conducting during analysis, and a conducting surface coating was applied to provide a proper path for the incident electrons to flow to the ground during analysis.

The following EDS detectors were used to analyze 8 mm^2 ceramic, coated ceramic and hydrophobic nanoparticles (Thermo Scientific, USA), a 10 mm^2, SDD (Bruker, Germany), a 100 mm^2, SDD (Thermo Scientific, USA), with an annular 60 mm2 Flat QUAD SDD (Bruker, Germany). The SDD annular is being inserted between the pole shoe and the experimental sample to give a very large solid angle of the X-rays being emitted by the sample. For the TEM analysis, the samples were not polished since the coated nanoparticles were on the surface of the membrane. A standard TEM thin foil 3mm in diameter were prepared for analysis by electrolytic twin-jet (at −30ºC, 30 V) in Struers Tenupol 2 filled with 6% solution of perchloric acid in methanol. It was imperative to analyze the uncoated sample for ceramic membrane and its descriptive statistical analysis to detect elements in it and to observe the surface properties.

3.3.3 Comparison of the newly designed ceramic membrane with the previously designed ceramic membrane from previous the literature

Correlation will be done between the current results obtained in this study with the results obtained from the previous literature to demonstrate the improvement from the newly designed ceramic membrane. The parameters modelled during manufacturing of the nanostructured ceramic membrane in this study will be compared with the parameters modelled during manufacturing of the nanostructured ceramic membrane from the previous literature. Wettability tests conducted by the previous researchers will be observed and the parameters they used to validate their membranes will be also be observed.

3.3.4 Summary of the Methodology

This chapter was intended to discuss the research methodology, which forms the foundation of any research study. The chapter shows that the study employed the relevant theoretical models in modelling surface energy-driven separability. The stochastic effects of nanoparticle size, the morphology of membrane channels and spatial distribution of membrane on surface energy were studied in this part of the thesis for efficient and stable wettability. The relationship between surface tension and surface energy in membrane viscous flow during oil/water separation was also examined for the design of the current membrane technology with more controlled wettability. The relationship between parameters of flow during nanoparticle coating and surface energy-driven separability during oil/water separation was also analysed for a stable wettability process.

Membrane dynamic forces on surface energy and their impact during oil/water separation were also analysed to be applicable in the design of the current membrane technology. Membrane inter-separation distances during nanoparticle scattering were also modelled theoretically to obtain the optimal inter-separation distances that gave optimal wettability, as revealed in this part of the dissertation. A new membrane technology, which is efficient with stable wettability during oil/water separation, was established after the theoretical models were developed in the methodology. The relevant engineering simulation was done using Engineering Equation Solver (EES).

The nanostructured ceramic membrane was done using jet-spray coating under different coating rounds. During coating, the following parameters were monitored, the coating distance was varied between 10-24 mm to achieve optimal coating distance, the coating angle was varied between 1 to 9º with reference from the vertical axis to the membrane surface to achieve optimal coating angle. These parameters were maintained when coating all-ceramic beads. Four coating rounds were employed on different ceramic grains for both LP and HP coating. Membranes were coated in first coat, second coat, third coat and fourth coat for both HP and LP rounds of coating. The coating was done in two minutes intervals between coating rounds for both LP and HP.

Correlation was be done between the current results obtained in this study with the results obtained from the previous literature to demonstrate the improvement from the newly designed ceramic membrane. The parameters modelled during manufacturing of the nanostructured ceramic membrane in this study were compared with the parameters modelled during manufacturing of the nanostructured ceramic membrane from the previous literature.

CHAPTER FOUR

RESULTS AND DISCUSSION

4.1 Theoretical modelling and simulation of surface energy-driven separability

In this section, the theoretical results obtained during modelling and simulation is discussed. The impact of membrane surface clusters during jet spray coating is discussed together with different parameters that led to a decrease in these clusters.

The obtained results are shown in Fig.4.1 (a-b) revealed the relationship between total force during jet spray coating and jet spray distance and cluster sizes during the coating process. It was revealed, as shown in Fig.4.1 (a-b), that increasing the total force and coating distance in the jet spray gun, the sizes of membrane clusters increases, as shown in Fig. 4.1 (b). This is because the mobility of nanoparticles vibrates at a higher deposition speed during the coating process. This impacts the scattering of nanoparticles, which creates more membrane clusters during the the coating process. It was also shown that as the coating distance increases with coating total force in the jet spray gun, an optimal coating distance gave optimal membrane cluster minimization during the coating process, as shown in Fig. 4.1 (a-b).

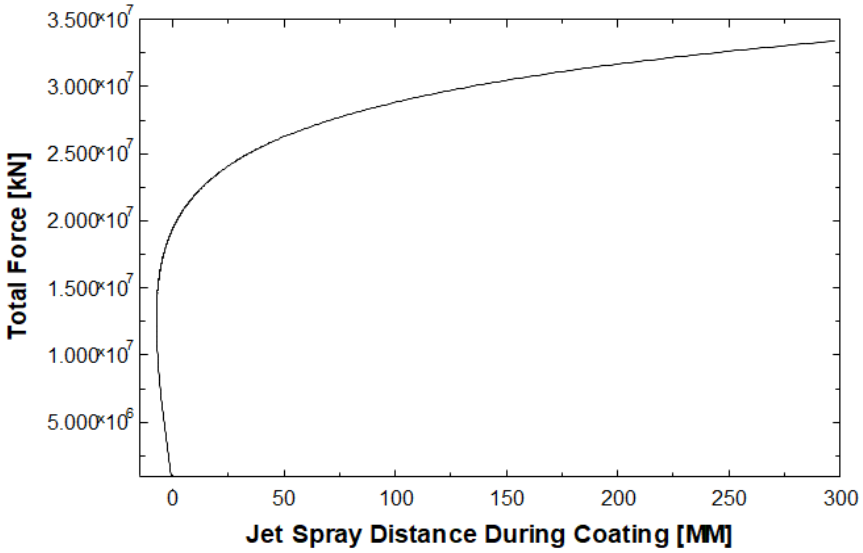

(a)

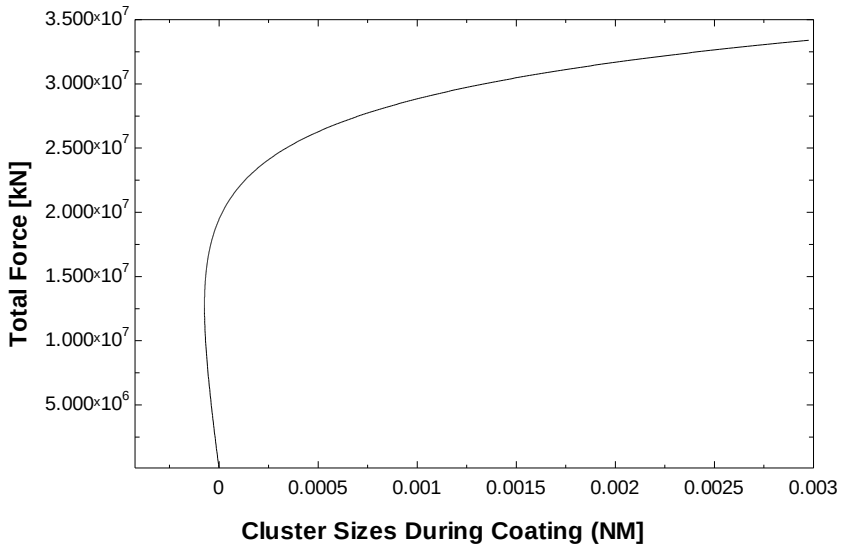

(b)

Figure 4.1 (a) Jet spray distance during coating [cm] against Total Force from the jet spray gun [kN] (b) showing cluster sizes during coating [nm] against Total Force from the jet spray gun during coating [kN]

The cluster size minimization also gave uniform scattering of nanoparticles on the membrane surface, giving a smooth membrane surface and a lowered surface energy to increase membrane wettability. This can be explained as the coating process began, more membrane clusters were created, which created a rough membrane surface. As more coating processes took place, a rough membrane surface became a smooth membrane surface because the increase in formation of membrane clusters was stabilized, which led to the creation of smooth membrane surfaces that lowered surface energy and increased membrane wettability. The relationship between jet spray angle during coating and total force during coating and their impact on the change in cluster size is revealed in Fig. 4.2 (a-b). The results revealed an increase in jet spray angle and total force in the jet spray during coating to an optimal level, accompanied by a decrease during the coating process. The increase in coating angles and total forces to an optimal level shown in Fig. 4.2 (a) led to a decrease in cluster sizes during the coating process, as shown in Fig. 4.2 (b). It was revealed, as shown in Fig. 4.2 (b), that during the initial process of jet spray coating, more membrane clusters were created, which revealed the initial increase, which was accompanied by a continuous decrease at the optimal point during the coating process. The reason for the initial increase, which was accompanied by a decrease, was because during the initial process of coating, more clusters were created on the membrane surface.

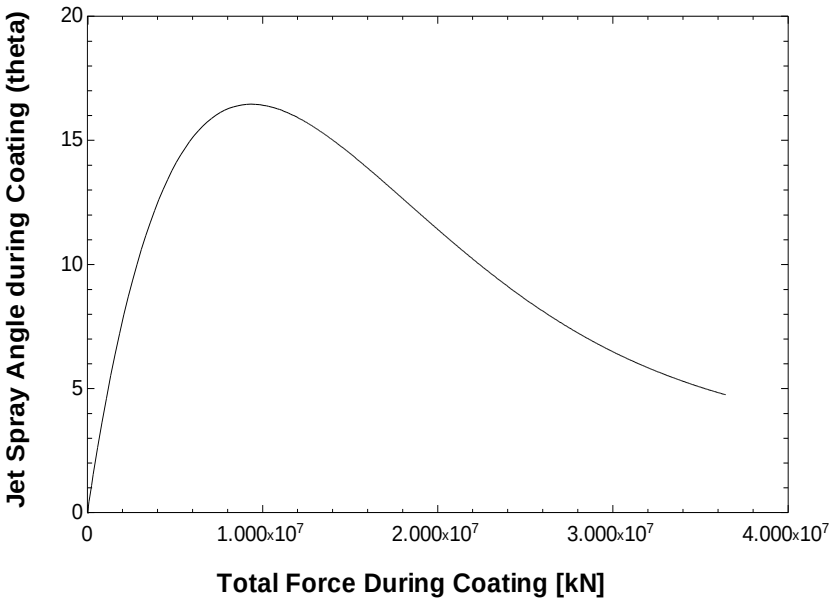

(a)

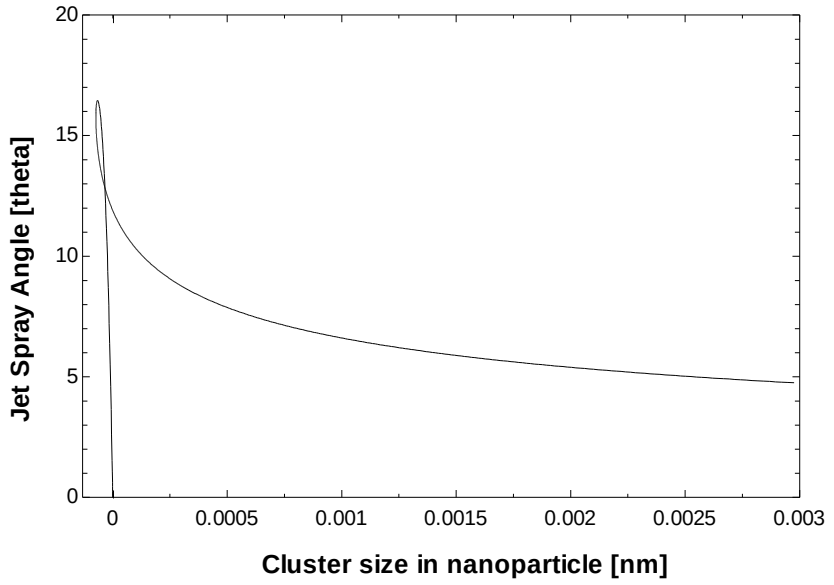

(b)

Figure 4.2 *(a) jet spray angle during coating [theta] against Total Force from the jet spray [kN] (b) showing Jet spray angle during coating [theta] against Cluster sizes during coating [nm].*

As more coating took place, these clusters were being minimized since the required coating force was produced to minimize the surface cluster on the membrane surface. Therefore, at optimal coating forces, optimal coating distance and at optimal coating angles, membrane clusters were minimized. Membranes with minimized clusters leads to smoother surfaces with lowered surface energy and improved surface wettability (Cai *et al.*, 2016) (Zhou *et al.*, 2015). The formation of membrane clusters during the initial coating process created a more rough membrane surface, which increased surface energy. As the coating

pressure and angles increased during coating, these clusters were minimized since the rough surfaces became smooth surfaces. This resulted in a lowered surface energy with improved membrane surface wettability, as shown in Fig.4.3 (a-b). It was revealed that membrane surface energy increased to $1{,}8x10^8$ Joules, which is an optimal level of surface energy on a rough surface. This was because when rough membrane surfaces were initially generated during the initial process of jet spray coating, the membrane surface energy immediately increased, which decreased surface wettability. At the optimal point of coating when the membrane surface clusters began to minimize, rough membrane surfaces became smooth surfaces which lowered surface energy to $1{,}0x10^8$ Joules and increased membrane wettability during oil-water separation. The change in membrane clusters also impacts the aperture sizes, see Fig.4.3 (b). This is due to that the degree of surface roughness to smoothness during cluster minimization leads to a decrease in aperture sizes, which lowers surface energy and improves surface wettability.

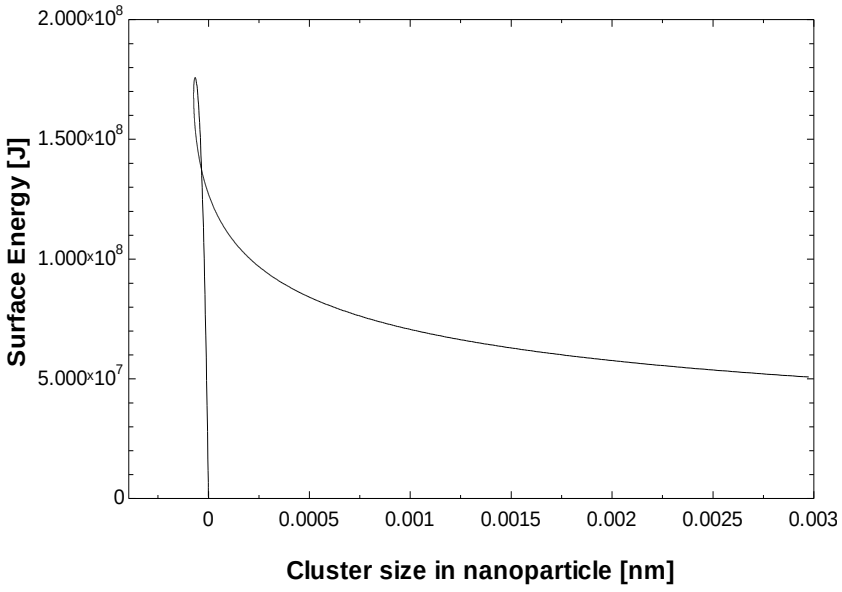

(a)

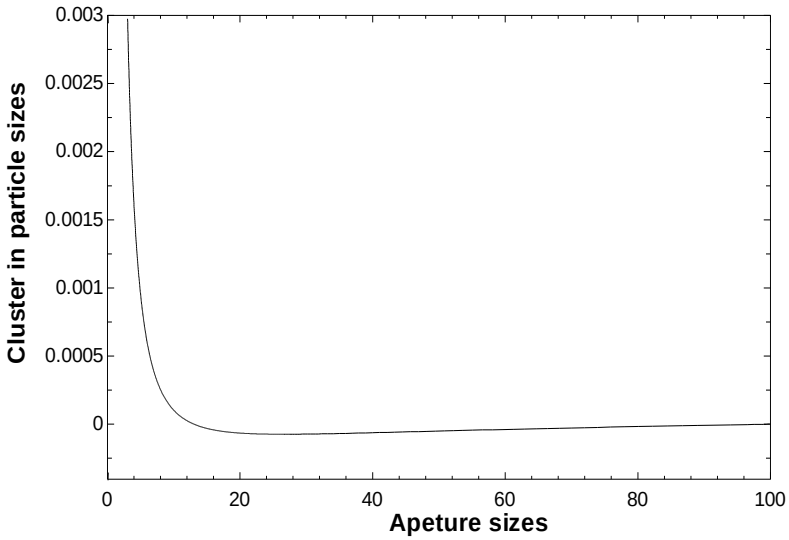

(b)

Figure 4.3 *(a) surface Energy [J] against Cluster sizes in nanoparticles during coating [nm] (b) showing cluster particle sizes during coating [nm] against aperture sizes during coating.*

4.2 Fabrication of ceramic membrane with minimized surface clusters for improved surface smoothness and increased wettability during oil-water separation

The current section of this dissertation provides an introduction and background as well as an outline of the new strategy to minimize membrane clusters and increase membrane wettability. This section broadens the understanding of the newly designed membrane with fewer surface clusters that led to smoother membrane surfaces with lowered surface energy and increased membrane wettability. The section deals with the experimental items, experimental setup, membrane materials, nanoparticle coating and microstructural analysis of the nanoparticles on the coated membrane surface. The section also revealed the main coating parameters that impact membrane clusters during coating, such as the coating force, coating distance and coating angle to be measured when coating the membranes in different coating rounds. The orientation of nanoparticles, surface morphology, surface spread, spatial distribution and size of nanoparticles were observed with the behaviour of fluorine (F) element on the membrane surface during coating. The scattering of F on the membrane was also observed in different coating rounds. The surface homogeneity and inhomogeneity were also observed in all coating rounds.

4.2.1 Ceramic control sample

The EDS and Statistical analysis revealed seven elements that were noticed on the ceramic control sample. The EDS shows the variation of intensity and kilo electrons volt (keV) on a full scale during EDS analysis, while the statistical analysis results revealed five spectrums (spectrum 1, spectrum 2, spectrum 3, spectrum 4 and spectrum 5) on which data was captured. The statistical analysis depicted different mean, standard deviation, max and min, which correspond to the varying peak, max spread, and min spread. The observed elements in both EDS and statistical analysis are oxygen (O), sodium (Na), magnesium (Mg), aluminium (Al), silicon (Si), potassium (K) and iron (Fe). These elements consist of different atomic numbers, electronegativity, oxidation states, atomic mass, chemical symbol, name and electron configuration. Spectrum 1 was chosen as a reference of analysis on the statistical analysis for all analyses in this dissertation. The ceramic sample was reported to have a very high content of oxygen, followed by silicon, iron and aluminium, as shown in Table 4.1. Sodium was reported to have the least content, followed by magnesium and potassium, as shown in Table 4.1. A good correlation can be seen between the results of EDS and statistical analysis. Oxygen was observed to have the highest peak or intensity, followed by Silicon, Iron, Aluminium, Potassium, Magnesium and Sodium.

Table 4.1: Composition of elements in the surface layer formed in the ceramic control sample.

ESD setting.

MAOME Project 1	Project	Owner	Site:	Sample	ID
	MAOME Project 1	INCA Operator	Site of Interest 2	CERAMIC Control Sample	CERAMIC Control Sample

Descriptive statistics

Spectrum	**In stats.**	**O**	**Na**	**Mg**	**Al**	**Si**	**K**	**Fe**	**Total**
Spectrum 1	Yes	53.26	0.33	0.36	9.37	24.19	2.03	10.47	100.00
Spectrum 2	Yes	51.92	0.36	0.26	11.25	26.56	2.86	6.78	100.00
Spectrum 3	Yes	53.16	0.37	0.38	11.07	24.07	2.54	8.41	100.00
Spectrum 4	Yes	53.46	0.39	0.42	11.62	24.02	2.99	7.09	100.00
Spectrum 5	Yes	54.52	0.67	0.39	9.75	25.40	2.45	6.82	100.00
Mean		53.26	0.43	0.36	10.61	24.85	2.57	7.91	100.00
Std. deviation		0.93	0.14	0.06	0.99	1.12	0.38	1.57	
Max.		54.52	0.67	0.42	11.62	26.56	2.99	10.47	
Min.		51.92	0.33	0.26	9.37	24.02	2.03	6.78	

All results in weight %

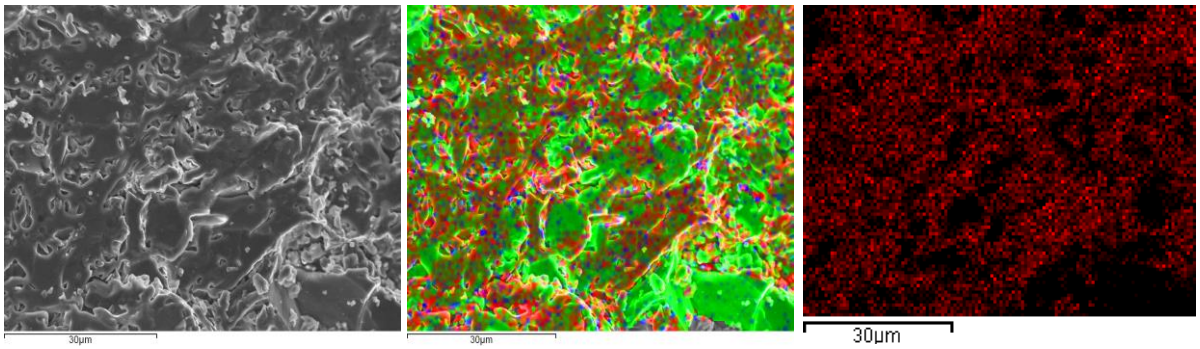

(a) (b) (c)

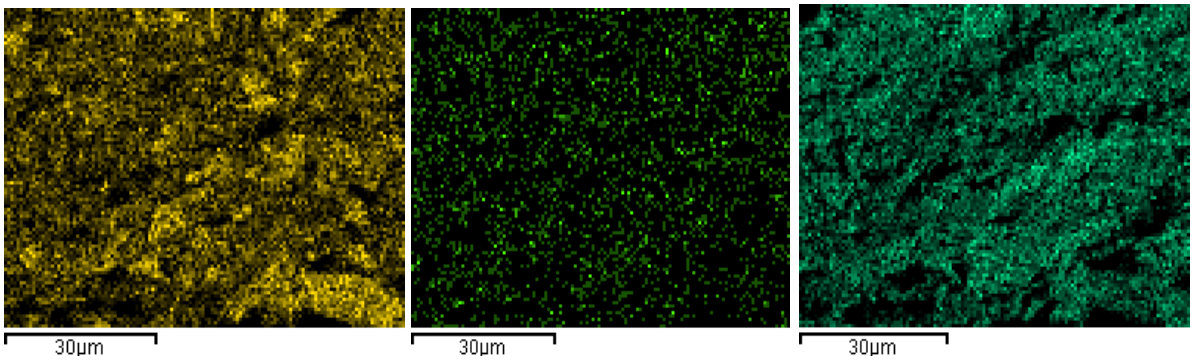

(d) (e) (f)

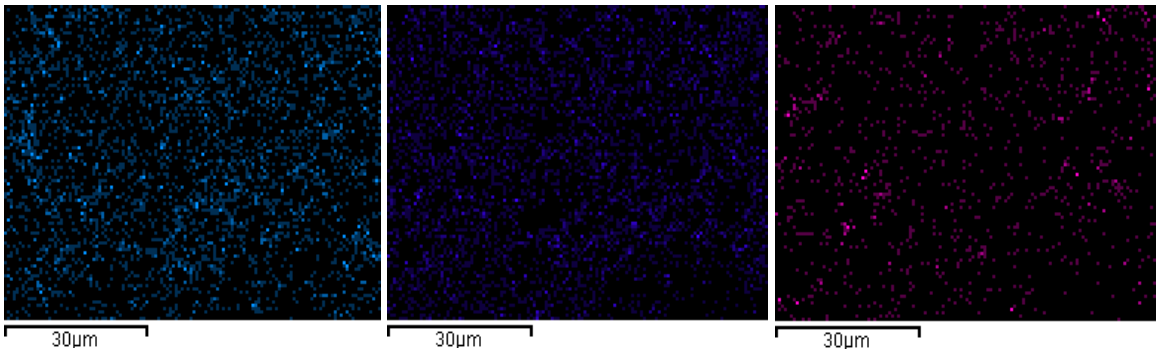

(g) (h) (i)

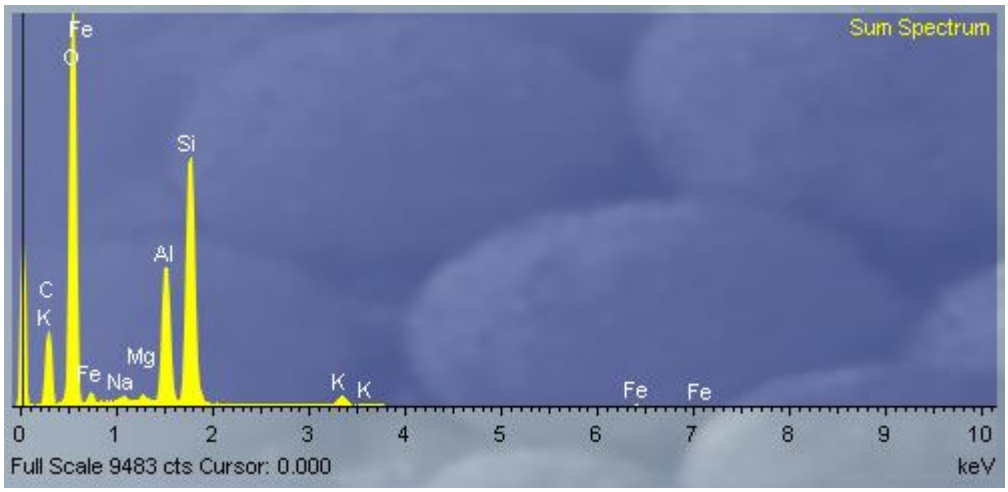

(j)

Figure 4.4(a-j) Ceramic control sample with different elements (a) Reference image (b) Mix showing all elements on the membrane surface (c) element Al (d) element Si (e) element Na (f) element O (g) element Mg (h) element K (i) element Fe and (j) Energy dispersion X-ray spectroscopy.

It was important to analyse the composition of hydrophobic nano4stone for ceramic used in membrane coating. The results for EDS and statistical analysis are depicted in Fig.4.5.

4.2.2 Nanoparticles control sample

It is observed from hydrophobic nano4stone control samples that four main elements are found, as shown in Table 4.2. These elements are oxygen (O), fluorine (F), silicon (Si) and sulphur (S). It is observed, as shown in Table 4.2, that there is a new element, Fluorine (F) which is not found in ceramic control samples. The nano4stone control sample was reported to have a very high content of fluorine, followed by oxygen, silicon and sulphur being the least element, as shown in Table 4.2. Fluorine (F) is the main element of hydrophobic nanoparticles, which created membrane hydrophobicity during the oil/water separation process. Therefore, F was the main scattering element that varied during HP and LP coating rounds. Therefore, the morphology, sizes, shape, orientation, and spatial distribution of F was changing during the coating rounds. This affected membrane clusters, resulting in different inter-separation distances of nanoparticles and surface clusters on the membrane surface, which impacted surface tension and surface energy.

Table 4.2: Composition of elements in the surface layer formed in Nano4Stone control sample.

ESD setting.

MAOME Project 1	Project	Owner	Site:	Sample	ID
	MAOME Project 1	INCA Operator	Site of Interest 2	Nano4Stone	Nano4Stone

Descriptive statistics

Spectrum	**In stats.**	**O**	**F**	**Si**	**S**	**Total**
Spectrum 1	Yes	32.54	57.01		10.45	100.00
Spectrum 2	Yes	22.92	71.20		5.87	100.00
Spectrum 3	Yes	24.82	61.88	7.13	6.18	100.00
Max.		32.54	71.20	7.13	10.45	
Min.		22.92	57.01	7.13	5.87	

All results in weight %

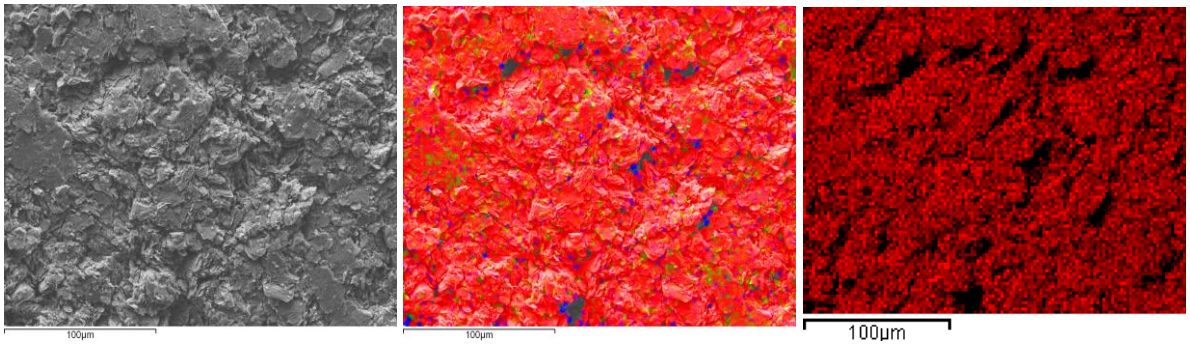

(a) (b) (c)

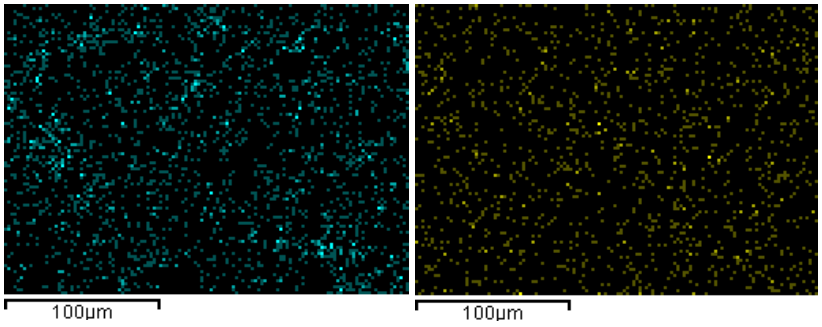

(d) (e)

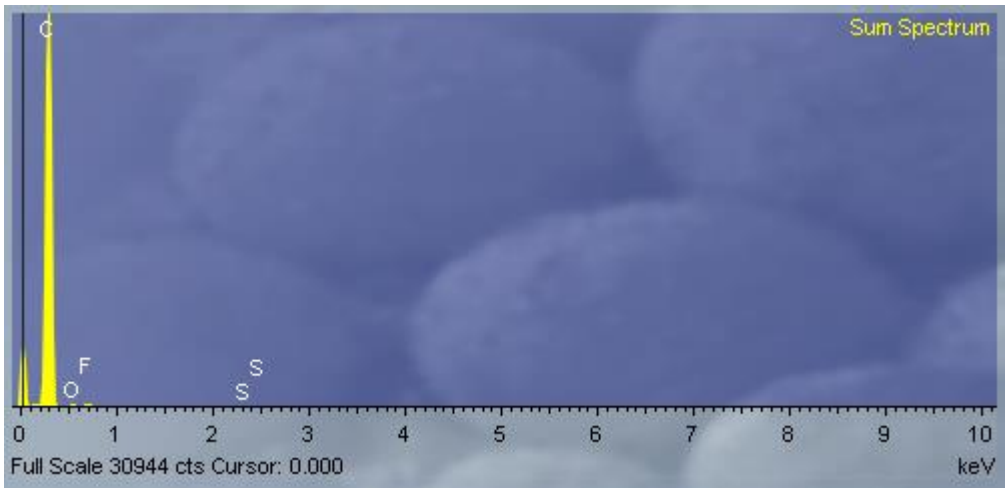

(f)

Figure 4.5(a-f) nano4stone control sample with different elements (a) Reference image (b) Mix showing all elements on in the Nano4stone control sample (c) element C (d) element F (e) element Si (f) Energy dispersion X-ray spectroscopy.

Since both control samples have been tested and analysed using SEM, it is now necessary to examine the rounds of HP and LP coating.

4.2.3 LP Coating Round 1

In Fig.4.6, the SEM and EDS results of the membrane surface layer formed on the ceramic membrane after the 1st round of hydrophobic nanoparticle LP coating are presented. All SEM photos show different spread of surface density of oxygen (O), iron (Fe), sodium (Na), magnesium (Mg), aluminium (Al), silicon (Si) and potassium (K) on the ceramic membrane surface. Oxygen was observed to have the highest peak or intensity, followed by Silicon, Aluminium, Iron, Potassium, Fluorine and Magnesium, while Sodium was observed to have the lowest peak or intensity. Clusters were observed on the reference image and mixed F element as shown in Fig.4.6(a) and 4.6(b). The cluster sizes are bigger, resulting in an inhomogeneous surface. The inter-separation distances are bigger, and morphology, spatial distribution, orientation, size and shape of the F element keeps changing on the surface. The size of clusters is big, and this indicates a rougher surface on the membrane, and this doesn't improve membrane wettability on the surface when related to the lotus effect on surface wettability. The lotus effect states that for enhanced wettability, the coated membrane surface must be smooth (Sob *et al.*, 2020) (Sob*et al.*, 2019) (Hurwitz *et al.*, 2010) (Quéré, 2008) (Miwa *et al.*, 2000). The wettability of coated membrane is characterized by measuring contact angles (Gao *et al.*, 2011).

Table 4.3: Composition of elements in the surface layer formed in ceramic 1st round LP after PEO

ESD setting

MAOME Project 1	Project	Owner	Site:	Sample	ID
	MAOME Project 1	INCA Operator	Site of Interest 2	CERAMIC 1 LP Type	CERAMIC 1 LP

Descriptive statistics

Spectrum	In stats.	O	F	Na	Mg	Al	Si	K	Fe	Total
Spectrum 1	Yes	48.50	1.98	0.31	0.38	10.45	29.35	2.97	6.07	100.00
Spectrum 2	Yes	56.27	2.85	0.40	0.35	8.95	24.39	2.02	4.76	100.00
Mean		52.39	2.42	0.35	0.36	9.70	26.87	2.49	5.42	100.00
Std. deviation		5.50	0.61	0.07	0.02	1.06	3.51	0.67	0.92	
Max.		56.27	2.85	0.40	0.38	10.45	29.35	2.97	6.07	
Min.		48.50	1.98	0.31	0.35	8.95	24.39	2.02	4.76	

All results in weight %

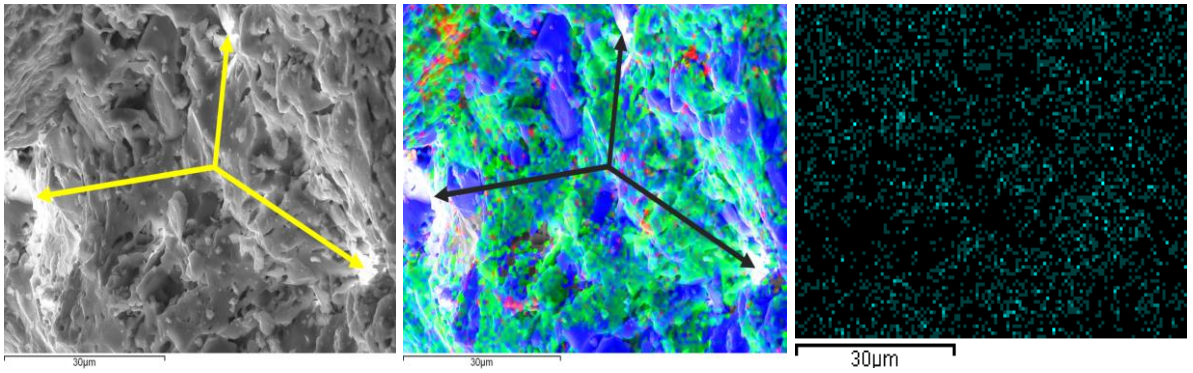

(a) (b) (c)

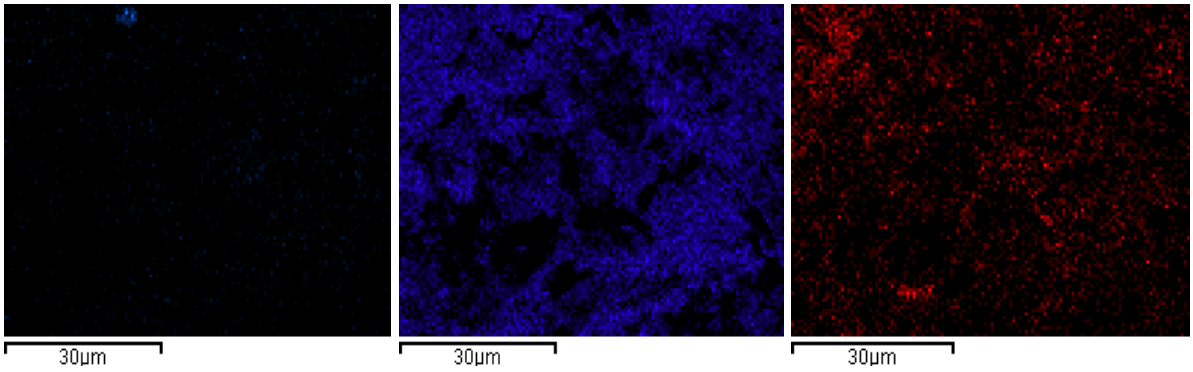

(d) (e) (f)

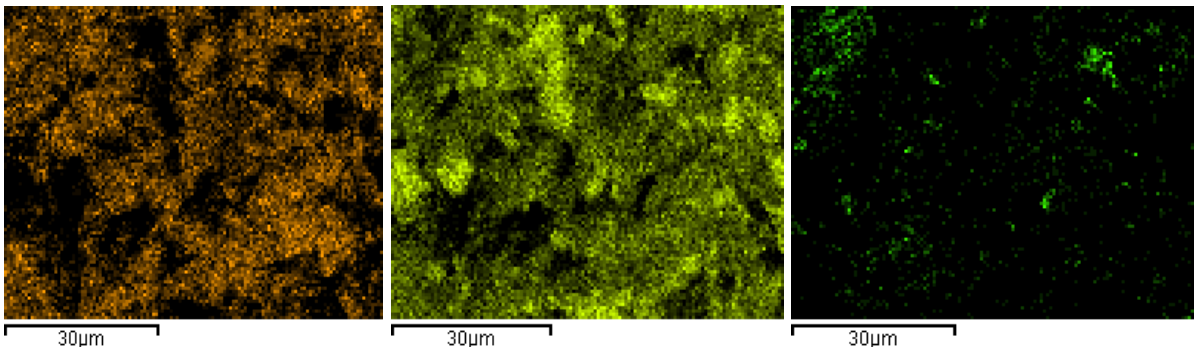

(g) (h) (i)

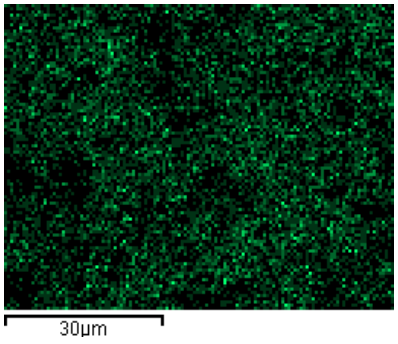

(j)

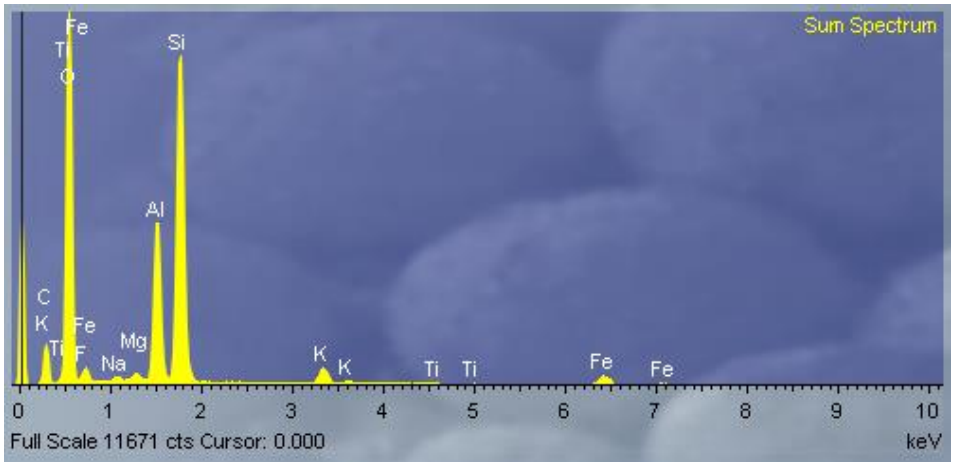

(k)

Figure 4.6(a-k) ceramic 1st LP coating with different elements (a) Reference image (b) Mix showing all elements on the membrane surface (c) element Na (d) element Mg (e) element O (f) element F (g) element Al (h) element Si (i) element Fe (j) element K (k) Energy dispersion X-ray spectroscopy.

Since the sizes of clusters are big on this membrane, indicating a rougher surface on the membrane, it was important to study the membrane surface after the 2nd round of LP coating, as shown in Table 4.4.

4.2.4 LP Coating Round 2

In Fig.4.7, the SEM and EDS results of the membrane surface layer formed on ceramic surface after 2nd round of hydrophobic nanoparticle LP coating are presented. All SEM photos show a different spread of surface density of O, F, Mg, Al, Si, K and Fe on the ceramic membrane surface. Oxygen was observed to have the highest peak or intensity, followed by Silicon, Aluminium, Potassium, Iron and Magnesium, while Sodium was observed to have the lowest peak or intensity. The 2rd LP coated surface with hydrophobic nanoparticles revealed a high concentration of O, followed by Si, Al, F, Fe, K, S, Na and Mg being the least, as shown in Table 4. This can be correlated with the EDS and statistical analysis results.

Additionally, more clusters are observed on the reference image and mix F element when compared with the 1st LP coating. The inter-separation distances are smaller when compared to 1st LP coating with a more visible distribution of clusters, nanoparticle morphology, nanoparticle spatial distribution, change in orientation of nanoparticle, change in sizes of nanoparticle and change in the shape of F. This is due to the fact that the coating distance and coating force were increased in this coating round as opposed to the 1st LP coating, in trying to identify the optimal levels of coating pressure for cluster minimization. This, however resulted in a rougher membrane surface, which affected wettability negatively.

Table 4.4: Composition of elements in the surface layer formed in ceramic 2nd round LP after PEO

ESD setting

MAOME Project 1	Project	Owner	Site:	Sample	ID
	MAOME Project 1	INCA Operator	Site of Interest 2	CERAMIC 2 LP Type	CERAMIC 2 LP

Descriptive statistics

Spectrum	**In stats.**	**O**	**F**	**Na**	**Mg**	**Al**	**Si**	**S**	**K**	**Fe**	**Total**
Spectrum 1	Yes	45.28	9.60	0.35	0.30	10.26	26.43	0.46	2.37	4.95	100.00
Spectrum 2	Yes	50.19		0.43	0.48	11.23	27.93	0.41	2.90	6.44	100.00
Spectrum 3	Yes	44.50	10.90	0.37	0.48	9.98	23.43	0.49	2.34	7.52	100.00
Spectrum 4	Yes	48.40	3.28	0.55	0.39	11.60	26.35	0.38	3.10	5.94	100.00
Spectrum 5	Yes	53.39		0.61	0.42	10.30	24.40		2.43	8.45	100.00
Mean		45.28	9.60	0.35	0.30	10.26	26.43	0.46	2.37	4.95	100.00
Std. deviation		0.00	0.00	0.00	0.00	0.00	0.00	0.00	0.00	0.00	
Max.		45.28	9.60	0.35	0.30	10.26	26.43	0.46	2.37	4.95	
Min.		45.28	9.60	0.35	0.30	10.26	26.43	0.46	2.37	4.95	

All results in weight %

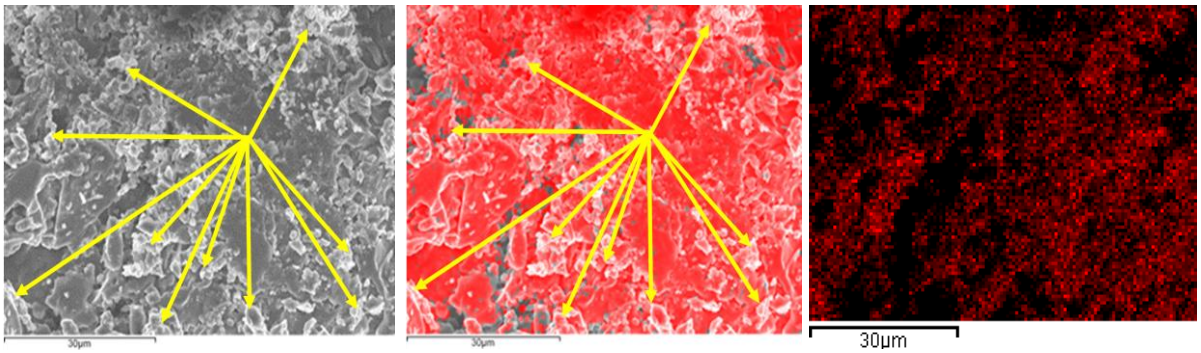

(a) (b) (c)

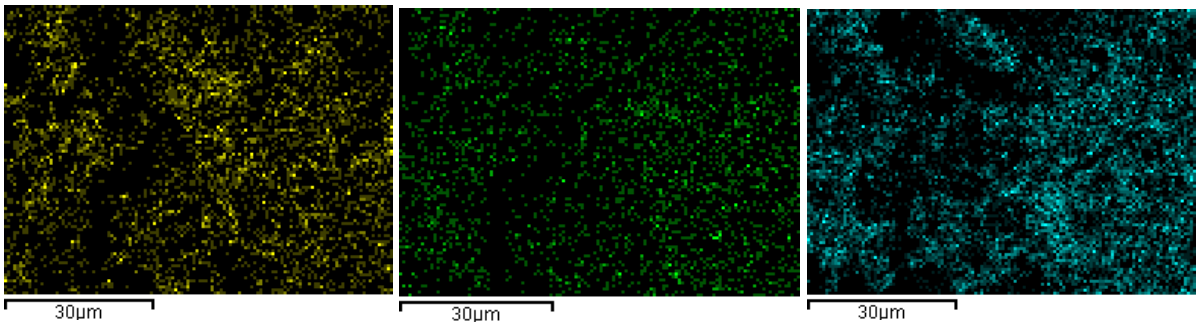

(d) (e) (f)

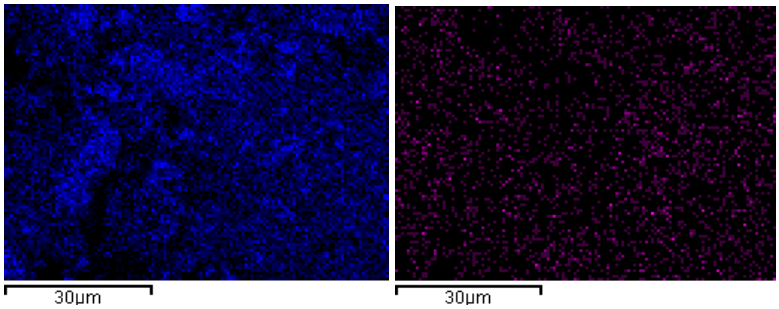

(g) (h)

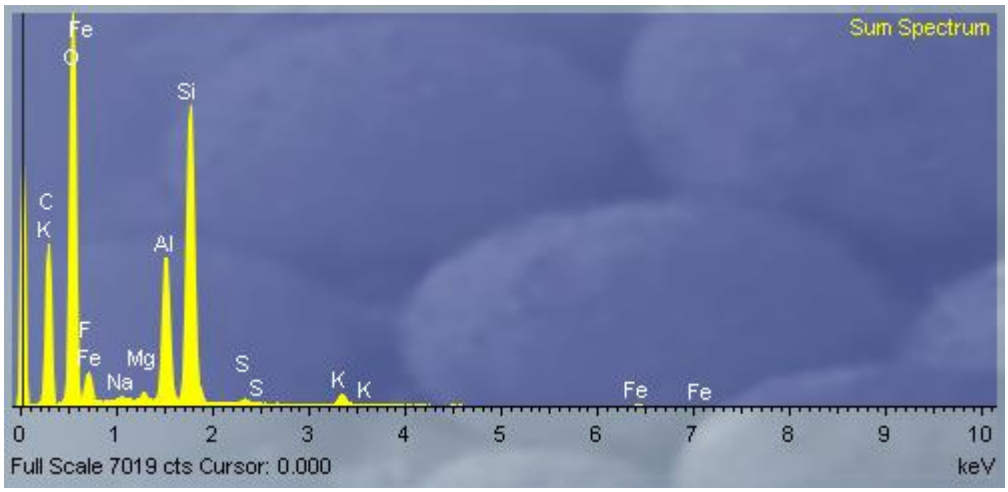

(i)

Figure 4.7(a-i) ceramic 2nd LP coating with different elements (a) Reference image (b) Mix showing all elements on the membrane surface (c) element O (d) element F (e) element Mg (f) element Al (g) element Si (h) element K (i) Energy dispersion X-ray spectroscopy.

Since more visible distribution of clusters were observed in this membrane, this resulted in a rougher membrane surface. It was therefore, necessary to observe the trend of results in LP 3rd round of coating as shown in Table 4.5.

4.2.5 LP Coating Round 3

In Fig.4.8, the SEM and EDS results of the membrane surface layer formed on ceramic surface after 3rd LP hydrophobic nanoparticle coating are presented. All SEM photos show a different spread of surface density of O, Si, Al, K, Ca, F, S and Na on the ceramic membrane surface. Oxygen was observed to have the highest peak or intensity, followed by Silicon, Potassium, Aluminium, Iron and Magnesium, while Sodium was observed to have the lowest peak or intensity. Clusters are observed on the reference image and mix F element but better than 1st LP and 2nd LP coating. On the coated hydrophobic nanoparticle mixed surface, the inter-separation distances are small when compared with 1st LP coating and 2nd LP coating. Moreover, the orientation of nanoparticles after 3rd LP coating differs from 1st LP coating and 2nd LP coating with small cluster sizes, and the shape of F keeps changing on the membrane surface. Although the inter-separation distances are small when compared with 1st LP coating and 2nd LP coating, there's still visible distribution of clusters. This is due to the fact that the coating distance, coating angle and coating force were increased furthermore in this coating round as opposed to the 1st LP coating and 2nd LP coating in trying to identify the optimal level of coating pressure for further cluster minimization. This authenticates why clusters are minimised better on the 3rd LP coating round as compared to the 1st LP coating and 2nd LP coating. Although the produced membrane after the 3rd LP

coating round had better minimised and small clusters, it was imperative to coat the 4th LP round to further produce a membrane with more minimised clusters to give the most enhanced surface wettability.

Table 4.5: Composition of elements in the surface layer formed in ceramic 3rd round LP after PEO

ESD setting

MAOME Project 1	Project	Owner	Site:	Sample	ID
	MAOME Project 1	INCA Operator	Site of Interest 2	CERAMIC 3 LP Type	CERAMIC 3 LP

Descriptive statistics

Spectrum	**In stats.**	**O**	**F**	**Na**	**Mg**	**Al**	**Si**	**S**	**K**	**Fe**	**Total**
Spectrum 1	Yes	44.03	8.23	0.36	0.52	11.26	26.65	0.44	3.56	4.95	100.00
Spectrum 2	Yes	49.98		0.50	0.47	12.46	25.46		3.28	7.86	100.00
Spectrum 3	Yes	40.34	22.01	0.49	0.35	8.80	20.60	1.20	2.14	4.06	100.00
Spectrum 4	Yes	45.14	3.20	0.46	0.51	11.12	29.09	0.61	3.16	6.71	100.00
Spectrum 5	Yes	51.86	3.59	0.57	0.44	9.85	24.51	1.42	2.17	5.59	100.00
Max.		51.86	22.01	0.57	0.52	12.46	29.09	1.42	3.56	7.86	
Min.		40.34	3.20	0.36	0.35	8.80	20.60	0.44	2.14	4.06	

All results in weight %

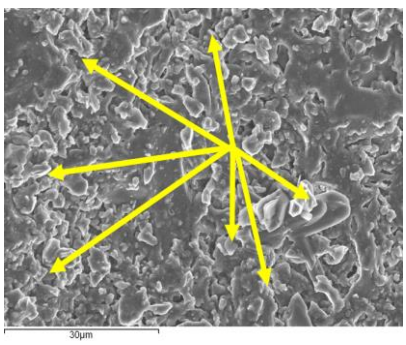

(a)

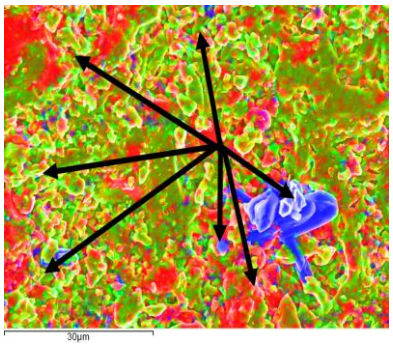

(b)

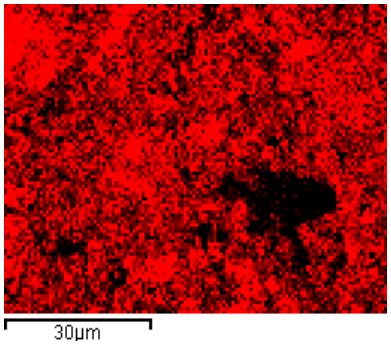

(c)

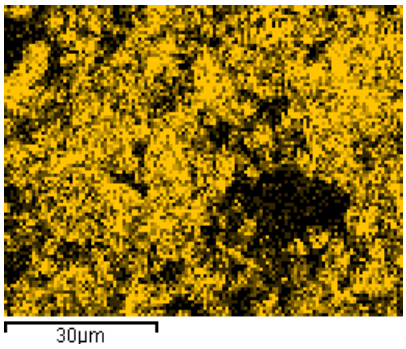

(d)

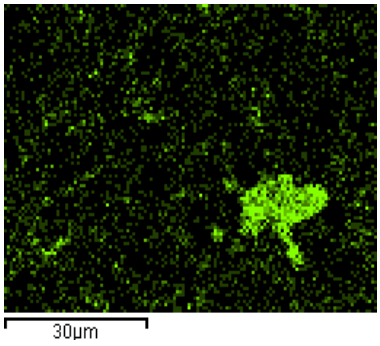

(e)

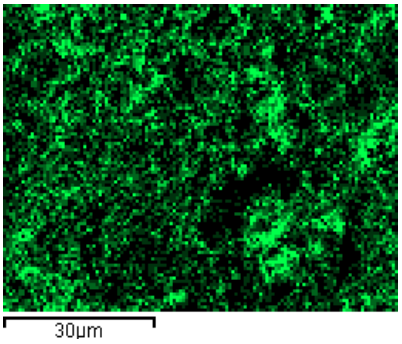

(f)

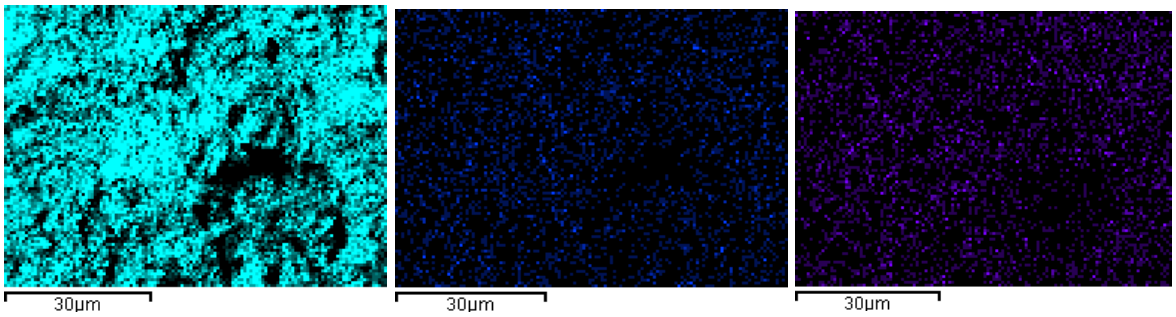

(g) (h) (i)

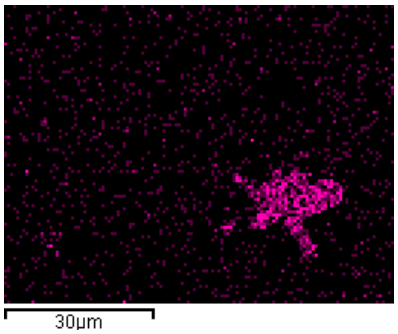

(j)

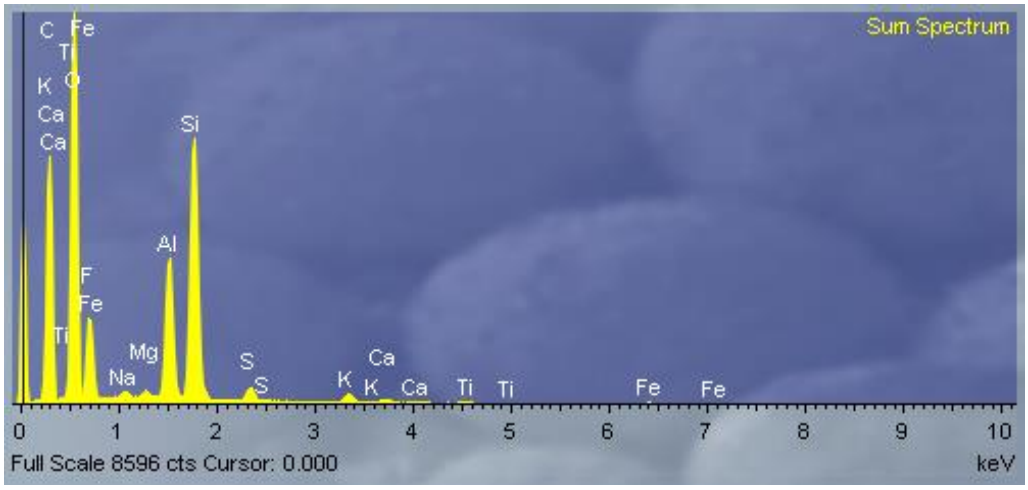

(k)

Figure 4.8(a-k) Showing ceramic 3rd LP coating with different elements (a) Reference image (b) Mix showing all elements on the membrane surface (c) element Si (d) element Al (e) element S (f) element F (g) element O (h) element Na (i) element K (j) element Ca (k) Energy dispersion X-ray spectroscopy.

Since there were still visible clusters on this membrane, this resulted in a rougher membrane surface. It was therefore, necessary to observe the trend of results in LP 4th round of coating as shown in Table 4.6.

4.2.6 LP Coating Round 4

In Fig.4.9, the SEM and EDS results of the membrane surface layer formed on ceramic surface after 4th LP hydrophobic nanoparticle coating are presented. All SEM photos show a different spread of surface density of O, Si, Al, F, K, and Na on the ceramic membrane surface. Oxygen was observed to have the highest peak or intensity, followed by Silicon, Potassium, Aluminium, Iron and Magnesium, while Sodium was observed to have the lowest peak or intensity. On the coated hydrophobic nanoparticle mixed surface, the inter-separation distances are small when compared with the 3rd LP coating. This gave more clusters observed on the reference image and mixed F element when compared with the 3rd LP coating. The coating distance and coating angle were decreased in trying to get the optimal levels of coating to get more clusters minimised. The pressure maintained in this coating round didn't reach the optimal level; therefore, it gave poor membrane wettability as compared to the 3rd LP coating. This therefore produced poor surface wettability on the membrane surface.

Table 4.6: Composition of elements in the surface layer formed in ceramic 4th round LP after PEO

ESD setting

MAOME Project 1	Project	Owner	Site:	Sample	ID
	MAOME Project 1	INCA Operator	Site of Interest 2	CERAMIC 4 LP Type	CERAMIC 4 LP

Descriptive statistics

Spectrum	**In stats.**	**O**	**F**	**Na**	**Mg**	**Al**	**Si**	**S**	**K**	**Fe**	**Total**
Spectrum 1	Yes	50.29	1.60	0.45	0.42	10.53	25.34	1.12	2.67	7.57	100.00
Spectrum 2	Yes	47.60	2.86	0.43	0.40	10.77	29.05	0.48	2.82	5.58	100.00
Spectrum 3	Yes	46.19	3.72	0.38	0.41	12.79	25.86	0.31	3.17	7.17	100.00
Mean		48.03	2.73	0.42	0.41	11.36	26.75	0.64	2.89	6.78	100.00
Std. deviation		2.08	1.06	0.04	0.01	1.24	2.01	0.42	0.26	1.05	
Max.		50.29	3.72	0.45	0.42	12.79	29.05	1.12	3.17	7.57	
Min.		46.19	1.60	0.38	0.40	10.53	25.34	0.31	2.67	5.58	

All results in weight %

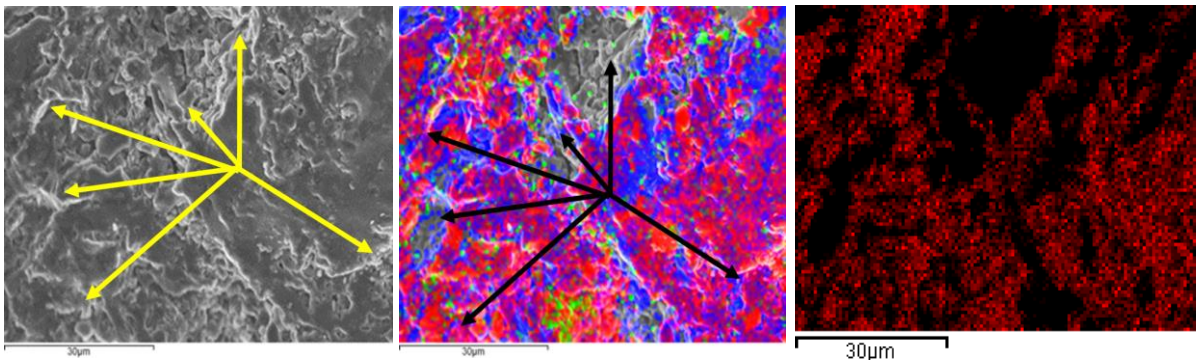

(a) (b) (c)

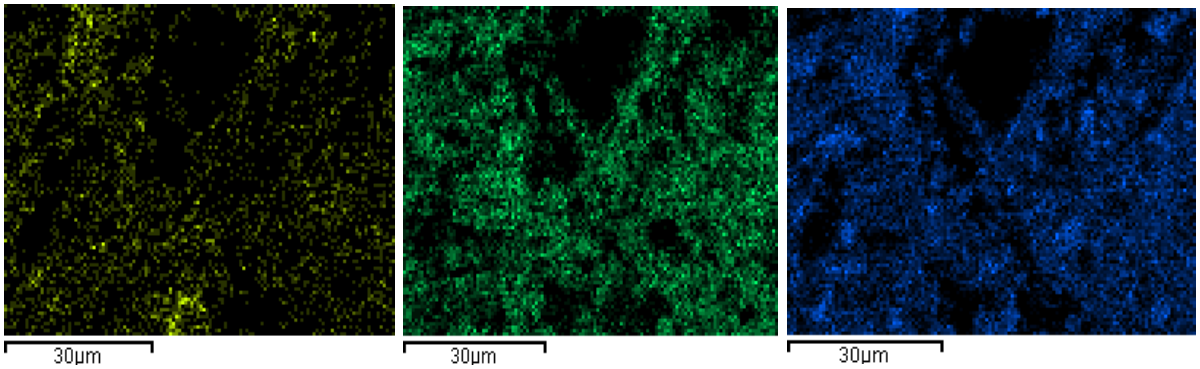

(d) (e) (f)

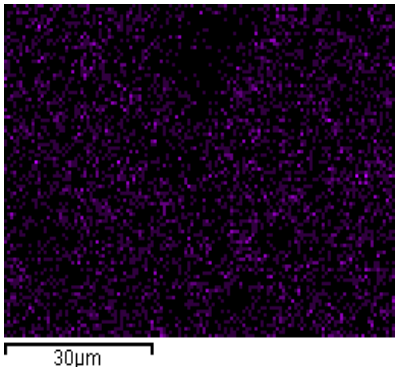

(g)

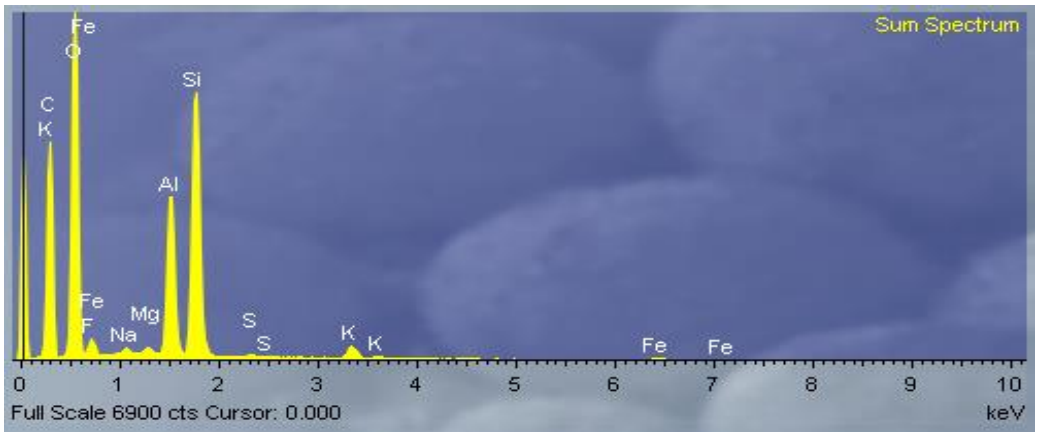

(h)

Figure 4.9(a-h) Showing ceramic 4th LP coating with different elements (a) Reference image (b) Mix showing all elements on the membrane surface (c) element O (d) element F (e) element Al (f) element Si (g) element K (h) Energy dispersion X-ray spectroscopy.

Since more clusters were observed on this membrane, it gave poor membrane wettability, resulting to poor surface wettability on the membrane surface. It was, therefore, important to study HP coating and its impact on wettability.

4.2.7 HP Coating Round 1

In Fig.4.10, the SEM and EDS results of the membrane surface layer formed on ceramic after 1st HP hydrophobic nanoparticle coating are presented. Spectrum 2 was chosen as a reference of analysis on the statistical analysis for 1st HP and 4th HP coating analysis due to that some elements were not detected on Spectrum 1, as shown in Table 4.7 and Table 4.10. All SEM photos show a different spread of surface density of O, Al, Si, Fe, K, Na, Mg and F on the ceramic membrane surface. Oxygen was observed to have the highest peak or intensity, followed by Silicon, Aluminium, Iron, Potassium, Fluorine, Sodium, and Magnesium, while Sulphur was observed to have the lowest peak or intensity. The surfaces coated with hydrophobic nanoparticles have high O, Si, Al, and Fe, which overpowered F, and this can be correlated with the EDS and statistical analysis results. Additionally, few clusters are observed on the reference image and mix F element when compared with 1st LP, 2nd LP, 3rd LP and 4th LP coating. The inter-separation distances are big, thus creating a rough membrane surface. The orientation of nanoparticles, morphology, spread, spatial distribution, and size of nanoparticles are changing with F on the membrane surface. The scattering of F shows an inhomogeneous surface. This is due to clusters that are observed on the surface. This resulted in a rough membrane surface being produced, and this impacted membrane wettability negatively. The pressure was increased in this coating round to reach the optimal level, but it was not high enough to maintain optimum cluster minimization. It gave better

membrane wettability as compared to a 1st LP, 2nd LP, 3rd LP and 4th LP coating, but still, clusters were observed on the membrane, resulting in an inhomogeneous membrane.

Table 4.7: Composition of elements in the surface layer formed in ceramic 1st round HP after PEO

ESD setting

MAOME Project 1	Project	Owner	Site:	Sample	ID
	MAOME Project 1	INCA Operator	Site of Interest 2	CERAMIC 1 HP Type	CERAMIC 1 HP

Descriptive statistics

Spectrum	**In stats.**	**O**	**F**	**Na**	**Mg**	**Al**	**Si**	**S**	**K**	**Fe**	**Total**
Spectrum 1	Yes	50.27		0.43	0.43	10.76	29.26		2.93	5.93	100.00
Spectrum 2	Yes	49.27	2.65	0.51	0.44	10.87	26.61	0.27	2.67	6.70	100.00
Spectrum 3	Yes	50.58	1.21	0.51	0.37	10.90	26.13		2.82	7.48	100.00
Spectrum 4	Yes	46.02	6.11	0.37	0.39	10.13	25.11	0.52	2.55	8.80	100.00
Spectrum 5	Yes	48.64	4.15	0.42	0.34	9.76	26.53		2.42	7.75	100.00
Max.		50.58	6.11	0.51	0.44	10.90	29.26	0.52	2.93	8.80	
Min.		46.02	1.21	0.37	0.34	9.76	25.11	0.27	2.42	5.93	

All results in weight %

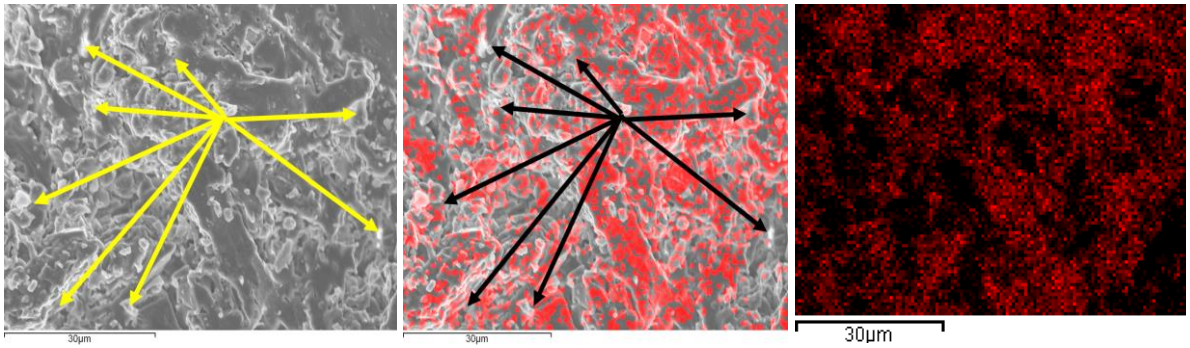

(a) (b) (c)

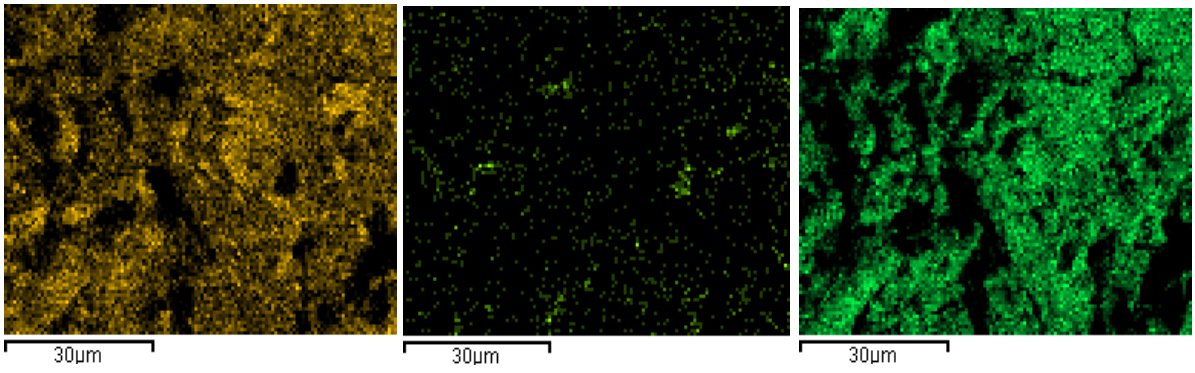

(d) (e) (f)

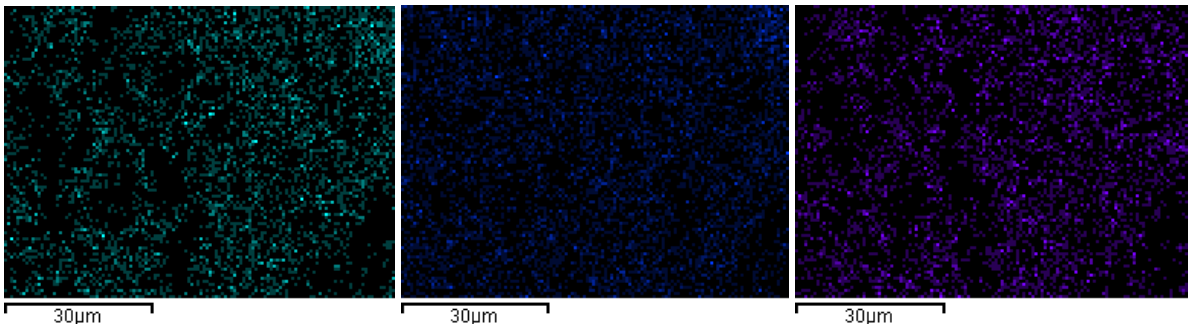

(g) (h) (i)

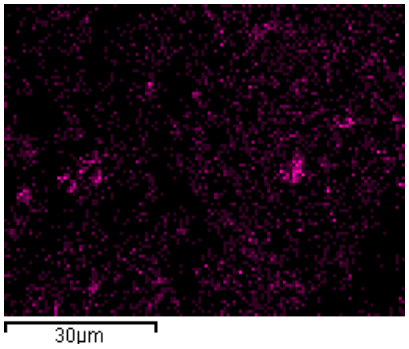

(j)

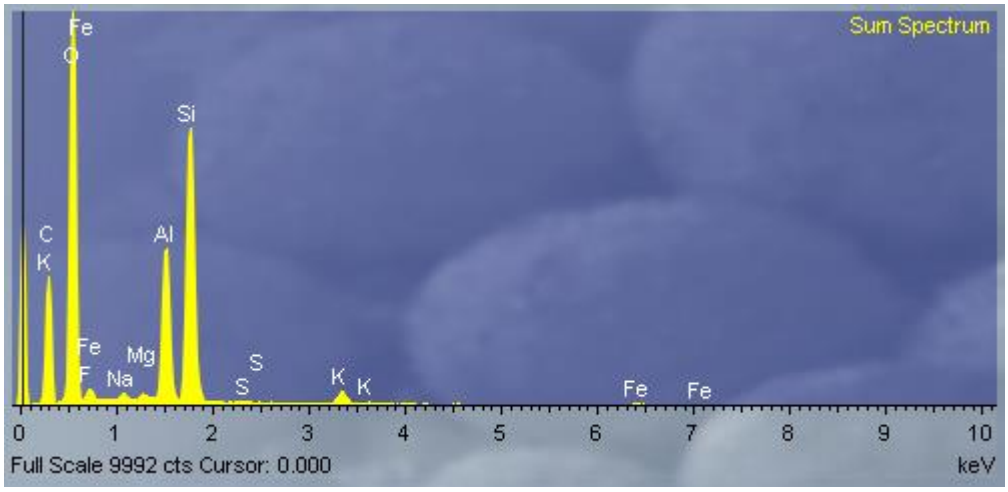

(k)

Figure 4.10(a-k) Showing ceramic 1st HP coating with different elements (a) Reference image (b) Mix showing all elements on the membrane surface (c) element Al (d) element Si (e) element Fe (f) element O (g) element Na (h) element K (i) element Mg (j) element F (k) Energy dispersion X-ray spectroscopy.

Due to the produced rough membrane surface on the 1st HP coating, there was a need to study the 2nd round of HP coating to produce a membrane surface with fewer clusters for better surface properties to give more efficient and stable wettability.

4.2.8 HP Coating Round 2

In Fig.4.11, the SEM and EDS results of the membrane surface layer formed on ceramic after 2nd HP hydrophobic nanoparticle coating are presented. Spectrum 1 was chosen as a reference of analysis on the statistical analysis for 2nd HP and 3rd HP coating analysis. All SEM photos show a different spread of surface density of O, Al, Si, K, Mg and F on the ceramic membrane surface. Oxygen was observed to have the highest peak or intensity, followed by Silicon, Aluminium, Fluorine, Iron, Potassium, Sulphur, and Sodium, while Magnesium was observed to have the lowest peak or intensity. Additionally, few clusters are observed on the reference image and mix F element when compared with 1st LP, 2nd LP, 3rd LP, 4th LP and 1st HP coating. The inter-separation distances are slightly big, still creating a rough membrane surface but better than 1st LP, 2nd LP, 3rd LP, 4th LP and 1st HP coating rounds. The orientation of nanoparticles, morphology, spread, spatial distribution, and size of nanoparticles are changing with F on the membrane surface. The surfaces coated with hydrophobic nanoparticles have high O, Si, Al, and F, and this can be correlated with the EDS and statistical analysis results.

Table 4.8: Composition of elements in the surface layer formed in ceramic 2nd round HP after PEO

ESD setting

MAOME Project 1	Project	Owner	Site:	Sample	ID
	MAOME Project 1	INCA Operator	Site of Interest 2	CERAMIC 2 HP Type	CERAMIC 2 HP

Descriptive statistics

Spectrum	In stats.	O	F	Na	Mg	Al	Si	S	K	Fe	Total
Spectrum 1	Yes	42.66	8.47	0.61	0.45	12.13	25.02	1.14	3.23	6.31	100.00
Spectrum 2	Yes	54.69		0.62	0.36	10.73	23.05	0.23	2.83	7.48	100.00
Spectrum 3	Yes	51.90	7.08	0.43	0.39	9.43	20.85	0.57	2.08	7.28	100.00
Spectrum 4	Yes	55.22		0.37	0.45	9.77	23.66		2.39	8.14	100.00
Spectrum 5	Yes	50.82		0.48	0.33	11.91	26.37		2.94	7.15	100.00
Max.		55.22	8.47	0.62	0.45	12.13	26.37	1.14	3.23	8.14	
Min.		42.66	7.08	0.37	0.33	9.43	20.85	0.23	2.08	6.31	

All results in weight %

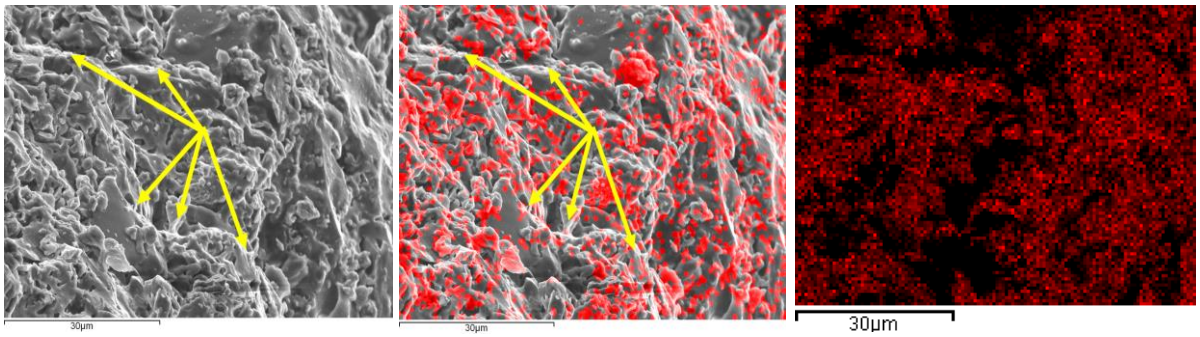

(a) (b) (c)

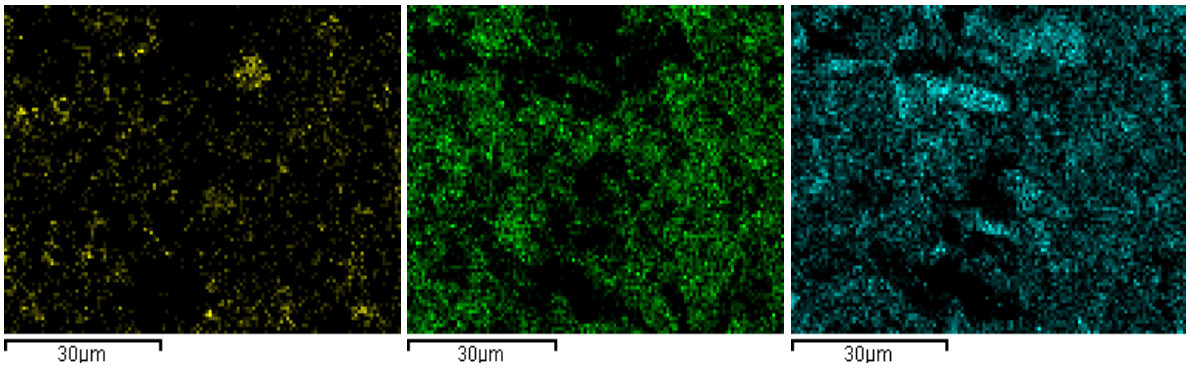

(d) (e) (f)

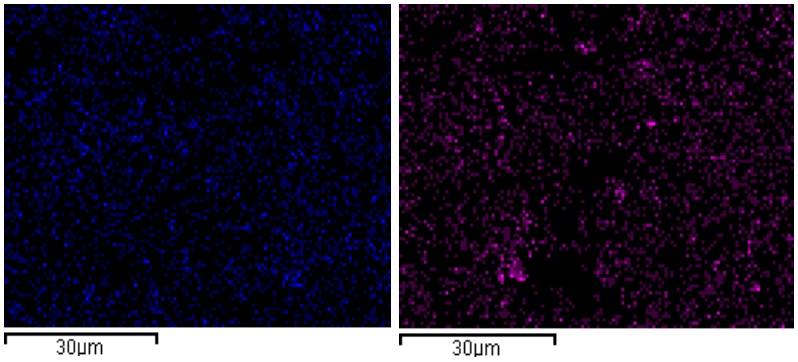

(g) (h)

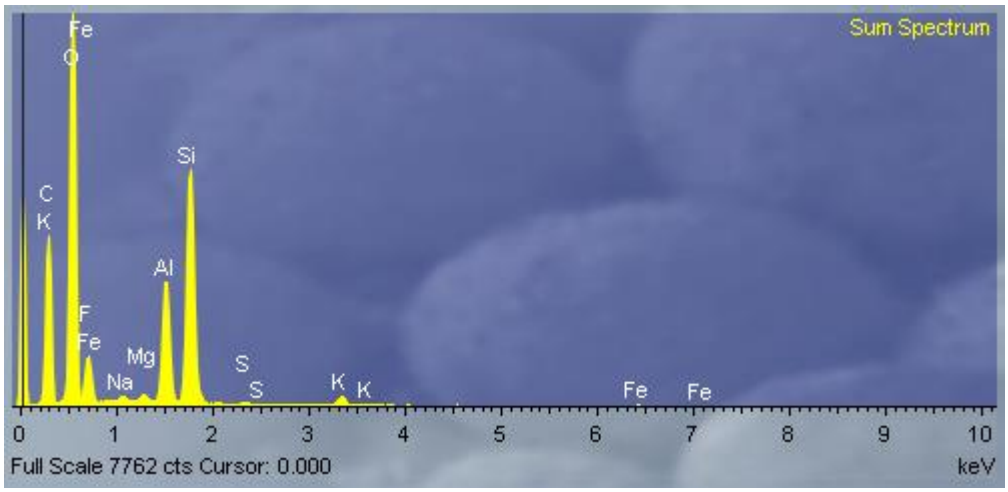

(i)

Figure 4.11(a-i) Showing ceramic 2nd HP coating with different elements (a) Reference image (b) Mix showing all elements on the membrane surface (c) element O (d) element F (e) element Al (f) element Si (g) element K (h) element Mg (i) Energy dispersion X-ray spectroscopy.

Due to that, this still created a rough membrane surface. Therefore, there was a need to study 3rd round of HP coating to produce membrane surface with more enhanced wettability for oil-water separation.

4.2.9 HP Coating Round 3

In Figure 4.12, the SEM and EDS results of the membrane surface layer formed on ceramic after 3rd HP hydrophobic nanoparticle coating are presented. All SEM photos show a different spread of surface density of O, F, Na, Mg, Al, Si, S, K, Ca, and Fe on the ceramic membrane surface. Oxygen was observed to have the highest peak or intensity, followed by Silicon, Aluminium, Iron, Fluorine, Potassium, Sulphur, and Sodium, while Magnesium was observed to have the lowest peak or intensity. The surfaces coated with hydrophobic nanoparticles have high O, Si, Al, which overpowered F, and this can be correlated with the EDS and statistical analysis results. Fewer clusters are observed on the reference image and mix F element when compared with 1st LP, 2nd LP, 3rd LP, 4th LP, 1st HP and 2nd HP coating. The inter-separation distances are small, thus creating a better smooth membrane surface as compared to 1st LP, 2nd LP, 3rd LP, 4th LP, 1st HP and 2nd HP coating rounds. The surface was still inhomogeneous due to the orientation of nanoparticles, surface morphology, spread, spatial distribution, and size of nanoparticles. The orientation of nanoparticles, morphology, spread, spatial distribution, and size of nanoparticles are changing with F on the membrane surface. The scattering of Fluorine is far better than on 1st LP, 2nd LP, 3rd LP, 4th LP, 1st HP and 2nd HP coating rounds.

Table 4.9: Composition of elements in the surface layer formed in ceramic 3rd round HP after PEO

ESD setting

MAOME Project 1	Project	Owner	Site:	Sample	ID
	MAOME Project 1	INCA Operator	Site of Interest 1	CERAMIC 3 HP Type	CERAMIC 3 HP

Descriptive statistics

Spectrum	In stats.	O	F	Na	Mg	Al	Si	S	K	Fe	Total
Spectrum 1	Yes	49.52	2.94	0.43	0.42	11.03	25.29	0.86	2.67	6.84	100.00
Spectrum 2	Yes	50.25	3.30	0.41	0.44	10.25	25.94	0.31	2.36	6.74	100.00
Spectrum 3	Yes	43.27	9.62	0.40	0.36	10.32	27.73	0.33	2.74	5.22	100.00
Spectrum 4	Yes	50.62		0.65	0.30	10.47	27.98		3.23	6.76	100.00
Spectrum 5	Yes	46.87	9.57	0.36	0.38	9.84	22.53		2.88	7.56	100.00
Sum Spectrum	Yes	46.65	4.36	0.82	0.40	10.24	25.98	3.06	2.75	5.72	100.00
Max.		50.62	9.62	0.82	0.44	11.03	27.98	3.06	3.23	7.56	
Min.		43.27	2.94	0.36	0.30	9.84	22.53	0.31	2.36	5.22	

All results in weight %

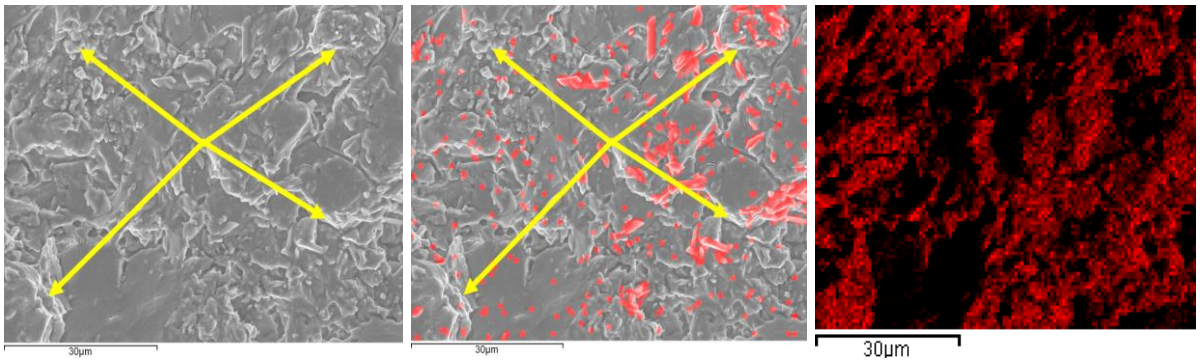

(a) (b) (c)

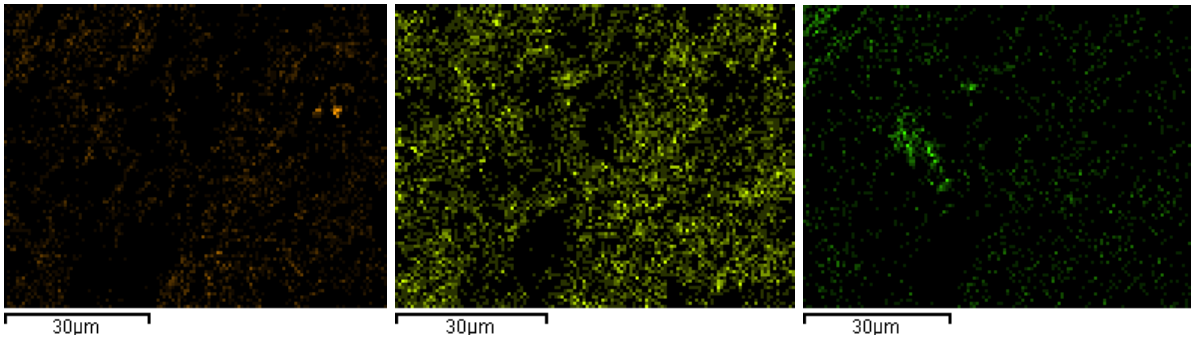

(d) (e) (f)

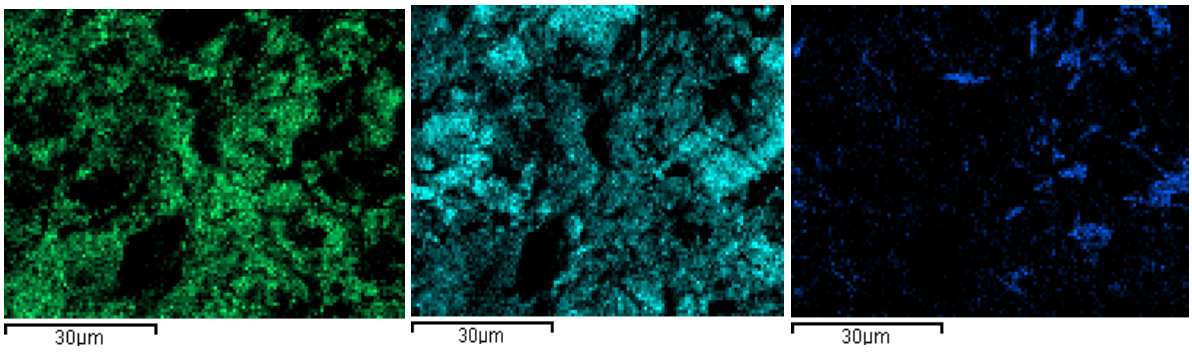

(g) (h) (i)

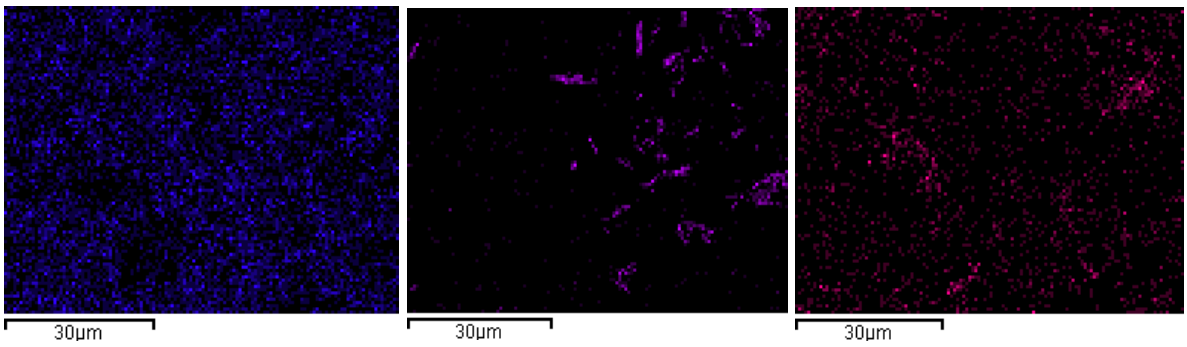

(j) (k) (l)

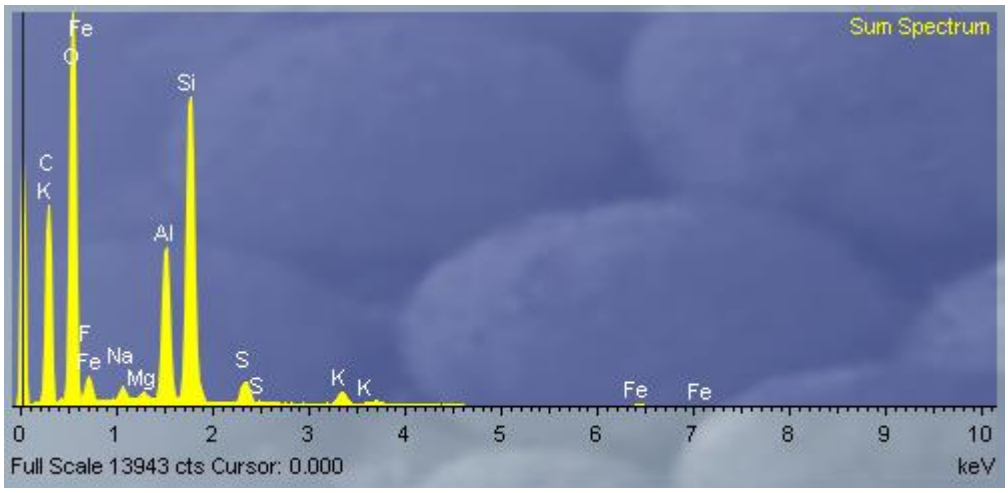

(m)

Figure 4.12(a-m) Showing ceramic 3rd HP coating with different elements (a) Reference image (b) Mix showing all elements on the membrane surface (c) element O (d) element F (e) element Na (f) element Mg (g) element Al (h) element Si (i) element S (j) element K (k) element Ca (l) element Fe (m) Energy dispersion X-ray spectroscopy.

Although the membrane gave better surface properties as compared to 1st LP, 2nd LP, 3rd LP, 4th LP, 1st HP and 2nd HP coating rounds, the surface was still inhomogeneous due to the orientation of nanoparticles, surface morphology, spread, spatial distribution, and size of nanoparticles. It was

therefore imperative to do 4th round of HP coating to produce a membrane surface with further reduced clusters to give a smoother surface with more minimised clusters to give better surface wettability.

4.2.10 HP Coating Round 4

In Figure 4.13, the SEM and EDS results of the membrane surface layer formed on ceramic surface after 4th LP hydrophobic nanoparticle coating are presented. All SEM photos show a different spread of surface density of O, Si, Al, F, and K on the ceramic membrane surface. Oxygen was observed to have the highest peak or intensity, followed by Silicon, Fluorine, Aluminium, Iron, Potassium, Sulphur and Sodium, while Magnesium was observed to have the lowest peak or intensity. On the coated hydrophobic nanoparticle mixed surface, the inter-separation distances are small when compared with the 3rd HP coating. This gave lesser clusters observed on the reference image and mix F element when compared with 1st LP, 2nd LP, 3rd LP, 4th LP, 1st HP, 2nd HP and 3rd HP coating. The inter-separation distances are small, thus creating a better smooth membrane surface as compared to 1st LP, 2nd LP, 3rd LP, 4th LP, 1st HP, 2nd HP and 3rd HP coating rounds. The orientation of nanoparticles, morphology, spread, spatial distribution, and size of nanoparticles are not changing much with F on the membrane surface. The scattering of F is even on the membrane surface due to surface uniformity, thus creating a smoother membrane surface. The produced membrane during this coating is more homogeneous as compared to 1st LP, 2nd LP, 3rd LP, 4th LP, 1st HP, 2nd HP and 3rd HP coating. This shows further reduced clusters on the membrane surface as compared to 1st LP, 2nd LP, 3rd LP, 4th LP, 1st HP, 2nd HP and 3rd HP coating rounds. This was achieved by varying the coating pressure, coating distance and coating angle until the optimal levels of coating was reached and maintained. The pressure reached during this coating round reached an optimal level to produce a smoother membrane. This improved membrane wettability on the surface when related to the lotus effect on surface wettability.

Table 4.10: Composition of elements in the surface layer formed in ceramic 4th round HP after PEO ESD setting

MAOME Project 1	Project	Owner	Site:	Sample	ID
	MAOME Project 1	INCA Operator	Site of Interest 2	CERAMIC 4 HP Type	CERAMIC 4 HP

Descriptive statistics

Spectrum	In stats.	O	F	Na	Mg	Al	Si	S	K	Fe	Total
Spectrum 1	Yes	46.11	1.58	0.48	0.52	14.17	26.84		3.77	6.53	100.00
Spectrum 2	Yes	44.41	17.10	0.60	0.28	8.98	20.67	1.67	2.34	3.96	100.00
Spectrum 3	Yes	46.93	6.25	0.44	0.37	10.10	27.27	0.49	2.59	5.57	100.00
Spectrum 4	Yes	37.72	37.17	1.30		9.79	9.23	4.79			100.00
Spectrum 5	Yes	54.34		0.35	0.40	8.64	27.54	0.34	2.19	6.20	100.00
Max.		54.34	37.17	1.30	0.52	14.17	27.54	4.79	3.77	6.53	
Min.		37.72	1.58	0.35	0.28	8.64	9.23	0.34	2.19	3.96	

All results in weight %

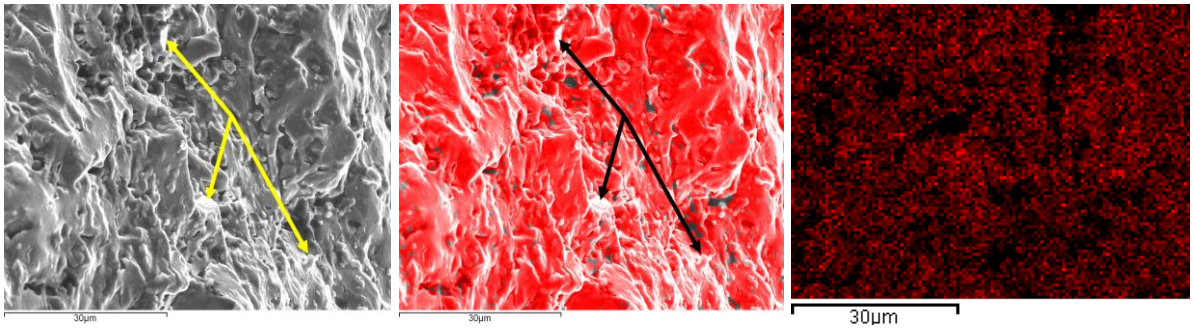

(a) (b) (c)

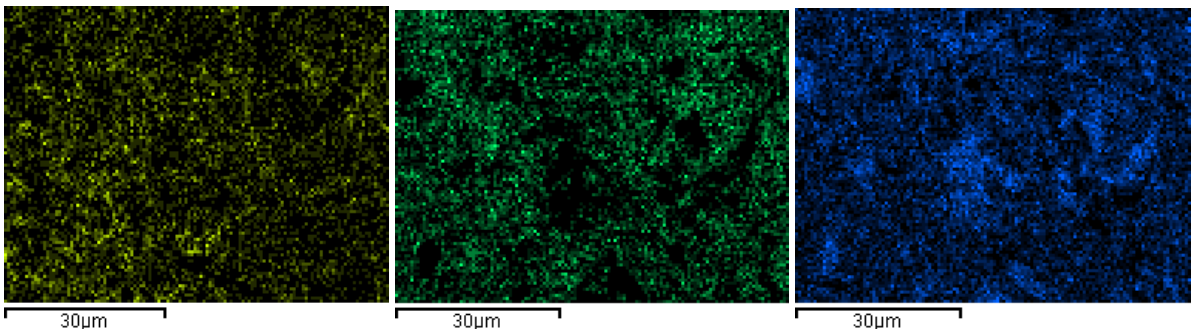

(d) (e) (f)

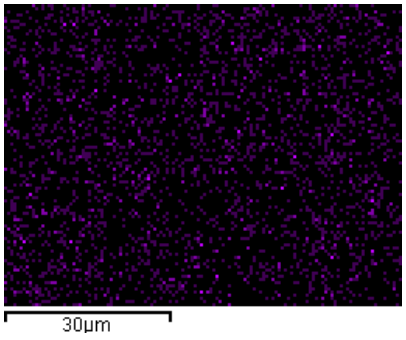

(g)

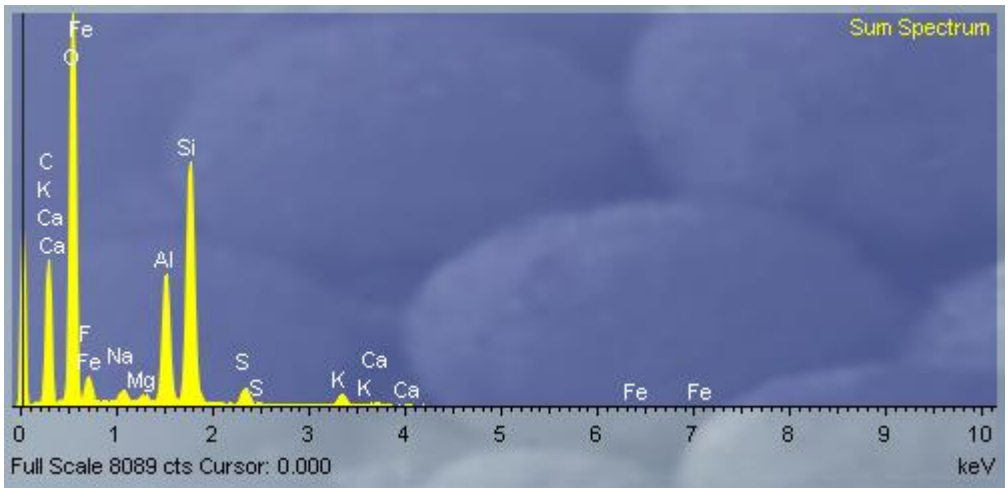

(k)

Figure 4.13(a-k) Showing ceramic 4th HP coating with different elements (a) Reference image (b) Mix showing all elements on the membrane surface (c) element O (d) element F (e) element Al (f) element Si (g) element K (h) element S (i) element K (j) element Fe (k) Energy dispersion X-ray spectroscopy.

The 3rd HP, 2nd HP and 1st HP, 4th LP, 3rd LP, 2nd LP and 1st LP coating revealed numerous clusters, and this resulted in an inhomogeneous surface. The scattering of the Fluorine element is not uniform due to the orientation of nanoparticles, surface morphology, spread, spatial distribution, and size of nanoparticles. This created rough membrane surfaces in those coating rounds. This resulted in increased surface energy and worst wettability for oil-water separation. The results in the 4th HP coating revealed more reduced clusters and smaller sizes on the membrane surface as compared to 1st LP, 2nd LP, 3rd LP, 4th LP, 1st HP, 2nd HP and 3rd HP coating rounds. The following parameters were varied during all coating rounds: coating force, coating distance, and coating angle. This was done to achieve optimal levels of coating so that cluster minimization could be achieved. The optimal coating pressure for cluster minimization was achieved during the 4th HP coating. The scattering of Fluorine in 4th HP coating is uniform, resulting in a homogeneous membrane with fewer clusters produced when compared to 1st LP, 2nd LP, 3rd LP, 4th LP, 1st HP, 2nd HP and 3rd HP coating rounds. The membrane produced during the 4th HP coating was smooth, with lowered surface energy. This improved wettability for oil-water separation; hence the objective of this study was to produce a ceramic membrane with minimal clusters for the most enhanced wettability in oil-water separation. Since the produced membrane after the 4th HP coating offered a smoother membrane and homogeneous surface as compared to all other coating rounds, there was no need to study 5th round HP coating.

4.3 Comparison of the newly designed ceramic membrane surface with the previously designed ceramic membrane surfaces from the previous literature

4.3.1 Different clusters observed on nanostructured ceramic membranes during coating from the current study

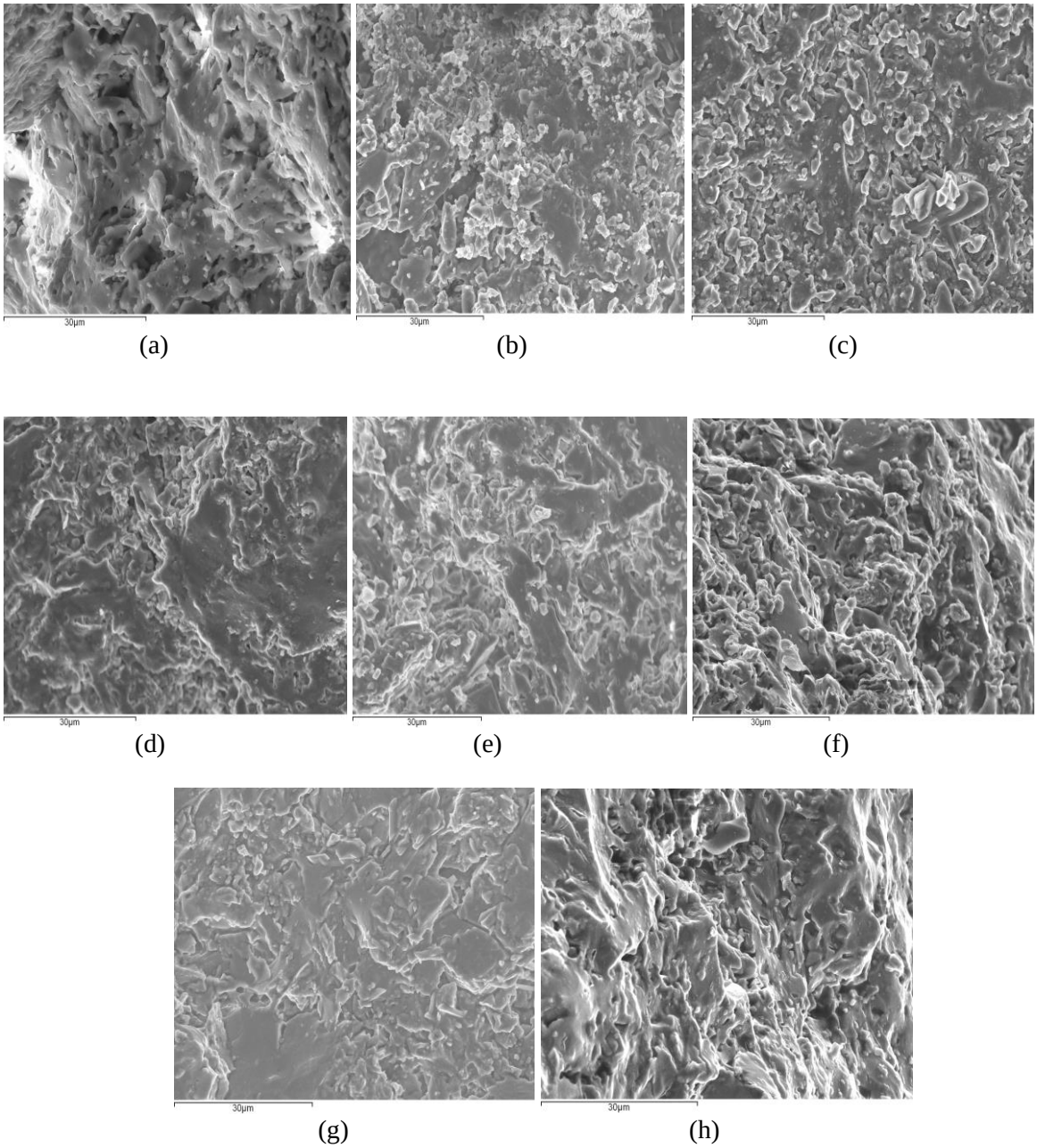

Figure 4.14 SEM images of clusters on ceramic membrane surface after rounds of jet spray coating in this current study (a) 1st LP coating (b) 2nd LP coating (c) 3rd LP coating (d) 4th LP coating (e) 1st HP coating(f) 2nd HP coating(g) 3rd HP coating and (h) 4th HP coating.

Fig. 4.14 (a-h) show different surface morphology with clusters developed during different LP and HP coating rounds in this study. The results from figure 4.14 (h) revealed a smooth and homogeneous membrane with fewer clusters and in small sizes on the surface as compared to 3rd HP, 2nd HP, 1st HP, 4th LP, 3rd LP, 2nd LP and 1st LP coating rounds, see Fig. 4.14 (a-h). This resulted in a lowered surface energy on the membrane with the most enhanced wettability, as this is the focus of this dissertation. This can be related to the lotus effect on surface wettability. The lotus effect on surface wettability states that the coated membrane surface must be smooth so as to give more enhanced wettability during oil-water separation (Ge *et al.*, 2019) (Sob *et al.*, 2019) (Kubiak *et al.*, 2011) (Miwa *et al.*, 2000). The rough surface doesn't improve wettability when related to the lotus effect on surface wettability (Ge *et al.*, 2019) (Sob *et al.*, 2019) (Kubiak *et al.*, 2011) (Miwa *et al.*, 2000). This is due to bigger nanoparticles' inter-separation distances and morphology on the surface. Nanoparticle cluster sizes play a significant role in membrane wettability. Small size clusters give less impact on membrane wettability, while bigger clusters give more roughness on the surface (Ge *et al.*, 2019) (Sob *et al.*, 2019) (Kubiak *et al.*, 2011) (Miwa *et al.*, 2000). More clusters are reported to increase surface roughness, resulting to poor wettability during oil-water separation.

4.3.2 Different clusters observed on nanostructured ceramic membranes during coating (Chen et al., 2018)

Fig. 4.15 (a) shows a rough ceramic membrane surface before coating, and Fig. 4.15 (b) shows a rough membrane surface with clusters after the first round of coating, and Fig. 4.15 (c) shows a smooth membrane surface having fewer clusters developed after the second round of coating (Chen *et al.*, 2018).

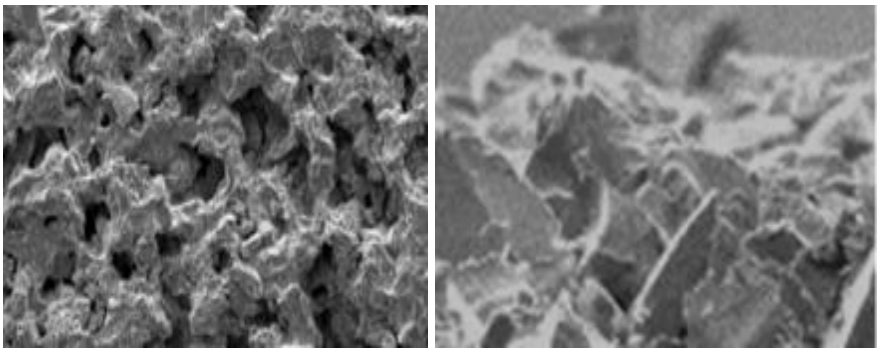

(a) (b)

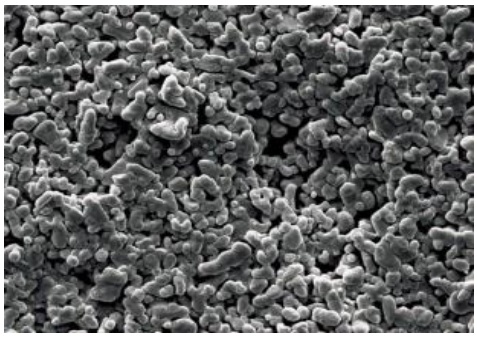

(c)

Figure 4.15 SEM images of ceramic membrane surfaces (a) before coating (b) after 1st round of coating and (c) after 2nd round of coating (Chen et al., 2018).

4.3.3 Different clusters observed on nanostructured ceramic membranes during coating (Raji et al., 2021)

Fig. *4.16* (a) shows a rough ceramic membrane surface before coating, and Fig. *4.16* (b) shows surface morphology with fewer nanoparticle clusters developed after dip coating on a nanostructured kaolin-based ceramic membrane (Raji *et al.*, 2021). As it can be seen, this membrane revealed a smooth surface after the researchers used poly diallyl dimethyl ammonium chloride (PDDA) to improve the efficiency of oil-water separation. Raji et al. (2021) reported this membrane to be homogeneous and has a lowered surface energy after coating.

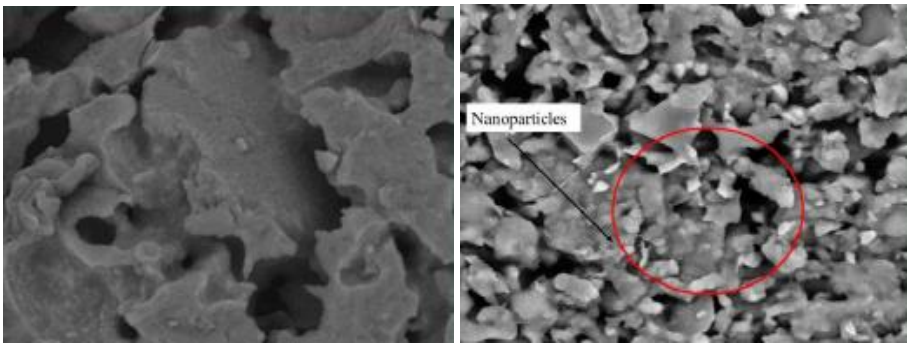

(a) (b)

Figure 4.16 SEM images of ceramic membrane surface (a) before coating (b) after coating (Raji et al., 2021).

4.3.4 Different clusters observed on nanostructured ceramic membranes during coating (L. H. Chen et al., 2018)

Fig. *4.17* (a) shows a rough ceramic membrane surface before coating, Fig. *4.17* (b) shows a rougher membrane surface with bigger clusters after the first round of coating and Fig. *4.17* (c) shows a smooth membrane surface having little and fewer clusters developed after the second round of coating (L. H.

Chen *et al.*, 2018). The coating method used is chemical bath deposition. L.H Chen et al. (2018) reported this membrane to have revealed a homogeneous surface after using zinc oxide (ZnO) as nanoparticles.

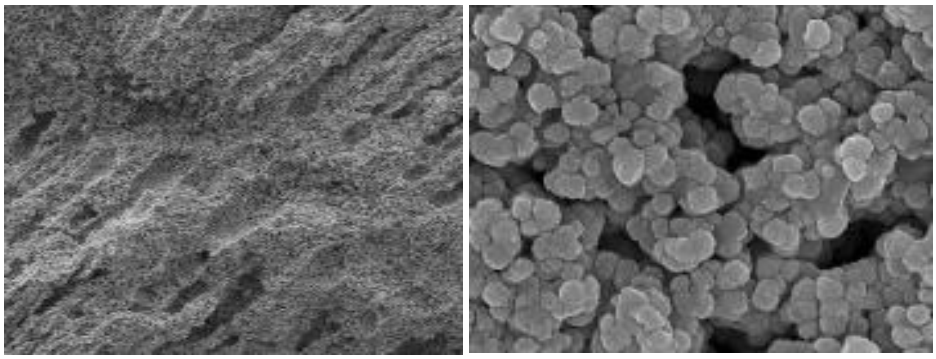

(a) (b)

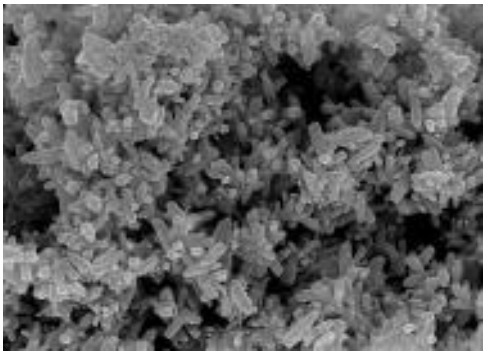

(c)

Figure 4.17 SEM images of ceramic membrane surfaces (a) before coating (b) after 1st round of coating and (c) after 2nd round of coating (L. H. Chen et al., 2018).

4.3.5 Different clusters observed on nanostructured ceramic membranes during coating (Sob et al., 2020)

Fig. *4.18* (a) shows a rough glass membrane surface after 2nd round of LP coating, Fig. *4.18* (b) shows a rougher glass membrane surface 3rd round of LP coating and Fig. *4.18* (c) shows a smooth glass membrane surface after 3rd round of HP coating (Sob *et al.*, 2020). Sob et al. (2020) reported 3rd round of HP coating on a glass surface to have little clusters on the membrane with low surface energy.

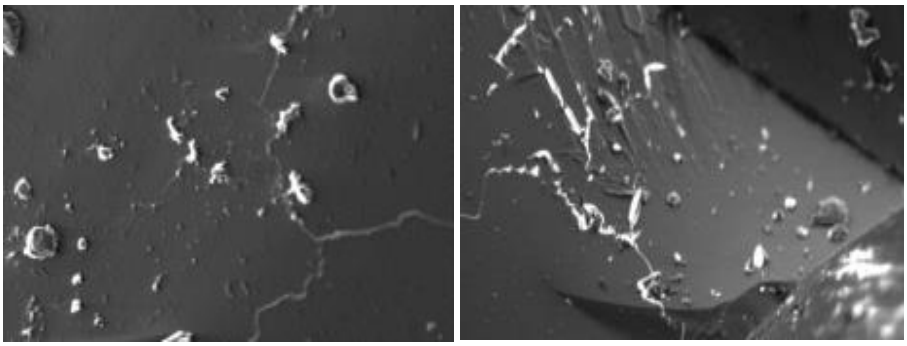

(a) (b)

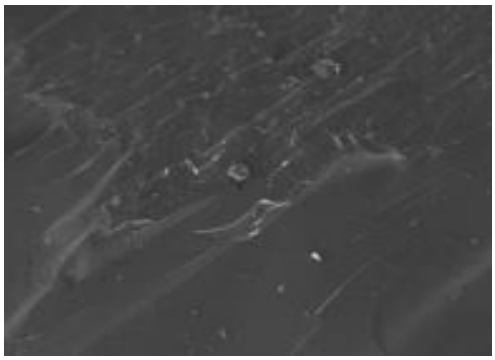

(c)

Figure 4.18 glass surface morphologies (a) after 2nd round of LP coating (b) after 3rd round of LP coating and (c) after 3rd round of HP coating (Sob et al., 2020).

4.4 Summary of the results and discussion

The current study revealed the following facts after modelling the minimization of membrane clusters. It was shown that, as the coating distance increases with coating total force in the jet spray gun, there was an optimal coating distance that gave optimal membrane clusters during the coating process. It was also revealed that at optimal coating distance, there was optimal cluster minimization which gave optimal surface spread of nanoparticles in the membrane surface, resulting in a smooth membrane surface which led to lowered surface energy. It was also shown that an increase in jet spray angle and total force in the jet spray during coating led to an optimal level, leading to a decrease in cluster sizes during nanoparticle coating. It was also revealed that during the initial process of jet spray coating, more membrane clusters were created. This gave a rough membrane surface. It was also revealed that as more coating took place, these clusters were minimized due to continuous coating which took place. This is due to the fact that the required coating force was produced to minimize the surface cluster on the

membrane surface. Therefore, it could be concluded that at the optimal coating forces, optimal coating distance and optimal coating angles, membrane clusters were properly minimized as revealed in the study.

This chapter dealt with the analyses of the produced nanostructured membrane used in oil-water separation. Ceramic was used to produce the membrane. This material was coated with nanoparticles using the jet-spray coating technique. This coating technique was done using both high- and low-pressure jets. Four coating rounds were done for both LP and HP, and the sampled membranes were allowed to dry for 24 hours under room temperature. During coating, the coating force, the coating distance and the coating angle were varied between $0{,}2x10^7$ kN to $2{,}4x10^7$ kN, 10 mm to 24 mm and 1º to 9º respectively, which led to optimal spread of nanoparticles on the membrane surface thus resulting to optimal cluster minimisation during the coating process. The samples were prepared for microscopy. SEM, TEM, EDS and Image J particle analysers were used for analysis. The results for SEM and EDS were correlated and characterized for optimal wettability. Different surface spread, orientation, morphology, spatial distribution and surface densities of nanoparticles were revealed after different coating rounds by low and high pressure. Different surface scattering, orientation, morphology and nanoparticle densities on the surface were revealed after different coating rounds by low and high pressure. A correlation was established between the theoretically derived model data on optimal nanoparticle scattering and inter-separation distances for efficient wettability. Membrane clusters were also revealed. These clusters created rough membrane surfaces that negatively impacted wettability. The membrane inter-separation distances were also measured using an Image J particle analyser and their impact on membrane surface roughness and smoothness on wettability was established. The scattering of fluorine on the membrane surface was observed to identify surface homogeneity.

The analysis revealed that optimal levels were reached at 4th HP coating round as compared to 3rd HP, 2nd HP and 1st HP, 4th LP, 3rd LP, 2nd LP and 1st LP. In this coating round, clusters were reduced to minimal levels. The membrane produced during this coating round was smooth, with lowered surface energy. This led to a membrane with better wettability as compared to other coating rounds hence it was the objective of this study to produce a ceramic membrane with minimal clusters for the most enhanced wettability in oil-water separation.

A correlation was be done between the current results obtained in this study with the results obtained from the previous literature to demonstrate the improvement of the newly designed ceramic membrane.

CHAPTER FIVE

CONCLUSION

5.1 Introduction

The main aim of the current study was to design a nanostructured ceramic membrane material with more improved surface properties for enhanced wettability to achieve efficient oil-water separation. To achieve this, it was imperative to investigate the best coating strategy to minimise the clustering of nanoparticles during the coating process. It was also necessary to investigate the parameters that impact membrane surface during jet spray coating. These parameters are coating force, coating distance and coating angle. The stochastic mechanics and fluid dynamics tools were used to study the random forces and parameters during jet spray coating. Therefore, the current chapter of this study presents the conclusions and recommendations of the theoretically modelled results and experimentally analysed results in membrane wettability for efficient oil-water separation.

5.2 Conclusion of theoretically modelled results for efficient wettability for oil-water separation

The first part of the study was to theoretically design a model and simulate the results to minimize clusters developed during coating for efficient wettability during oil-water separation. It was important to establish the effects of different nanoparticle coatings. The impact of membrane surface clusters during jet spray coating was discussed together with different parameters that led to a decrease in these clusters. These parameters are coating force, coating distance and coating angle. During theoretical modelling and simulation, the effect of random nanoparticle size, morphology, nanoparticle scattering and nanoparticle inter-separation distances on surface energy during wettability were investigated for efficient oil-water separation. To achieve the objective of the study, a proposed nanostructured membrane was designed. Main parameters and variables of the newly designed nanostructured membrane were modelled and simulated to observe the impact of nanoparticle size, morphology, nanoparticle scattering and nanoparticle inter-separation distances on surface energy. The following findings were observed and reported.

It was shown that increasing the total force from $0{,}2x10^7$ kN to $2{,}4x10^7$ kN , coating distance from 10 mm to 24 mm and coating from angle 1^o to 9^o in the jet spray region led to an optimal membrane clusters minimization during coating, which gave a smooth membrane surface. This is due to the that as the coating process began, more membrane clusters were created, which created a rough membrane surface. As more coating processes took place, a rough membrane surface became a smooth membrane surface because the formation of membrane clusters was stabilized. This led to the creation of smooth membrane surfaces, which lowered surface energy and increased membrane wettability. Smooth membrane surface

and minimized clusters on the membrane surface were reported to have lower surface energy on the membrane surface, and this improved membrane wettability for oil-water separation, as this was the focus of the current study. It was also revealed that the change in membrane clusters also impacts the membrane aperture sizes. This is because the degree of surface roughness to smoothness during cluster minimization led to a decrease in membrane aperture sizes, which lowered surface energy and improved surface wettability, as this was the focus of the current study.

5.3 Conclusion of experimentally designed membrane for efficient wettability for oil-water separation

The second part of the study was to fabricate an efficient ceramic membrane surface that will have fewer clusters with small sizes on the surface for better wettability during oil-water separation. Ceramics were used to produce wettable membranes using HP and LP coating techniques to achieve this. Four coating rounds were employed on different ceramic beads for LP and HP. Membranes were coated in the following order: first coat, second coat, third coat and fourth coat for HP and LP rounds. Different microstructures developed using ceramic materials were observed under microscopy for characterization. These microstructures revealed different surface densities of nanoparticles, mean particle sizes, surface roughness, surface smoothness and nanoparticles inter-separation distances. F was observed as the control element during characterization. The orientation of nanoparticles, surface morphology, nanoparticle scattering on the surface and size of nanoparticles were observed with the behaviour of the F element on the membrane surface during coating. The scattering of F on the membrane was also observed in different coating rounds. The surface homogeneity and inhomogeneity were also observed in all coating rounds. It was revealed that the sample, which gave better wettability with few and small clusters on the surface, is the 4^{th} HP coating round. Correlations were established from the SEM, EDS and descriptive statistics of the quantities of elements in the surface layer formed after different coating rounds. It was also revealed that nanoparticle scattering on the membrane surface during coating was varied, resulting in minimised clusters. This resulted in rougher membranes being smoother, which impacted membrane wettability positively. This was achieved during the 4^{th} HP coating round. The results show that rough membrane surfaces created higher surface energy, their inter-separation distances were bigger, and this affected membrane wettability negatively. Smooth membrane surfaces created lower surface energy; their inter-separation distances were smaller, and this affected membrane wettability positively, as this was the focus of the study.

A comparison was be done between the current results obtained in this study with the results obtained from the previous literature to demonstrate the improvement of the newly designed ceramic membrane.

The produced nanostructured ceramic membranes in this study were compared with the produced nanostructured ceramic membranes in the previous literature to observe clusters on the surfaces.

5.4 Summary of the Conclusion

In summary, this chapter discussed the conclusion and recommendation of the newly designed nanostructured ceramic membrane used in oil-water separation. The first part concluded on the results obtained from theoretical modelling. It was shown that the effect of random nanoparticle size, morphology, nanoparticle scattering and nanoparticle inter-separation distances on surface energy during wettability were investigated for efficient oil-water separation. It was shown that the formation of membrane clusters during the initial process of coating created rougher membrane surface, which increased surface energy on the membrane, which negatively affected wettability. It was revealed that a smooth membrane surface with minimized clusters on the surface results in low surface energy on the membrane surface, and this improved membrane wettability for oil-water separation, and this was the focus of the current study. As more coating took place, these clusters were being minimized due to continuous coating. It was also revealed that membrane clusters were minimised at optimal coating forces, optimal coating distance and optimal coating angles since the rough surfaces became smooth surfaces. This is because the degree of surface roughness to smoothness during cluster minimization led to a decrease in aperture sizes, which lowered surface energy and improved surface wettability for oil-water separation, which was the focus of the current study.

During experimental analysis, fluorine scattering was observed on sampled ceramic beads under microscopic view. The orientation of nanoparticles, surface morphology, nanoparticle scattering on the surface and size of nanoparticles were observed with the behaviour of F element on the membrane surface during coating. The surface homogeneity and inhomogeneity were also observed in all coating rounds. Correlations were established from the SEM, EDS and descriptive statistics of the quantities of elements in the surface layer formed after different coating rounds. The optimal coating round that resulted in efficient wettability on the membrane surface is the 4^{th} HP coating round. This membrane was rough before coating and became smoother during coating, which impacted membrane wettability positively. This was achieved during the 4^{th} HP coating round due to that the following parameters were varied during coating: the coating force, coating distance and coating angle. This research focused on surface energy-driven separability, while the previous research focused only on surface tension driven separability.

A comparison was done between the current results obtained in this study with the results obtained from the previous literature to demonstrate the improvement of the newly designed ceramic membrane.

5.5 Applications

The designed membrane might be useful in membrane technology. It might be used globally by industrial sectors, mining sectors, municipal sectors, medical & pharmaceutical sectors and industries during offshore oil exploration.

5.6 Value of the Research

It is believed that the research will have a great impact across the globe since it will produce the ceramic membrane material with more improved wettability for oil-water separation. The university will sell the patent to industrial, mining and government sectors since it will improve their productivity and environmental standards compliance. The derived theoretical models will contribute greatly to the field of nanoscience and nanotechnology. The successful execution of this research project will give credit to the Vaal University of Technology and its contribution to the study of nanoscience and nanotechnology. I will be honoured with a Masters degree in Mechanical Engineering and my successive publications through the research output.

CHAPTER SIX

RECOMMENDATIONS

Limited interest has been shown from the previous literature on the durability enhancement on the ceramic membrane for steady oil-water separation. This was also not investigated in this study. Future studies should be done in this topic, to create more stable wettability during oil-watersepartion.

REFERENCES

Abbasi, M., Mirfendereski, M.., Nikbakht, M., Golshenas, M. and Mohammadi, T. (2010) 'Performance study of mullite and mullite – alumina ceramic MF membranes for oily wastewaters treatment', *DES*. Elsevier B.V., 259(1–3), pp. 169–178. doi: 10.1016/j.desal.2010.04.013.

Achilli, A., Cath, T. Y., Marchand, E. A. and Childress, A. E. (2009) 'The forward osmosis membrane bioreactor : A low fouling alternative to MBR processes', *DES*. Elsevier B.V., 239(1–3), pp. 10–21. doi: 10.1016/j.desal.2008.02.022.

Ben, M., Hamdi, N., Rodriguez, M. and Mahmoudi, M. K. (2018) 'Preparation and characterization of new ceramic membranes for ultrafiltration', Ceramics International, 44(2), pp. 2328–2335. doi: 10.1016/j.ceramint.2017.10.199.

Atallah, C., Tremblay, A. Y. and Mortazavi, S. (2017) 'Silane surface modified ceramic membranes for the treatment and recycling of SAGD produced water', Journal of Petroleum Science and Engineering, 157, pp. 349–358. doi: 10.1016/j.petrol.2017.07.007.

Bai, X., Zhao, Z., Yang, H. and Li, J. (2019) 'Separation and Puri fi cation Technology ZnO nanoparticles coated mesh with switchable wettability for on-demand ultrafast separation of emulsi fi ed oil / water mixtures', Separation and Purification Technology, 221(April), pp. 294–302. doi: 10.1016/j.seppur.2019.04.003.

Balzarotti, R., Cristiani, C. and Francis, L. F. (2019) 'Combined dip-coating / spin-coating depositions on ceramic honeycomb monoliths for structured catalysts preparation', Catalysis Today, 334(June 2018), pp. 90–95. doi: 10.1016/j.cattod.2019.01.037.

Ten Brink, G. H., Foley, N., Zwaan, D., Kooi, B. J. and Palasantzas, G. (2015) 'Roughness controlled superhydrophobicity on single nanometer length scale with metal nanoparticles', RSC Advances, 5(36), pp. 28696–28702. doi: 10.1039/c5ra02348c.

Cai, Y., Coyle, T.W., Azimi, G. and Mostaghimi, J. (2016) 'Superhydrophobic Ceramic Coatings by Solution Precursor Plasma Spray', *Nature Publishing Group*. Nature Publishing Group, pp. 1–7. doi: 10.1038/srep24670.

Cai, Y., Chen, D., Li, N., Xu, Q., Li, H., He, J. and Lu, J. (2018) 'A smart membrane with antifouling capability and switchable oil wettability for high-efficiency oil/water emulsions separation', *Journal of Membrane Science*. Elsevier B.V., 555(March), pp. 69–77. doi: 10.1016/j.memsci.2018.03.042.

Cao, L., Price, T. P., Weiss, M. and Gao, D (2008) 'Super water- and oil-repellent surfaces on intrinsically hydrophilic and oleophilic porous silicon films', Langmuir, 24(5), pp. 1640–1643. doi: 10.1021/la703401f.

Chen, L., Guan, K., Zhu, W., Peng, C. and Wu, J. (2018) 'Preparation and mechanism analysis of high performance ceramic membrane by spray coating'. Royal Society of Chemistry, pp. 39884–39892. doi: 10.1039/c8ra07258b.

Chen, L., Guan, K., Zhu, W., Peng, C. and Wu, J. (2018) 'Nanostructure depositions on alumina hollow fiber membranes for enhanced wetting resistance during membrane distillation', Journal of Membrane Science, 564, pp. 227–236. doi: 10.1016/j.memsci.2018.07.011.

Chen, T., Duan, M. and Fang, S. (2016) 'Fabrication of novel superhydrophilic and underwater superoleophobic hierarchically structured ceramic membrane and its separation performance of oily wastewater', Ceramics International, 42(7), pp. 8604–8612. doi: 10.1016/j.ceramint.2016.02.090.

Cheng, Z., Lai, H., Du, Y., Fu, K., Hou, R., Zhang, N. and Sun, K (2013) 'Underwater superoleophilic to superoleophobic wetting control on the nanostructured copper substrates', ACS Applied Materials and Interfaces, 5(21), pp. 11363–11370. doi: 10.1021/am403595z.

Cheng, Z., Wang, J., Lai, H., Du, Y., Hou, R., Li, C., Zhang, N. and Sun, K. (2015) 'PH-controllable on-demand oil/water separation on the switchable superhydrophobic/superhydrophilic and underwater low-adhesive superoleophobic copper mesh film', Langmuir, 31(4), pp. 1393–1399. doi: 10.1021/la503676a.

Cheryan, M. and Rajagopalan, N. (1998) 'Membrane processing of oily streams. Wastewater treatment and waste reduction', Journal of Membrane Science, 151(1), pp. 13–28. doi: 10.1016/S0376-7388(98)00190-2.

Chu, L., Wang, S. and Chen, W. (2005) 'Surface Modification of Ceramic-Supported Polyethersulfone Membranes by Interfacial Polymerization for Reduced Membrane Fouling', pp. 1934–1940. doi: 10.1002/macp.200500324.

Chu, Z., Feng, Y. and Seeger, S. (2015) 'Oil / Water Separation with Selective Superantiwetting / Superwetting Surface Materials Angewandte', pp. 2328–2338. doi: 10.1002/anie.201405785.

CNN. (2018). Oil Spills fast fact on CNN.com May 2018.

Das, B., Chakrabarty, B. and Barkakati, P. (2016) 'Preparation and characterization of novel ceramic membranes for micro-filtration applications', Ceramics International, 42(13), pp. 14326–14333. doi: 10.1016/j.ceramint.2016.06.125.

Dion, I.., Bordenave, L., Lefebvre, F., Bareille, R., Baquey, C., Monties, J. R. and Havlik, P. (1994) 'Physico-chemistry and cytotoxicity of ceramics - Part II Cytotoxicity of ceramics', Journal of Materials Science: Materials in Medicine, 5(1), pp. 18–24. doi: 10.1007/BF00121148.

Ditsch, A., Laibinis, P. E., Wang, D. I. C. and Hatton, T. A. (2005) 'Controlled clustering and enhanced stability of polymer-coated magnetic nanoparticles', *Langmuir*, 21(13), pp. 6006–6018. doi: 10.1021/la047057+.

Duan, C., Zhu, T., Guo, J., Wang, Z., Liu, X., Wang, H., Xu, X., Jin, Y., Zhao, N. and Xu, J. (2015) 'Smart enrichment and facile separation of oil from emulsions and mixtures by superhydrophobic/superoleophilic particles', ACS Applied Materials and Interfaces, 7(19), pp. 10475–10481. doi: 10.1021/acsami.5b01901.

Ebrahimi, M., Willershausen, D., Ashaghi, K. S., Engel, L., Placido, L., Mund, P., Bolduan, P. and Czermak, P. (2010) 'Investigations on the use of different ceramic membranes for efficient oil-field produced water treatment', Desalination, 250(3), pp. 991–996. doi: 10.1016/j.desal.2009.09.088.

Emani, S., Uppaluri, R. and Purkait, M. K. (2014) 'Cross fl ow micro fi ltration of oil – water emulsions using kaolin based low cost ceramic membranes', DES, 341, pp. 61–71. doi: 10.1016/j.desal.2014.02.030.

Fang, Z. (2015) 'Formation of hydrophobic coating on glass surface using atmospheric pressure non-thermal plasma in ambient air', (May). doi: 10.1088/0022-3727/37/16/007.

Fauchais, P. and Vardelle, A. (2011) 'Innovative and emerging processes in plasma spraying : from micro- to nano-structured coatings'. doi: 10.1088/0022-3727/44/19/194011.

Feng, L., Li, S., Li, Y., Li, H., Zhang, L., Zhai, J., Song, Y., Liu, B., Jiang, L. and Zhu, D. (2002) 'Super-hydrophobic surfaces: From natural to artificial', Advanced Materials, 14(24), pp. 1857–1860. doi: 10.1002/adma.200290020.

Feng, L., Zhang, Y., Xi, J., Zhu, Y., Xia, F. and Jiang, L. (2008) '花びら効果.Pdf', (18), pp. 4114–4119.

Ferrando, R., Jellinek, J. and Johnston, R. L. (2008) 'Nanoalloys : From Theory to Applications of Alloy Clusters and Nanoparticles', 108(3).

Gao, N., Yan, Y. Y., Chen, X. Y. and Mee, D. J. (2011) 'Superhydrophobic surfaces with hierarchical structure', Materials Letters, 65(19–20), pp. 2902–2905. doi: 10.1016/j.matlet.2011.06.088.

Gao, N. and Xu, Z. K. (2019) 'Ceramic membranes with mussel-inspired and nanostructured coatings for water-in-oil emulsions separation', Separation and Purification Technology, 212(November 2018), pp. 737–746. doi: 10.1016/j.seppur.2018.11.084.

Gao, N. and Yan, Y. (2012) 'Characterisation of surface wettability based on nanoparticles', Nanoscale, 4(7), pp. 2202–2218. doi: 10.1039/c2nr11736c.

Garmsiri, E., Rasouli, Y., Abbasi, M. and Izadpanah, A. A. (2017) 'Chemical cleaning of mullite ceramic microfiltration membranes which are fouled during oily wastewater treatment', Journal of Water Process Engineering, 19(July), pp. 81–95. doi: 10.1016/j.jwpe.2017.07.012.

Ge, D., Deng, J., Duan, R., Li, X., Liu, Y. and Yue, H. (2019) 'Effect of surface wettability on tribological properties of Al2O3/TiC ceramic under wet lubrication', Ceramics International, 45(18), pp. 24554–24563. doi: 10.1016/j.ceramint.2019.08.184.

Gestel, T.V., Sebold, D., Meulenberg, W. A., Bram, M. and Buchkremer, H. (2008) 'Manufacturing of new nano-structured ceramic – metallic composite microporous membranes consisting of ZrO 2 , Al 2 O 3 , TiO 2 and stainless steel ☆', 179, pp. 1360–1366. doi: 10.1016/j.ssi.2008.02.046.

Gu, J., Ren, C., Zong, X., Chen, C. and Winnubst, L. (2016) 'Preparation of alumina membranes comprising a thin separation layer and a support with straight open pores for water desalination', Ceramics International, 42(10), pp. 12427–12434. doi: 10.1016/j.ceramint.2016.04.183.

Huang, J.-Y. and Lai, Y.-K. (2015) 'TiO2 -Based Surfaces with Special Wettability – From Nature to Biomimetic Application', Wetting and Wettability. doi: 10.5772/60826.

Hurwitz, G., Guillen, G. R. and Hoek, E. M. V. (2010) 'Probing polyamide membrane surface charge, zeta potential, wettability, and hydrophilicity with contact angle measurements', Journal of Membrane Science, 349(1–2), pp. 349–357. doi: 10.1016/j.memsci.2009.11.063.

Jiang, F. and Hsieh, Y. Lo (2014) 'Amphiphilic superabsorbent cellulose nanofibril aerogels', Journal of Materials Chemistry A, 2(18), pp. 6337–6342. doi: 10.1039/c4ta00743c.

Ke, Q., Jin, Y., Jiang, P. and Yu, J. (2014) 'Oil/Water separation performances of superhydrophobic and superoleophilic sponges', Langmuir, 30(44), pp. 13137–13142. doi: 10.1021/la502521c.

Khan, M. (2015) '美国科学院学报 Materials Chemistry A 材料化学 a', Journal of Materials Chemistry A, (207890), p. 121.

Kim, S. C., Yeom, H. J., Kim, Y. W., Song, I. H. and Ha, J. H. (2017) 'Processing of alumina-coated glass-bonded silicon carbide membranes for oily wastewater treatment', International Journal of Applied Ceramic Technology, 14(4), pp. 692–702. doi: 10.1111/ijac.12693.

Kong, J. and Li., K. (1999) 'Oil removal from oil-in-water emulsions using PVDF membranes', Separation and Purification Technology, 16(1), pp. 83–93. doi: 10.1016/S1383-5866(98)00114-2.

Kong, L., Wang, Q., Xiong, S. and Wang, Y. (2014) 'Turning low-cost filter papers to highly efficient membranes for oil/water separation by atomic-layer-deposition-enabled hydrophobization', Industrial and Engineering Chemistry Research, 53(42), pp. 16516–16522. doi: 10.1021/ie502864u.

Kubiak, K. J., Wilson, M. C.T., Mathia, T. G. and Carval, P. (2011) 'Wettability versus roughness of engineering surfaces', *Wear*, 271(3–4), pp. 523–528. doi: 10.1016/j.wear.2010.03.029.

Kumar, R. V., Ghoshal, A. K. and Pugazhenthi, G. (2015) 'Elaboration of novel tubular ceramic membrane from inexpensive raw materials by extrusion method and its performance in micro fi ltration of synthetic oily wastewater treatment', Journal of Membrane Science, 490, pp. 92–102. doi: 10.1016/j.memsci.2015.04.066.

Le, N. L. and Nunes, S. P. (2016) 'Materials and membrane technologies for water and energy sustainability', Sustainable Materials and Technologies, 7, pp. 1–28. doi: 10.1016/j.susmat.2016.02.001.

Liu, H., Gao, S. W., Cai, J. S., He, C. L., Mao, J. J., Zhu, T. X., Chen, Z., Huang, J. Y., Meng, K., Zhang, K. Q., Al-Deyab, S. S. and Lai, Y. K. (2016) 'Recent progress in fabrication and applications of superhydrophobic coating on cellulose-based substrates', Materials, 9(3), pp. 1–37. doi: 10.3390/ma9030124.

Liu, X., Ge, L., Li, W., Wang, X. and Li, F. (2015) 'Layered Double Hydroxide Functionalized Textile for E ff ective Oil / Water Separation and Selective Oil Adsorption', (3).

Long, L., Xianguang, X., Jinzhi, Z., Rongchao, C., Jianhua, W., Shuang, L. and Haijun, Y. (2016) 'Application of innovative high-temperature high-density oil-based drilling fluid technology in the efficient exploration and development of ultra-deep natural gas resources in West China', International Petroleum Technology Conference 2016, IPTC 2016. doi: 10.2523/iptc-18600-ms.

Ma, Q., Cheng, H., Fane, A. G., Wang, R. and Zhang, H. (2016) 'Recent Development of Advanced Materials with Special Wettability for Selective Oil/Water Separation', *Small*, 12(16), pp. 2186–2202. doi: 10.1002/smll.201503685.

Ma, Q., Cheng, H., Fane, A. G., Wang, R. and Zhang, H. (2017) 'Preparation of Superhydrophilic and Underwater Superoleophobic Nanofiber-Based Meshes from Waste Glass for Multifunctional Oil / Water Separation', 1700391, pp. 1–7. doi: 10.1002/smll.201700391.

Masuda, T., Asoh, H., Haraguchi, S. and Ono, S. (2015) 'Fabrication and characterization of single phase α-alumina membranes with tunable pore diameters', Materials, 8(3), pp. 1350–1368. doi: 10.3390/ma8031350.

Meena, M. K., Sinhamahapatra, A., & Kumar, A. (2019). Superhydrophobic polymer composite coating on glass via spin coating technique. *Colloid and Polymer Science*, *297*(11–12), 1499–1505. https://doi.org/10.1007/s00396-019-04560-z

Mittal, P., Jana, S. and Mohanty, K. (2011) 'Synthesis of low-cost hydrophilic ceramic – polymeric composite membrane for treatment of oily wastewater', DES, 282, pp. 54–62. doi: 10.1016/j.desal.2011.06.071.

Miwa, M., Nakajima, A., Fujishima, A., Hashimoto, K. and Watanabe, T. (2000) 'Effects of the surface roughness on sliding angles of water droplets on superhydrophobic surfaces', *Langmuir*, 16(13), pp. 5754–5760. doi: 10.1021/la991660o.

Munirasu, S., Haija, M. A. and Banat, F. (2016) 'Use of membrane technology for oil field and refinery produced water treatment - A review', Process Safety and Environmental Protection, 100, pp. 183–202. doi: 10.1016/j.psep.2016.01.010.

NEWS 24. (2019).

Neumann, A., Reske, T., Held, M., Jahnke, K., Ragoß, C. and Maier, H. R. et al. (2004) 'Comparative investigation of the biocompatibility of various silicon nitride ceramic qualities in vitro', Journal of Materials Science: Materials in Medicine, 15(10), pp. 1135–1140. doi: 10.1023/B:JMSM.0000046396.14073.92.

O.V. Magdysyuk, F. Adams, H-P. Liermann, I. Spanopoulos, P.N. Trikalitis, M. Hirscher, R.E. Morris, M.J. Duncan, L.J. McCormick, R. E. D. (2016) 'Understanding the Adsorption Mechanism of Noble Gases Kr and Xe in CPO-27-Ni, CPO-27-Mg, and ZIF-8', pp. 1–6. doi: 10.1039/x0xx00000x.

Ogi, T., Iskandar, F., Itoh, Y. and Okuyama, K. (2006) 'Characterization of dip-coated ITO films derived from nanoparticles synthesized by low-pressure spray pyrolysis', pp. 343–350. doi: 10.1007/s11051-005-9006-0.

Padaki, M., Murali, R. S., Abdullah, M. S., Misdan, N., Moslehyani, A., Kassim, M. A., Hilal, N. and Ismail, A. F. (2015) 'Membrane technology enhancement in oil – water separation . A review', *Desalination*. Elsevier B.V., 357, pp. 197–207. doi: 10.1016/j.desal.2014.11.023.

Peng, H., Wang, H., Wu, J., Meng, G., Wang, Y., Shi, Y., Liu, Z. and Guo, X. (2016) 'Preparation of Superhydrophobic Magnetic Cellulose Sponge for Removing Oil from Water', Industrial and Engineering Chemistry Research, 55(3), pp. 832–838. doi: 10.1021/acs.iecr.5b03862.

Prasad, D. V. V., Reddy, Y. V. and Pandey, V. K. (2008) 'An unique prediction model of the interconnect geometry for a full-custom design style', Journal of Applied Sciences, 8(19), pp. 3503–3507. doi: 10.3923/jas.2008.3503.3507.

Quéré, D. (2008) 'Wetting and roughness', Annual Review of Materials Research, 38, pp. 71–99. doi: 10.1146/annurev.matsci.38.060407.132434.

Radjenović, J., Petrović, M., Ventura, F. and Barceló, D. (2008) 'Rejection of pharmaceuticals in nanofiltration and reverse osmosis membrane drinking water treatment', Water Research, 42(14), pp. 3601–3610. doi: 10.1016/j.watres.2008.05.020.

Raji, Y. O., Othman, M. H. D., Nordin, N. A. H. S., Kurniawan, T. A., Ismail, A. F., Rahman, M. A. Jaafar, J., Adam, M. R. Bi., Alftessi, S. A., El-badawy, T. and Farag, T. M. (2021) 'Wettability improvement of ceramic membrane by intercalating nano-Al2O3 for oil and water separation', Surfaces and Interfaces, 25, p. 101178. doi: 10.1016/j.surfin.2021.101178.

Ramachandran, R. and Nosonovsky, M. (2016) 'Vibrations and Spatial Patterns Change Effective Wetting Properties of Superhydrophobic and Regular Membranes'. doi: 10.3390/biomimetics1010004.

Ren, C., Fang, H., Gu, J., Winnubst, L. and Chen, C. (2015) 'Preparation and characterization of hydrophobic alumina planar membranes for water desalination', Journal of the European Ceramic Society, 35(2), pp. 723–730. doi: 10.1016/j.jeurceramsoc.2014.07.012.

Rezaei, S., Abadi, H., Reza, M., Hemati, M., Rekabdar, F. and Mohammadi, T. (2011) 'Ceramic membrane performance in micro fi ltration of oily wastewater', *DES*. Elsevier B.V., 265(1–3), pp. 222–228. doi: 10.1016/j.desal.2010.07.055.

Riley, F. L. (2000) 'Silicon nitride and related materials', Journal of the American Ceramic Society, 83(2), pp. 245–265. doi: 10.1111/j.1151-2916.2000.tb01182.x.

Shahien, M. and Suzuki, M. (2017) 'Low power consumption suspension plasma spray system for ceramic coating deposition', Surface and Coatings Technology, 318, pp. 11–17. doi: 10.1016/j.surfcoat.2016.07.040.

Shannon, M. A., Bohn, P. W., Elimelech, M., Georgiadis, J. G., Marĩas, B. J. and Mayes, A. M. (2008) 'Science and technology for water purification in the coming decades', *Nature*, 452(7185), pp. 301–310. doi: 10.1038/nature06599.

Si, Y., Fu, Q., Wang, X., Zhu, J., Yu, J., Sun, G. and Ding, B. (2015) 'Superelastic and Superhydrophobic Nanofiber-Assembled Cellular Aerogels for Effective Separation of Oil/Water Emulsions', ACS Nano, 9(4), pp. 3791–3799. doi: 10.1021/nn506633b.

Sob, P. B., Alugongo, A. A. and Tengen, T. B. (2019) 'Scanning Electron Microscopy , Energy Dispersive X-ray Spectroscopy and Statistica Analysis of High and Low Pressure Coatings on Sediments Membrane for Stable and Efficient Wettability', 12(12), pp. 1–22.

Sob, P. B., Alugongo, A. A. and Tengen, T. B. (2020) "*Controllability and stability of selectively wettable nanostructured membrane for oil / water separation*,"A thesis submitted in fulfilment of the requirements for the degree Doctorate Technologiae in Mechanical Engineering in the Faculty of Engineering & Technology.

Solomon, B. R., Hyder, M. N. and Varanasi, K. K. (2014) 'Separating oil-water nanoemulsions using flux-enhanced hierarchical membranes', Scientific Reports, 4, pp. 1–6. doi: 10.1038/srep05504.

Song, J., Lu, Y., Luo, J., Huang, S., Wang, L., Xu, W. and Parkin, I.P. (2015) 'Barrel-Shaped Oil Skimmer Designed for Collection of Oil from Spills', pp. 1–8. doi: 10.1002/admi.201500350.

Song, J. and Rojas, O. J. (2013) 'Approaching super-hydrophobicity from cellulosic materials: A review', Nordic Pulp and Paper Research Journal, 28(2), pp. 216–238. doi: 10.3183/npprj-2013-28-02-p216-238.

Stebounova, L. V, Guio, E. and Grassian, V. H. (2011) 'Silver nanoparticles in simulated biological media : a study of aggregation , sedimentation , and dissolution', pp. 233–244. doi: 10.1007/s11051-010-0022-3.

Subhash, L. S., Basavraj, G. A., Shridhar M. C. and Shrikant V. R. (2012) 'Recent Progress in Preparation of Superhydrophobic Surfaces: A Review', Journal of Surface Engineered Materials and Advanced Technology, 02(02), pp. 76–94. doi: 10.4236/jsemat.2012.22014.

Suresh, K., Kumar, M., Pugazhenthi, G. and Uppaluri, R. (2017) 'Enhanced mechanical and thermal properties of polystyrene nanocomposites prepared using organo-functionalized Ni–Al layered double hydroxide via melt intercalation technique', Journal of Science: Advanced Materials and Devices, 2(2), pp. 245–254. doi: 10.1016/j.jsamd.2017.05.003.

Tai, M. H., Gao, P., Tan, B. Y. L., Sun, D. D. and Leckie, J. O. (2015) 'A Hierarchically-Nano Structured TiO2-Carbon Nanofibrous Membrane for Concurrent Gravity-Driven Oil-Water Separation', *International Journal of Environmental Science and Development*, 6(8), pp. 590–595. doi: 10.7763/ijesd.2015.v6.663.

Tuteja, A., Choi, W., Mabry, J. M., McKinley, G. H. and Cohen, R. E. (2008) 'Robust omniphobic surfaces', Proceedings of the National Academy of Sciences of the United States of America, 105(47), pp. 18200–18205. doi: 10.1073/pnas.0804872105.

Tuyen, D. V., Park, Y. J., Kim, H. D. and Lee, B. T. (2009) 'Formation of rod-like Si3N4 grains in porous SRBSN bodies using 6Y2O3-2MgO sintering additives', Ceramics International, 35(6), pp. 2305–2310. doi: 10.1016/j.ceramint.2009.01.010.

Wang, B., Liang, W., Guo, Z. and Liu, W. (2015) 'Biomimetic super-lyophobic and super-lyophilic materials applied for oil/water separation: A new strategy beyond nature', Chemical Society Reviews, 44(1), pp. 336–361. doi: 10.1039/c4cs00220b.

Wang, H., Hu, X., Ke, Z., Du, C. Z., Zheng, L., Wang, C. (2018) 'Review: Porous Metal Filters and Membranes for Oil–Water Separation', Nanoscale Research Letters, 13. doi: 10.1186/s11671-018-2693-0.

Wang, J., Wong, J. X. H., Kwok, H., Li, X. and Yu, H. Z. (2016) 'Facile preparation of nanostructured, superhydrophobic filter paper for efficient water/oil separation', PLoS ONE, 11(3), pp. 1–12. doi: 10.1371/journal.pone.0151439.

Wang, Y., Wang, X., Liu, Y., Ou, S., Tan, Y. and Tang, S. (2009) 'Refining of biodiesel by ceramic membrane separation', 90, pp. 422–427. doi: 10.1016/j.fuproc.2008.11.004.

Wei, Y., Qi, H., Gong, X. and Zhao, S. (2018) 'Specially Wettable Membranes for Oil – Water Separation', 1800576, pp. 1–27. doi: 10.1002/admi.201800576.

Weston, J. S., Jentoft, R. E., Grady, B. P., Resasco, D. E. and Harwell, J. H (2015) 'Silica Nanoparticle Wettability: Characterization and E ff ects on the Emulsion Properties'. doi: 10.1021/ie504311p.

Wu, L., Li, L., Li, B., Zhang, J. and Wang, A. (2015) 'Magnetic, durable, and superhydrophobic polyurethane@Fe3O4@SiO2@fluoropolymer sponges for selective oil absorption and oil/water separation', ACS Applied Materials and Interfaces, 7(8), pp. 4936–4946. doi: 10.1021/am5091353.

Xing, W. (2017) Chapter 14 - Ceramic Membranes, Membrane-Based Separations in Metallurgy. Elsevier Inc. doi: 10.1016/B978-0-12-803410-1/00014-1.

Xu, L., Karunakaran, R. G. Guo, J. and Yang, S. (2012) 'Transparent, superhydrophobic surfaces from one-step spin coating of hydrophobic nanoparticles', *ACS Applied Materials and Interfaces*, 4(2), pp. 1118–1125. doi: 10.1021/am201750h.

Yan, Y. Y., Gao, N. and Barthlott, W. (2011) 'Mimicking natural superhydrophobic surfaces and grasping the wetting process: A review on recent progress in preparing superhydrophobic surfaces', Advances in Colloid and Interface Science, 169(2), pp. 80–105. doi: 10.1016/j.cis.2011.08.005.

Yang, C., Tartaglino, U. and Persson, B. N. J. (2006) 'Influence of surface roughness on superhydrophobicity', Physical Review Letters, 97(11), pp. 1–4. doi: 10.1103/PhysRevLett.97.116103.

Yang, X. and Cranston, E. D. (2014) 'Chemically cross-linked cellulose nanocrystal aerogels with shape recovery and superabsorbent properties', Chemistry of Materials, 26(20), pp. 6016–6025. doi: 10.1021/cm502873c.

Yu, L., Han, M. and He, F. (2017) 'A review of treating oily wastewater', Arabian Journal of Chemistry, 10, pp. S1913–S1922. doi: 10.1016/j.arabjc.2013.07.020.

Zhang, J. and Seeger, S. (2011) 'Polyester materials with superwetting silicone nanofilaments for oil/water separation and selective oil absorption', Advanced Functional Materials, 21(24), pp. 4699–4704. doi: 10.1002/adfm.201101090.

Zhang, L., Wu, J., Wang, Y., Long, Y., Zhao, N. and Xu, J. (2012) 'Combination of Bioinspiration: A General Route to Superhydrophobic Particles'.

Zhang, L., Zhang, Z. and Wang, P. (2012) 'Smart surfaces with switchable superoleophilicity and superoleophobicity in aqueous media: Toward controllable oil/water separation', NPG Asia Materials, 4(2). doi: 10.1038/am.2012.14.

Zhang, W., Shi, Z., Zhang, F., Liu, X., Jin, J. and Jiang, L. (2013) 'Superhydrophobic and superoleophilic PVDF membranes for effective separation of water-in-oil emulsions with high flux', *Advanced Materials*, 25(14), pp. 2071–2076. doi: 10.1002/adma.201204520.

Zheng, X., Guo, Z., Tian, D., Zhang, X., Li, W. and Jiang, L. (2015) 'Underwater self-cleaning scaly fabric membrane for oily water separation', ACS Applied Materials and Interfaces, 7(7), pp. 4336–4343. doi: 10.1021/am508814g.

Zhong, Z., Xing, W. and Zhang, B. (2013) 'Fabrication of ceramic membranes with controllable surface roughness and their applications in oil / water separation', Ceramics International, 39(4), pp. 4355–4361. doi: 10.1016/j.ceramint.2012.11.019.

Zhou, J. E., Chang, Q., Wang, Y., Wang, J. and Meng, G. (2010) 'Separation of stable oil-water emulsion by the hydrophilic nano-sized ZrO2 modified Al2O3 microfiltration membrane', Separation and Purification Technology, 75(3), pp. 243–248. doi: 10.1016/j.seppur.2010.08.008.

Zhou, X., Zhang, Z., Xu, X., Men, X. and Zhu, X. (2013) 'Facile fabrication of superhydrophobic sponge with selective absorption and collection of oil from water', Industrial and Engineering Chemistry Research, 52(27), pp. 9411–9416. doi: 10.1021/ie400942t.

Zhou, Y., Li, M., Zhong, X., Zhu, Z., Deng, P. and Liu, H. (2015) 'Hydrophobic composite coatings with photocatalytic self-cleaning properties by micro / nanoparticles mixed with fl uorocarbon resin', Ceramics International, 41(4), pp. 5341–5347. doi: 10.1016/j.ceramint.2014.12.090.

Zhu, Q., Chu, Y., Wang, Z., Chen, N., Lin, L., Liu, F. and Pan, Q. (2013) 'Robust superhydrophobic polyurethane sponge as a highly reusable oil-absorption material', Journal of Materials Chemistry A, 1(17), pp. 5386–5393. doi: 10.1039/c3ta00125c.

Zhu, X., Tu, W., Wee, K. and Bai, R. (2014) 'Effective and low fouling oil / water separation by a novel hollow fi ber membrane with both hydrophilic and oleophobic surface properties', *Journal of Membrane Science*. Elsevier, 466, pp. 36–44. doi: 10.1016/j.memsci.2014.04.038.

Zhu, Y., Wang, D., Jiang, L. and Jin, J. (2014) 'Recent progress in developing advanced membranes for emulsified oil / water separation', *NPG Asia Materials*. Nature Publishing Group, 6(5), pp. e101-11. doi: 10.1038/am.2014.23.